Molecular Magnetic Switches – Synthesis and Characterisation of Novel Iron Spin Crossover Compounds

Von der Naturwissenschaftlichen Fakultät der

Gottfried Wilhelm Leibniz Universität Hannover

zur Erlangung des Grades

Doktor der Naturwissenschaften

Dr. rer. nat.

genehmigte Dissertation von

M. Sc. Christoph Krüger

geboren am 09.02.1987 in Berlin

2016

Referent: Prof. Dr. Franz Renz

Korreferent: Prof. Dr. Ralf Sindelar

Tag der Promotion: 25.02.2016

M. Sc. Christoph Krüger

Molecular Magnetic Switches –

Synthesis and Characterisation of Novel Iron Spin Crossover Compounds

2016

Abstract

More than eight decades ago the spin crossover phenomenon was discovered and is now attractive for the design of novel functional switchable materials. A spin crossover can occur in iron coordination compounds and also be induced by temperature, pressure or light. The switching properties offer a variety of opportunities in the development of magnetic materials for potential applications such as temperature and pressure sensors, as well as optical devices.

The major part of this dissertation is devoted to the synthesis and characterisation of novel mononuclear Fe^{III} coordination compounds $[Fe^{III}(L^5)L^1]$ involving a pentadentate Schiff base ligand (L^5), as well as a sixth easy replaceable monomer (L^1). Two pentadentate Schiff base families have been developed to a series of novel thermal-induced spin crossover compounds. Investigations on structure-magnetism relationships were performed as well. The greatest achievement in this class of complexes is the adjustment of the transition temperature by using specific monomers. It is shown that thiocyanate and selenocyanate monodentate ligands offer a possibility in tuning the transition temperature, providing that the structure is equal. Further compounds exhibit gradual spin crossover either near room temperature or hysteretic behaviour at around 100 K.

Further results of this thesis were achieved through investigation of chiral bimetallic square complexes. Crystal structures provide unusual cyanide-bridge geometry of Ni-N≡C with an astonishing acute angle which is unique to our state of knowledge in molecular assemblies. The research of those novel functional systems reflects a modern trend in molecular materials science. Such systems might find applications in hydrogen storage, as molecular sieves and in nanoscale devices.

Inhaltsübersicht

Seit der Entdeckung des Spin-Crossover-Phänomens vor mehr als acht Jahrzehnten wurden im Laufe der Zeit äußerst vielversprechende Erkenntnisse in der Entwicklung neuer funktionaler schaltbarer Materialien erzielt. Spin-Übergänge werden überwiegend in Eisen-Koordinationsverbindungen beobachtet und können unter anderem durch Temperatur-, Druck- oder Lichteinflüsse induziert werden. Diese schaltfähigen Eigenschaften bieten zahlreiche Möglichkeiten in der Entwicklung von Temperatur- und Drucksensoren, sowie optischen Materialien.

Der größte Teil dieser Dissertation befasst sich mit der Synthese und Charakterisierung neuer mononuklearer Fe^{III}-Koordinationsverbindungen $[Fe^{III}(L^5)L^1]$, welche sich aus einem Pentadentat-Schiff-Base-Ligand (L^5) und einem in sechster Koordination einfach austauschbarem Monomer (L^1) zusammensetzen. Zwei Pentadentat-Schiff-Base-Familien wurden für die Entwicklung einer Anzahl neuer thermisch-induzierter Spin-Crossover-Verbindungen hergestellt und auf strukturelle und magnetische Eigenschaften untersucht. Eine Erkenntnis dieser Arbeit ist die Steuerbarkeit der Übergangstemperatur mittels spezifischer Monomere. Es hat sich gezeigt, dass die Co-Liganden Thiocyanat und Selenocyanat eine geeignete Möglichkeit bieten, um die Übergangstemperatur bei gleicher Kristallstruktur einzustellen. Weitere Spin-Crossover-Verbindungen zeigen einen Übergang nahe Raumtemperatur oder eine Hysterese im Bereich von 100 K.

Weitere Erkenntnisse dieser Arbeit wurden durch Untersuchungen neuer chiraler bimetallischer quadratischer Ni-Fe Komplexe gewonnen. Strukturanalysen von Einkristallen zeigen eine ungewöhnliche Cyanid-verbrückende Geometrie von Ni-N≡C mit einem erstaunlich scharfen Winkel auf, der nach unserem Kenntnisstand einzigartig auf der molekularen Ebene ist. Das Entwickeln solch neuer funktionaler Systeme spiegelt einen modernen Trend in der molekularen Materialwissenschaft wieder. Mögliche Anwendungen können diese Systeme in Wasserstoffspeicher, als Molekularsieb und in nanoskalierten Applikationen finden.

Stichwörter: Molekulare Schalter · Eisen(III)-Koordinationsverbindungen · Spin-Crossover · Schiff'sche Base · Ligandendesign · Pseudohalid · Square-Komplex

Danksagung

Mein Dank gilt zunächst meinem Doktorvater, Herrn Prof. Dr. Franz Renz, der es mir ermöglichte Forschungen in dem von mir gewünschten Feld vorzunehmen. Mit seiner Unterstützung war es mir möglich sowohl an der Tsukuba University in Japan zu studieren als auch an der Stanford University in den USA für meine Dissertation zu forschen.

Herrn Prof. Dr-Ing. Ralf Sindelar von der Hochschule Hannover danke ich für die Übernahme des Korreferats. Bei Herrn Prof. Dr. Jens-Uwe Grabow vom Institut für physikalische Chemie der Leibniz Universität Hannover bedanke ich mich für die Übernahme des Prüfungsvorsitzes.

Besonders hervorheben möchte ich auch unsere Kooperationspartner, Herrn Prof. Dr. Roman Boča und Herrn Dr. Lubor Dlhan von der Slovak University of Technology in Bratislava, für ihre Unterstützung mit magnetischen Messungen und der hervorragenden Zusammenarbeit an Publikationen.

Meine ereignisreiche und wertvolle Doktorandenzeit verdanke ich dem gesamten Arbeitskreis Renz. Durch unsere fachlichen Diskussionen konnte ich meinen Horizont in vielen Bereichen erweitern. Ihr wart mir jedoch nicht nur Kollegen, sondern wurdet mir zu treuen Freunden. Ich erinnere mich sehr gerne an unsere gemeinsamen Unternehmungen und zwar ganz besonders an die stets lustigen Abende, die wir gemeinsam mit Speis, Trank und Gesang im Sozialraum verbrachten. Vielen Dank an Bastian Dreyer, Lars Heyer, Dr. Patrick Homenya, Moritz Jahns, Stephen Klimke, Emi Lagerspets, Torben Meyer mit Lasse, Annika Preiss, Daniel Unruh und Dagmar Wengerowsky.

Meinen HiWis Stephen Klimke und Annika Preiss und den Gaststudenten Heather Cavers, Joseph Dey und Jana Ockova mit Unterstützung des DAAD RISE danke ich für die Hilfe bei wichtigen Synthesearbeiten.

Außerdem bedanke ich mich bei allen Studenten, die ich während Ihrer Bachelorarbeit betreuen durfte. Ich wünsche Stephen Klimke, Annika Preiss, Arthur Lysov, Marina Vellguth, Piotr Wemhoff und Christopher Hinse alles Gute für Ihre Zukunft.

Nicht unerwähnt sollen unsere chemisch-technischen Assistentinnen Dagmar Grüne und Kirsten Eiben bleiben. Ohne Ihre Hilfe und Erfahrung wäre so manches Praktikum sehr viel schwieriger verlaufen.

Ich danke auch dem Sekretariat Birgitt Förster, Merle Feldt und Sonja Thiele für die hervorragende Arbeit.

Ein besonderes Dankeschön möchte ich Herrn Prof. Dr. Hiroki Oshio aussprechen, der mir ein wirklich guter Freund geworden ist. Ich hatte eine unbeschreibliche Zeit in Japan.

Außerdem danke ich Herrn Prof. Dr. Richard. N. Zare bzw. Dick für die großartige Erfahrung an der Stanford University. Seine Erfolge sind das Produkt seiner einzigartigen wissenschaftlichen Arbeit, die ich sehr bewundere.

Insbesondere möchte ich mich bei meiner mir stets für mich einstehenden Familie danken. Meine Eltern, Marita und Andreas Krüger, haben mich während meines gesamten Studiums emotional und finanziell unterstützt. Sie haben mich immer aufgefangen und mir ihr offenes Ohr geschenkt. Ohne ihre Förderung hätte ich es mit Sicherheit viel schwieriger gehabt. Danke auch an meine Schwester Denise Krüger.

Zu guter Letzt bedanke ich mich bei Caroline Eickmeier. Ihre Unterstützung hat mir gerade in persönlich schwierigen Zeiten viel Kraft und Mut gegeben.

Preface

The presented results within this dissertation were achieved in the last four years during my work as scientific assistant at the Institute of Inorganic Chemistry of Gottfried Wilhelm Leibniz Universität Hannover in the group of Prof. Dr. Franz Renz. The studies were supported by Prof. Dr. Roman Boča and Prof. Dr. Hiroki Oshio. The main part of my thesis consists of three peer-reviewed articles and another already submitted manuscript written by me as the first author. They are dealing with the synthesis and characterisation of novel iron coordination compounds.

Great thanks to all co-authors for the cooperation and support during the manuscript preparations.

The first article in section 6.1 deals with the synthesis and characterisation of novel Fe^{III} spin crossover compounds with the general formula $[Fe^{III}(salpet)L^1]$ and $[Fe^{III}(napet)L^1]$. The first salpet complex family has been synthesised and characterised by myself. I performed single-crystal X-ray diffraction measurements in the group of Prof. Dr. Hiroki Oshio from Tsukuba University and partly with Dr. Michael Wiebcke from Leibniz Universität Hannover. Magnetic measurements were carried out in the Oshio group by me and additional calculations by Prof. Dr. Boča from Slovak University of Technology in Bratislava. The latter napet family has been synthesised and characterised by Prof. Dr. Roman Boča and Peter Augustin.

The article in section 6.2 is devoted to extended results of the previous work which provide a deeper understanding of structure-magnetism relationships within the salpet family. Preparation of four iron complexes was performed half by Peter Augustin and his colleagues and half by me. The single-crystal X-ray diffraction measurements were carried out by me with the help of Fabian Kempf from Leibniz Universität Hannover and Dr. Ivan Nemec from Palacky University in Czech Republic. Prof. Dr. Roman Boča and Dr. Lubor Dlhan performed magnetic measurements and calculations.

The submitted manuscript in section 6.3 presents novel salpet compounds including a spin crossover complex that exhibit a hysteresis. Preparations and characterisations of the compounds were mainly performed by me with the help of Annika Preiss and Daniel Unruh from Leibniz Universität Hannover. Magnetic measurements have been carried out and fitted by Prof. Dr. Roman Boča and Dr. Lubor Dlhan.

The last presented article in section 6.4 introduces a novel polycano building block which forms a tetranuclear Ni-Fe square complex with unusual cyanide bridges. The work was performed in the Oshio group by me. Preparations and characterisations involving single-crystal X-ray diffraction and magnetic measurements were carried out by me and were supervised by Dr. Takuya Shiga, Dr. Graham N. Newton and Dr. Takuto Matsumoto.

Further non published results gained within the scope of this thesis are given in the conclusions in section 7.

Table of Contents

1   Introduction

The fulfilment of the highest demands of potential future applications is probably one of the strongest and also most inspiring driving forces in recent research. The design of novel functional materials that exhibit switchable features has attracted the interest of a large number of chemists and physicists for over more than eight decades. After the first discovery of the spin crossover (SCO) phenomenon - also known as spin transition (ST) - by Cambi *et al.* in the early 1930s the development of switchable molecular materials increased rapidly.[1–3] Their investigations opened the door to a diverse research area in coordination chemistry. In 1999, the spin crossover has been defined by IUPAC as "a type of molecular magnetism that is the result of electronic instability caused by external constraints, which induce structural changes at molecular and lattice levels".[4] The possibility of switching between a diamagnetic low spin (LS) and a paramagnetic high spin (HS) state by external physical or chemical stimuli offers a huge variety of practical functions. Spin crossover has a high impact on the physical properties of the material including magnetism, colour, dielectric constant and electrical resistance. Several potential applications such as sensors, display and memory devices, electrical and electroluminescent devices, as well as temperature-sensitive MRT contrast agents are objectives currently under investigations.[5]

Development efforts in the molecule design of novel switchable molecular materials are controlling the magnetic properties nowadays.[5] From a chemical perspective, the preparation, as well as crystallisation plays an important role often involving challenging organic ligand synthesis. Although spin crossover can occur in any phase of matter, solid materials often show inter- and intramolecular cooperativity including short- and long-range interactions through the whole lattice. Due to the fact that these interactions go hand in hand with properties of crystals, the challenge remains the crystal engineering. Several switchable materials that also show pronounced hysteresis have been prepared in the course of development for specific technologically useful properties.[5–7]

Within the scope of this thesis, mononuclear Fe^{III} coordination compounds involving Schiff base ligands have been primarily investigated.[8–10] Here, Schiff base and Schiff base-like ligands are gaining more and more attention due to their flexibility and they appear to be highly suitable for the design of simple spin crossover materials.

Organic chemistry offers a variety of modified Schiff base ligands which can be easily modified for fine tuning the ligand field and magnetic properties. The ligands are usually classified into categories depending on available donor atoms. Mononuclear complexes in an octahedral sphere can contain, for example, a pentadentate ligand with a $\{N_5, N_3O_2, N_3S_2, \text{etc.}\}$ sphere, as well as a monodentate pseudohalide coligand. The easy replaceable coligand offers a further possibility for fine tuning the transition metal environment by varying anions of the spectrochemical series. Moreover, this type of mononuclear complexes is also a beneficial unit for the design of multinuclear clusters. Instead of the coligand, bridging units such as cyanide can serve as a connection between a metal centre and e.g. six monomers resulting in a star-shaped heptanuclear metal complex. This type of clusters can exhibit interesting magnetic properties due to the large number of metal ions. Renz *et al.* published the first star-shaped heptanuclear mixed-valence iron spin crossover complex in 2009,[11] providing the fundamental idea for this thesis.

Despite the benefits of star-shaped multinuclear cyanide-bridged Fe^{III} Schiff base complexes, this thesis deals also with the research of tetranuclear cyanide-bridged square compounds emerges from the possibility to create clusters in analogy to Prussian blue.[12] Prussian blue itself is a 3D network in which Fe^{II} and Fe^{III} centres are bridged by cyanide showing ferromagnetic interaction.[13] The cyanide bridge offers a valuable unit for the construction of molecular assemblies with magnetic and electronic interactions between neighbouring metal centres.[14] Due to the physical properties in Prussian blue analogues including photomagnetism, spin crossover, and electrochromicity, possible uses in hydrogen storage, as molecular sieves, and in nanoscale devices have been suggested for various applications.[12] Both the star-shaped cluster and the cyanide-bridged tetranuclear square complex can be considered as an analogous model of the infinite Prussian blue structure. Since the first studies on iron-copper high spin square complexes reported by Oshio *et al.* in 1999,[15] a great variety of cyanide-bridged homo- and heterometallic molecules have been prepared with an ongoing focus on applications as high-T_c magnetic materials,[16–19] spin crossover materials,[7,20–23] vapochromic materials,[24] as well as in photo-induced magnetism,[25–29] host-guest chemistry,[20,30–32] magnetochirality,[33–35] etc.[36]

Within the presented work, a large number of novel mononuclear Fe^{III} complexes are presented and have been discussed in three publications.[8–10] Two pentadentate ligand families (salpet, napet) have been developed to a series of novel thermal-induced spin crossover compounds. Investigations are focused within the salpet family on tuning the transition temperature by using specific monomers. The transition or critical temperature T_c varies in the temperature range from 90 to 326 K and the magnetic behaviour is either gradual or partial abrupt. In spite of the fact that the intermolecular cooperativity is usually rather weak in this class of compounds, hysteretic behaviour can occur within the salpet family. However, the obtained results provide new opportunities in the design of star-shaped heptanuclear complexes as well.

The fourth presented publication in this thesis introduces two novel bimetallic rectangular Ni-Fe clusters with unusual cyanide bridges.[37] Both enantiomeric square complexes exhibit ferromagnetic interactions between the nickel and iron ions and to our knowledge the most acute Ni-N≡C angle observed to date. The explored square design offers new opportunities in the development of cyanide-bridged complexes.

2   Spin Crossover Phenomenon

2.1   Historical Overview

In 1931, Cambi and Szegö from University of Milan published a couple of Fe^{III} derivates with anomalous temperature-dependent magnetic properties for the first time.[1–3] They discovered unknowingly a new type of transition metal coordination compounds with a fascinating phenomenon which has been developed further over almost nine decades and is known as spin crossover or spin transition.

Between 1931 and the 1960s, in order of World War II, developments in the field of spin crossover stagnated. The further progress in the research of switchable mononuclear complexes started in the 1960s and can be labelled as "the renaissance in mononuclear spin crossover compounds".[5] In 1963, Ewald *et al.* followed by Figgis *et al.* reported new discoveries in the Fe^{III} family including the first pressure-induced spin crossover.[38,39] Four years later, König and Madeja reported $[Fe^{II}(phen)_2(NCS)_2]^a$ which is nowadays one of the most intensively studied spin crossover compound.[40] This discovery was followed by a rapid increase in the research of mononuclear complexes with N-donor ligands. At that time, Ivanov *et al.* reported on Fe^{III} complexes in a $\{N_2S_2O_2\}$ sphere exhibiting sharp and hysteretic magnetic behaviour.[41] Subsequently, the first Fe^{III} spin crossover monomers containing a hexadentate $\{N_4O_2\}$ or $\{N_3O_3\}$ donor Schiff base ligand were studied,[42–45] followed by an emerging interest in complexes with a mixed heterocyclic/pseudohalide (N) donor set. Nowadays, these type of ligands are still a promising candidate for future developments.[5]

From 1980 to 2012 researchers were focused on the challenging multinuclear Fe^{II}, Fe^{III} and Co^{II} spin crossover chemistry. Multinuclear complexes have the ability to show sequential or simultaneous, as well as multistep transitions and the metal ions can cooperate between each other. Researchers have been focused on magnetic interactions across bridging groups resulting in cooperativity and thermal hysteretic behaviour in multi-dimensional systems such as 1D chains, 2D sheets or 3D frameworks.[5–7,46]

In 1987, the first dinuclear spin crossover complex was reported by Real *et al.* This was followed by trinuclear Fe^{II} complexes presented by Reedijk and Haasnoot *et al.* in which only the central ion shows a spin crossover with a weak cooperativity to

---

[a] phen: 1,10-phenanthroline

neighbouring atoms.[46–48] The first tetranuclear 2x2 grid $Fe^{II}_4L_4$ spin crossover complex, triggered by temperature, pressure and light, was published by Renz *et al.* in 2000.[49,50] In 2009, Duriska *et al.* presented the first hexanuclear spin crossover nanoball containing six Fe^{II} ions in a $\{N_6\}$ sphere.[51]

One of the latest developments in this area are investigations of spin crossover materials on the nanoscale.[52–60] Today´s pursuit is to combine the spin crossover phenomenon with other physical or chemical properties, such as liquid-crystalline and gel behaviour, electric conductivity, fluorescence and porous properties.[6] Up to now a variety of mono- and multinuclear spin crossover compounds have been discovered with an ongoing growth of interest on switchable molecular magnetic materials for future applications.[5]

The large subject of spin crossover has been summarised and reviewed plenty of times. Among these, the three-book set from the *Topics in Current Chemistry* monograph series, edited by Gütlich and Goodwin published in 2004.[7] In 2013, Halcrow extended this work as an editor of *Spin Crossover Materials: Properties and Applications*.[5] Alongside the above-mentioned books, numerous reviews reflect on the current state of research in great detail.[6,52,61,62]

2.2   Thermal-Induced Spin Crossover

The occurrence of spin crossover in coordination compounds of transition metal ions is expected for 3d transition elements with the electron configurations d^4-d^7 (Cr^{II}, Mn^{II}, Fe^{II}, Co^{II}, Mn^{III}, Fe^{III}, Co^{III}). For heavier 4d and 5d elements the ligand field energy increases notably in comparison to analogous 3d compounds. Therefore 4d and 5d metal complexes usually remain in the low spin state. Whether a compound exhibits the low or high spin state, corresponds to the distribution of electrons within the metal orbital energy levels that reveal the maximum (high spin, $S = 5/2$) and minimum (low spin, $S = 1/2$) number of unpaired electrons.[5,6]

The electron distributions in d-orbitals of metal organic coordination compounds can be described by the crystal field theory (CFT) for one-electron systems and the ligand field theory (LFT) for many-electron systems. In an electronic field the d-orbital energy splits up into the energy higher antibonding e_g and lower t_{2g} subsets in an octahedral coordination sphere. The energy difference Δ_O between the two subsets is crucial to the spin crossover. If Δ_O is greater than the interelectronic repulsion energy P, the configuration of the central metal ion will be low spin. In

contrast, if $\Delta_O < P$, the configuration will be high spin. Spin crossover can occur when Δ_O and P are similar ($\Delta_O \approx P$). In that situation, $|\Delta_O| - |P| = \Delta E_{HL}$ can be in the order of the magnitude of the thermal energy $\Delta E_{HL} \approx k_B T$ and a transition can be induced by external stimuli (T, p, hv, B).[63] The temperature at which the two states of different multiplicities are present in the ratio 1:1 is known as transition or critical temperature T_c. The term $T_c = \Delta H / \Delta S$ describes the dependence on the enthalpy, as well as the entropy due to the fact that the Gibbs energy at T_c is zero. The conversion from low to high spin is an entropy-driven reaction and with $\Delta S > 0$ and $\Delta H \sim kT > 0$ the conversion proceeds spontaneously. The relation between the equilibrium constant K and T is given by the van't Hoff equation with $\ln K = -\Delta H / RT + \Delta S / R$. A plot of $\ln K$ vs $1/T$ is a linear relationship. The equilibrium constant K can be described by $K = \chi_H / (1 - \chi_H)$ with the mole fraction χ_H of the high spin state as well.[64,65]

The spin crossover from low to high spin ($S = 1/2 \leftrightarrow 5/2$) in mononuclear Fe^{III} systems in an octahedral sphere occurs with following changes of electron configurations: $t_{2g}^5 e_g^0$ ($^2T_{2g}$, LS) $\leftrightarrow t_{2g}^3 e_g^2$ ($^6A_{1g}$, HS). With a higher occupation of the more antibonding e_g-orbitals during the transition the metal-to-ligand bond distances (r(Fe-L)) increase resulting in a larger molecular volume (Figure 1).[6] The high spin state is more populated with an increasing temperature while lowering the temperature favours the low spin state.

A detailed theoretical model including the interelectronic repulsion and spin-orbit coupling of the magnetic behaviour in mononuclear Fe^{III} spin crossover complexes was reported by Boča *et al.* in 2009.[63]
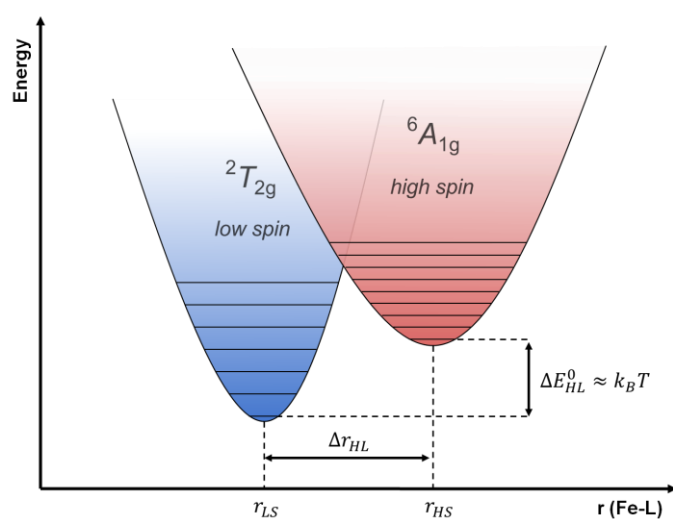
Figure 1. Potential well of the low spin ($^2T_{2g}$) and the high spin ($^6A_{1g}$) state for an octahedral Fe^{III} system.

Multinuclear compounds have the ability to show stepwise or simultaneous, as well as multistep transitions due to the fact that the number of energy levels increases with the number of nuclei. While the spin crossover in mononuclear complexes is associated with two minima (LS $\equiv$ L and HS $\equiv$ H) of the Gibbs energy, three spin pairs (LL, LH and HH) can occur in dinuclear complexes (assuming that the intermediate spin states and a difference between the LH and HL states can be ignored). In spite of the fact that the LH pair separates them by at least two energy gaps, Δ_1 (LL/LH) with $\Delta_1 = E(\text{LH}) - E(\text{LL})$ and Δ_2 (LH/HH) with $\Delta_2 = E(\text{HH}) - E(\text{LH})$, it does not have to be between LL and HH. Including the magnetic exchange coupling, the HH level splits up into six ($S = 0$ - 5), LH into two ($S = 2, 3$) and LL into two ($S = 0, 1$) sublevels (Figure 2).
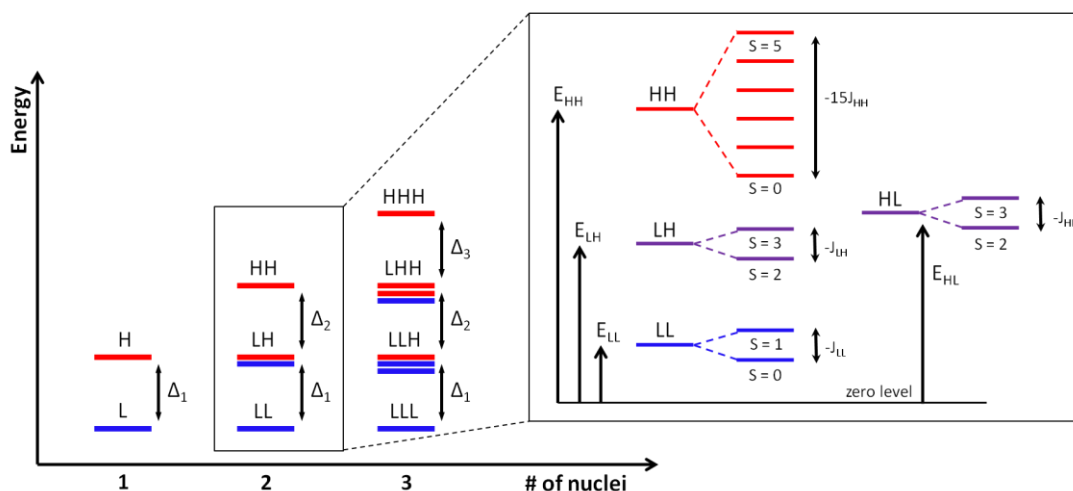

Figure 2. Reference states in multinuclear spin crossover complexes and the corresponding sub-spin-multiplets for a dinuclear Fe[III] system according to reference 65.

Various theoretical investigations on dinuclear spin crossover compounds have been reviewed. Among these, Bousseksou *et al.* presented a simple formulation of the theoretical model system Hamiltonian which is an extension of the Ising-like model originally formulated for mononuclear systems.[66] Also Boča *et al.* described a satisfying modelling for hysteretic and two-step transitions phenomena with three to six parameters and a change in theoretical efforts from reconstructions of T_c to the modelling of spatiotemporal evolution, clustering and critical phenomena of the spin crossover in a finite system.[67] Within the scope of this thesis, the theoretical aspect will not be further discussed. Theoretical foundations on molecular magnetism were

published by Boča and the current state of research have been summarised by Halcrow.[5,68]

One of the most challenging aspects in the development of mono- and multinuclear spin crossover materials with valuable properties is controlling the form of the transition. Five characteristic types of magnetic courses can occur (Figure 3): (i) gradual or (ii) abrupt, (iii) with or without hysteresis, (iv) in a single step or stepwise and (v) complete or inclompete.[5,63] Temperature-dependent spin transitions can take place in crystalline and amorphous solid states, as well as in liquid solutions. In the latter case, the mole fraction χ_H as a function of temperature follows a Boltzmann distribution law.[63] In contrast, solid state materials often show interactions transmitted by intramolecular pathways, as well as intermolecular between the metal complexes including exchange couplings which could be either antiferromagnetic or ferromagnetic. For a full understanding of the cooperativity of a spin transition in solid materials, a detailed knowledge of each structure properties and differences between the low and high spin states is necessary.[5] Due to the fact that the prediction of crystal structures and the correlating entropy is rather difficult in multinuclear systems the development of theoretical models still continues.
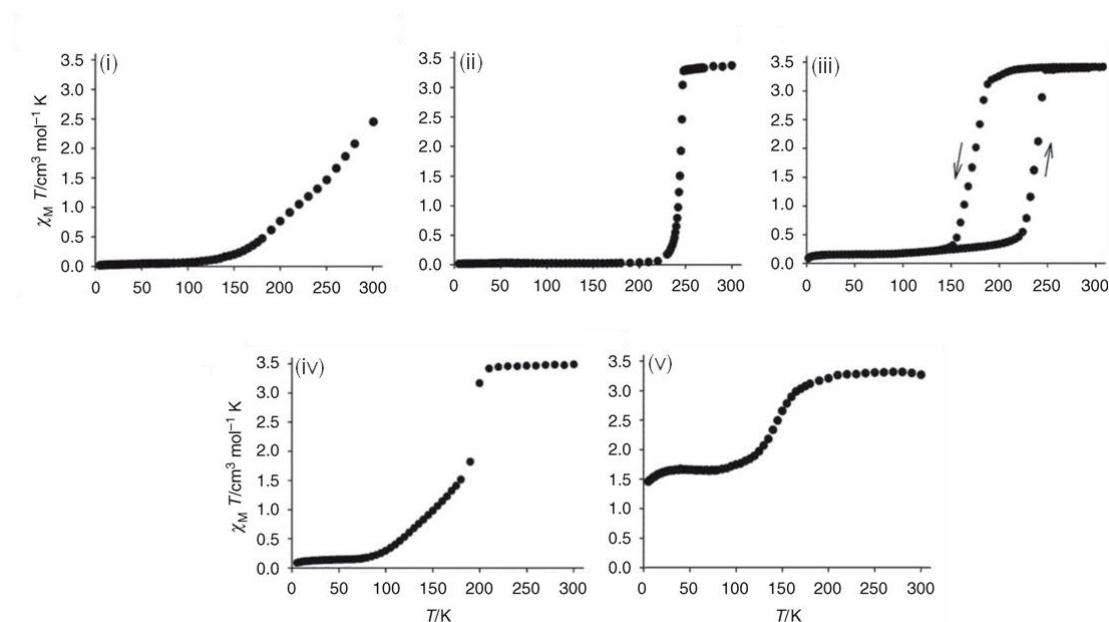
Figure 3. Spin crossover can occur in five characteristic types of magnetic courses according to reference 5: (i) gradual or (ii) abrupt, (iii) with thermal hysteresis, (iv) discontinuous and (v) incomplete.
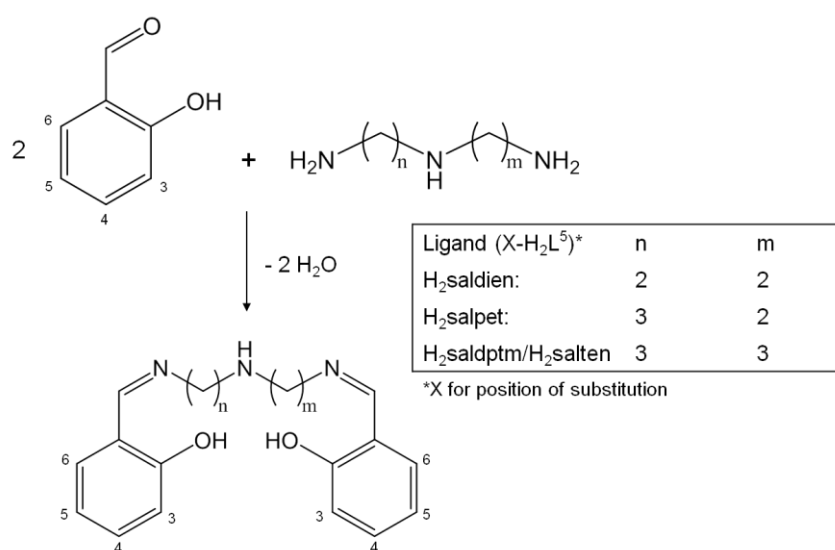
3 Mononuclear Iron Spin Crossover Compounds

3.1 Schiff Base Ligands

Imines, also known as azomethines or Schiff bases, have been reported on first by the Italian naturalized chemist Hugo Joseph Schiff in 1864.[69,70] The most common preparation for imines with the general formula $R_3R_2C=NR_1$ arises by a reaction of an aldehyde or ketone with a primary amine. Schiff base ligands are valuable to form complexes with a large number of transition metal ions and many reports on their applications in biology or catalysis have been published over the past few years.[71]

Spin crossover systems containing multidentate Schiff base-type ligands are one of the most widespread class used for the preparation of Fe^{III} spin crossover materials. Usually, they are classified into the number of donor atoms available for the coordination to the Fe^{III} ion. Di-, tri-, tetra-, penta- and hexadentate Schiff base-type complexes have been extensively reviewed by van Koningsbruggen *et al.* and Oshio *et al.* until 2007.[72,73] Among these, the most spin crossover complexes have been observed in a pentadentate $\{N_3O_2\}$ sphere including saldptm (or salten) in a pseudo-octahedral environment. Within the scope of this thesis, a pentadentate Schiff base ligand has been synthesised from a reaction of a variable diamino-aza compound with various salicylaldehyde derivatives (Figure 4). The following sections and publications introduce a number of spin crossover complexes containing the pentadentate H_2salpet ligand (salpet family), as well as the H_2napet derivative (napet family) whereas the latter is formed by a condensation of 2-hydroxynaphtaldehyde with di(3-aminopropyl)amine.

Ligand (X-H_2L^5)*	n	m
H_2saldien:	2	2
H_2salpet:	3	2
H_2saldptm/H_2salten	3	3

*X for position of substitution

Figure 4. Scheme of the synthetic method for the preparation of a pentadentate H_2L^5 ligand derived from salicylaldehyde derivatives and a diamine.

3.2 Pentadentate N₃O₂-Donating Schiff Base Complexes

The first mononuclear Fe[III] spin crossover compounds with a pentadentate Schiff base ligand were discovered by Matsumoto *et al.* in 1985.[42] In their study, a series of six-coordinated Fe[III] complexes were prepared with the {N₃O₂} donor ligand saldptm and different types of monodentate coligands (L[1]). They observed four high spin complexes (S = 5/2) with L[1] = chloride, azide, imidazole, N-methylimidazole and a further low spin complex (S = 1/2) with L[1] = cyanide in the temperature range from 10 to 300 K. They discovered as well four compounds with L[1] = pyridine, 3-methylpyridine, 3,4-dimethylpyridine and 2-methylimidazole exhibiting a gradual spin crossover from S = 1/2 → 5/2 (Figure 5).[42,74]
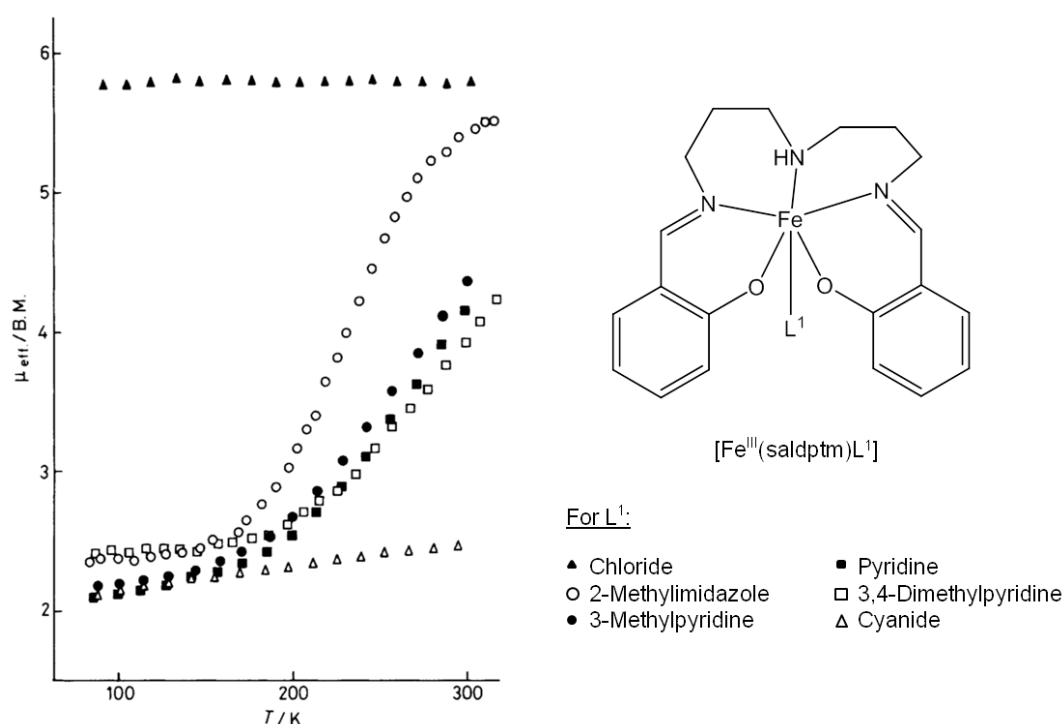
Figure 5. Effective magnetic moments of [Fe[III](saldptm)L[1]] involving L[1] = chloride, 2-methylimidazole, 3-methylpyridine, pyridine, 3,4-deimethylpyridine, cyanide are displayed according to reference 42.

In 2004 this class of Fe[III] complexes have been reviewed by van Koningsbruggen *et al.*[72] Followed by a further summary of Oshio *et al.* in 2007.[73] The progress in the development of mononuclear Fe[III] complexes with the general formula [Fe[III](X-salpet)L[1]]·Solv (X = substituent, L[1] = pseudohalide coligand, Solv = solvent molecule) started by Salitros *et al.* in 2009.[75] The Schiff condensed pentadentate ligand (H₂salpet) is derived from the reaction of an asymmetric 1,6-diamino-4-azahexane with salicylaldehyde. They published, inter alia, two complexes [Fe[III](salpet)Cl] and [Fe[III](MeBu-salpet)Cl] exhibiting only high spin

behaviour, as well as [Fe^{III}(salpet)CN]·MeOH which is in low spin state. Two years later, Nemec *et al.* investigated a series of novel mononuclear Fe^{III} Schiff base compounds and characterised them structurally and magnetically.[76] Their work was focused on complexes within the salpet family, as well as the napet family. While [Fe^{III}(3Bu5Me-salpet)(NCS)], [Fe^{III}(3MeO-salpet)(NCO)]· CH$_3$OH and [Fe^{III}(3MeO-salpet)(N$_3$)] complexes are high spin up to room temperature, compounds with H$_2$napet exhibit three different spin crossover phenomena: (i) from gradual and incomplete in [Fe^{III}(napet)(NCS)]· CH$_3$CN, (ii) to complete and relatively abrupt in [Fe^{III}(napet)(NCO)] and (iii) abrupt with a thermal hysteresis in [Fe^{III}(napet)(N$_3$)]. The obtained results provide a fine tuning of T_c by different pseudohalide coligands L^1 at the sixth labile coordination site which is still attractive for future studies. In comparison to previously reported spin crossover complexes with neutral monodentate ligands,[74] the neutral [Fe^{III}(napet)L^1] family containing charged ligands (L^1) shows cooperative interactions. According to the author, this could be explained by the asymmetric reduction of the aliphatic hydrocarbons of L^5. The higher rigidity of the molecule may play an important role in this class of compounds as a possible consequence.[76]

The first mononuclear spin crossover compounds containing the H$_2$salpet ligand were discovered by Krüger *et al.* in 2013 (section 6.1).[8] The two complexes [Fe^{III}(5Cl-salpet)(NCS)] and [Fe^{III}(5Cl-salpet)(NCSe)] were in focus of our investigations. Both exhibit a gradual spin crossover (S = 1/2 → 5/2) at T_c = 280 and 293 K and we pointed out that the solid-state cooperativeness is rather small in this class of compounds. Apart from that, we also described a couple of Fe^{III} spin crossover compounds containing naphthyl derivatives. One of them, α-[Fe^{III}(L$_2$)(NCS)], exhibit a hysteresis (S = 3/2 → 5/2) at T_c = 44, 40 K and [Fe^{III}(L$_1$)(NCS)] shows a gradual transition (S = 1/2 → 5/2) at T_c = 114 K.

A few month later Herchel and Travnicek published their investigations about the influence of 5-aminotetrazole (Hatz) as a monodentate ligand within the salpet family.[77] They synthesised and characterised four new high-temperature spin crossover compounds whereas the critical temperature T_c = 416 K could be calculated only from the magnetic data for [Fe^{III}(salpet)(atz)]. For [Fe^{III}(5Cl-salpet)(atz)], [Fe^{III}(5Br-salpet)(atz)] and [Fe^{III}(3,5Br-salpet)(atz)] they compared the temperature T_{min} at the point where the susceptibility starts to increase on heating (Table 1). In 2015, Krüger, Masarova and Nemec extended the series of mononuclear Fe^{III} Schiff base complexes.[9,78,79] Masarova *et al.* reported on

[Fe^{III}(3OEt-salpet)(NCS)] with an abrupt spin crossover at T_c = 84, 82 K and [Fe^{III}(napet)(NCS)] with a gradual magnetic behaviour at T_c = 174 K. Krüger *et al.* published two novel complexes [Fe^{III}(5Br-salpet)(N$_3$)]·CH$_3$OH (T_c = 143, 140 K) and [Fe^{III}(5Br-salpet)(NCSe)] (T_c = 326, 317 K) with a small hysteresis and weak cooperative interactions (section 6.2). We also explained the difference of the three isostructural spin crossover compounds [Fe^{III}(5Cl-salpet)(NCS)], [Fe^{III}(5Cl-salpet)(NCSe)], [Fe^{III}(5Br-salpet)(NCSe)] and the high spin complex [Fe^{III}(5Br-salpet)(NCS)] which crystallises in a different space group. Furthermore, Nemec *et al.* investigated the dependency on the structure and magnetic behaviour of two isostructural Fe^{III} complexes [Fe^{III}(napet)(NCX)]·Solv (X = S, Se) with different solvent molecules (Table 1). They found out that a stronger N-H···O hydrogen bond between the guest molecule and the amine group of the host molecule in [Fe^{III}(napet)NCX] implies a higher value of T_c. Even though they found no apparent correlation of T_c with other parameters like the guest volume, host cavity or its dielectric constant, their results are promising due to the capability to tune the spin transition point T_c and propagate cooperative interactions in the occurrence of abrupt spin crossover with thermal hysteresis using different solvents.[79] One of the latest discoveries within the salpet family is the Fe^{III} mononuclear complex [Fe^{III}(3,5Cl-salpet)(NCSe)] exhibiting a hysteresis loop of 24 K at T_c = 123, 99 K which was published by Krüger *et al.* (section 6.3).[10] On one hand the heating path shows a high cooperativity, on the other hand the cooling mode is rather gradual. Within the salpet family in mononuclear Fe^{III} spin crossover complexes with a pseudo-octahedral sphere, we observed the widest loop to date (Table 1).

Table 1. Summary and comparison of the spin transition temperature T_c of mononuclear Fe^{III} complexes containing an asymmetric (1,6-diamino-4-azahexane) pentadentate ligand napet (2-hydroxyacetonaphthone analogues) and salpet (salicylaldehyde derivatives).

	Spin	T_c (K)	Reference	Year
Naphthyl Derivatives (napet family)				
[Fe(napet)NCS)]·CH_3CN	1/2 → 5/2	151	Nemec et al.[76]	2011
[Fe(napet)NCSe)]·CH_3CN	1/2 → 5/2	170	Nemec et al.[76]	2011
[Fe(napet)(NCO)]	1/2 → 5/2	155	Nemec et al [76]	2011
[Fe(napet)(N_3)]	1/2 → 5/2	122, 117	Nemec et al.[76]	2011
α-[Fe(L_2)(NCS)]	3/2 → 5/2	44, 40	Krüger et al.[8]	2013
[Fe(L_1)(NCS)]	1/2 → 5/2	114	Krüger et al.[8]	2013
[Fe(napet)(NCS)]	1/2 → 5/2	174	Masarova et al.[78]	2015
[Fe(napet)(NCS)]·Butanone	1/2 → 5/2	84	Nemec et al.[79]	2015
[Fe(napet)(NCS)]·DMF	1/2 → 5/2	232, 235	Nemec et al.[79]	2015
[Fe(napet)(NCSe)]·DMF	1/2 → 5/2	244	Nemec et al.[79]	2015
[Fe(napet)(NCS)]·DMSO	1/2 → 5/2	127, 138	Nemec et al.[79]	2015
Salicyl Derivatives (salpet family)				
[Fe(5Cl-salpet)(NCS)]	1/2 → 5/2	280	Krüger et al.[8]	2013
[Fe(5Cl-salpet)(NCSe)]	1/2 → 5/2	293	Krüger et al.[8]	2013
[Fe(salpet)(atz)]	1/2 → 5/2	416	Herchel et al.[77]	2013
[Fe(5Cl-salpet)(atz)]	n. a.	334 (T_{min})*	Herchel et al.[77]	2013
[Fe(5Br-salpet)(atz)]	n. a.	362 (T_{min})*	Herchel et al.[77]	2013
[Fe(3,5Br-salpet)(atz)]	n. a.	370 (T_{min})*	Herchel et al.[77]	2013
[Fe(5Br-salpet)(N_3)]·CH_3OH	1/2 → 5/2	143, 140	Krüger et al.[9]	2015
[Fe(5Br-salpet)(NCSe)]	1/2 → 5/2	326, 317	Krüger et al.[9]	2015
[Fe(3OEt-salpet)(NCS)]	1/2 → 5/2	84, 82	Masarova et al.[78]	2015
[Fe(3,5Cl-salpet)(NCSe)]	1/2 → 5/2	123, 99	Krüger et al.[10]	2016

*T_c cannot be estimated from the magnetic data because it is shifted to values above 400 K.

4 Multinuclear Iron Spin Crossover Compounds

4.1 Multinuclear Complexes with Pentadentate Schiff Base Ligands

A couple of dinuclear and trinuclear complexes within the cyanide-bridged Fe^{III} salpet family were summarized and discussed by Boča *et al.* in 2009.[65] Therein they describe the interplay between the spin crossover phenomenon and its interference with the magnetic exchange interactions. Based on earlier results from Salitros *et al.*, Boča presented two Fe^{III} dinuclear complexes bridged by cyanide with a mixed spin behaviour.[75] The first compound $[L^5Fe^{III}(CN)Fe^{III}L^5](ClO_4) \cdot 2H_2O$ (L^5 = salpet) shows a mixture of LL and LH states at low temperatures, as well as an antiferromagnetic interaction between the C-coordinated Fe^{III} in low spin (L) and the N-coordinated Fe^{III} in high spin (H) state. By increasing the temperature the HH state primarily arises. The second compound $[L^5Fe^{III}(CN)Fe^{III}L^5](BPh_4) \cdot 2MeCN$ (L^5 = MeBu-salpet) exhibits a gradual spin crossover. At low temperatures the effective magnetic moment could present the LL pair as a ground state alone. However, the magnetization indicates a very strong asymmetric or eventually antisymmetric exchange.[65] A further trinuclear compound $[\{Fe^{II}(CN)_5(NO)\}\{Fe^{III}(L^5)\}_2] \cdot 3.65H_2O$ (L^5 = salpet) exhibits a high spin molar fraction of 0.45 at 20 K and 0.75 at 300 K. The LH (= HL) state is close to the LL level and both are populated at low temperatures. The magnetic data of two heterometallic trinuclear complexes containing the diamagnetic central units $[Ni^{II}(CN)_4]$ with L^5 = MeBu-salpet (1) and $[Pt^{II}(CN)_4]$ with L^5 = saldptm (2) display both a HH behaviour over the whole temperature range. The fit parameters $g_H = 2.010$ and $J_{HH}/hc = +0.069\ cm^{-1}$ in (1) shows a ferromagnetic exchange coupling ($J_{HH} > 0$) and the ground state is $S = 5$. In contrast, the parameters $g_H = 2.013$ and $J_{HH}/hc = -0.192\ cm^{-1}$ in (2) indicate a change from a ferromagnetic coupling to antiferromagnetic ($J_{HH} < 0$) by cooling which is explained by a more diffuse character of the Pt orbitals.[65]

Moreover, Renz and his co-workers presented a high spin Schiff base dinuclear complex $[(\mu^2\text{-bpyO}_2)\{Fe(BuMe\text{-salpet})\}_2](BPh_4)_2$ with a $\{FeN_3O_2O'\}$ sphere, bridged by a bidentate N-oxide ligand which is based on bipyridine.[80] The observed cooperativity is rather weak and can be explained by the long distance (11.85 Å) between the two iron ions.

A novel dinuclear Co^{III}-CN-Fe^{III} heterometallic system, $[\{Co(3EtO\text{-salpet})\}(\mu\text{-CN})\{Fe(L^4)(Cl)\}]$, was found by Nemec *et al.* in 2013.[81] The molecules form 1D

supramolecular chains in which each complex molecule is connected through intermolecular N-H--Cl hydrogen bonds. In spite of the fact that the magnetic data shows almost no exchange coupling between the Co^{III} low spin and Fe^{III} high spin centres, the building unit is a promising candidate for future Prussian blue analogues.[81]

A series of star-shaped multinuclear heterometallic complexes were also published by Renz *et al.* in 2009.[11,82,83] Among these, a cyanide-bridged pentanuclear complex $[((salpet)Fe^{III}–NC)_4Sn^{IV}]$ shows a multiple spin transition between Fe^{III} in low spin as well in high spin state. Mössbauer results indicate a tautomerism of the Sn centre between Sn^{IV} at room temperature and a partial Sn^{II} at 78 K. While one Sn^{II} centre oxidizes to Sn^{IV}, two Fe^{III} reduce to Fe^{II} and vice versa.[82] A further heptanuclear spin crossover system including cyanide bridges $[(LFe^{III}-X)_6Sb^V]Cl_5$ (X = CN⁻, NCS⁻) exhibits also a multiple spin transition between the Fe^{III} in high and low spin state. In contrast, all Fe^{III} monomers in the thiocyanate-bridged complex show high spin behaviour.[83]

A particular attention is paid to a novel heptanuclear mixed-valence iron spin crossover complex reported by Renz *et al.*[11] The compound $[Fe^{II}\{(CN)Fe^{III}(salpet)\}_6]Cl_2$ is composed of a $[Fe^{II}(CN)_6]^{4-}$ unit, as well as six peripheral monodentate $[Fe^{III}(salpet)]^+$ complexes which are linked by six cyanide bridges (Figure 6). While the diamagnetic Fe^{II} remains in the low spin state, the Fe^{III} centres have the ability to switch thermally. The high-temperature limit of six uncoupled Fe^{III} centres with $S = 5/2$ is $\mu_{eff}/\mu_B = g[6S(S + 1)]^{1/2} = 14.5$. The theoretical value is $\mu_{eff} = 12.1\,\mu_B$ and can be assigned to four high spin, as well as two low spin centres, reached at approximately 100 K (Figure 6). The magnetization $\mu_{eff} = 10.7\,\mu_B$ at 2 K was calculated for three high spin and three low spin states. The Mössbauer results show a 66 % high spin mole fraction at 78 K which is in agreement with the magnetic data. Theoretically, seven spin states might be possible: LLLLLL, LLLLLH, LLLLHH, LLLHHH, LLHHHH, LHHHHH and HHHHHH separated by six energy gaps Δ_i. For the first reference state (LLLLLL) $2^6 = 64$ magnetic energy levels and for the last one (HHHHHH) $6^6 = 46656$ magnetic energy levels with a substantial number of parameters (Δ_i, g_i and J_i) can be considered.[11]
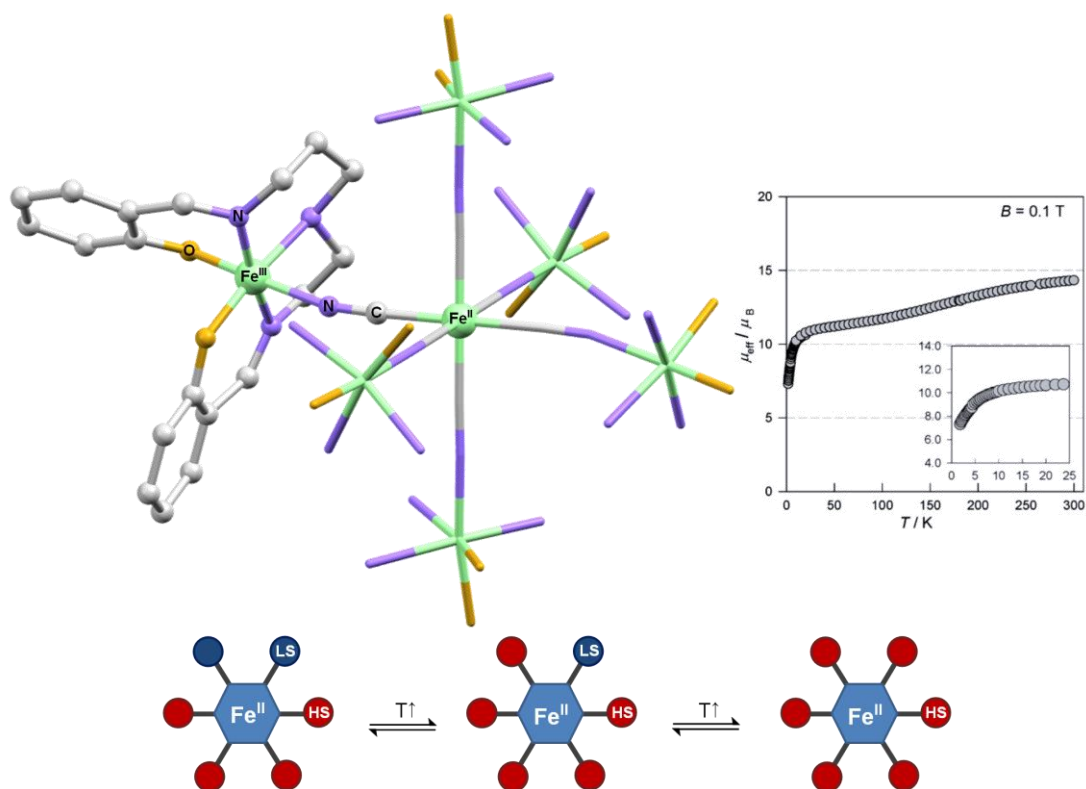
Figure 6. Crystal structure (left) and magnetic data (right) of a mixed-valence heptanuclear $[Fe^{II}\{(CN)Fe^{III}(salpet)\}_6]Cl_2$ spin crossover complex according to reference 11. Hydrogens and five salpet ligands are omitted for clarity. The Fe^{III} units switch sequentially by increasing temperature.

Further three mixed-valence heptanuclear iron complexes with ferromagnetic interactions were reported by Salitros *et al.* in 2012.[84] They presented three clusters constructed by six peripheral monodentate units $[Fe(L^5)]$ involving L^5 for (i) saldien, (ii) 3MeO-salpet and (iii) saldptm. Complex (i) and (ii) show similar magnetic behaviour, wherein all Fe^{III} are in high spin, as well as the central Fe^{II} in low spin state at all temperatures. The magnetic data for cluster (iii) show weak ferromagnetic interactions which were fitted by the Hamiltonian expression resulting in $J/hc = +0.057 \text{ cm}^{-1}$ and $g = 2.01$.[84] At low temperatures the Fe^{III} monomers are in low spin state which corresponds to thirty unpaired electrons. By increasing the temperature, the cluster indicates the presence of an either gradual and incomplete spin crossover or spin-admixing effect.[84]

A multinuclear system containing one of the highest nuclear number within the salpet family has been published by Renz *et al.* in 2007.[85] The dodecanuclear star-shaped complex $[((salpet)Fe^{III}-NC)_5Fe^{II}-CN-Co^{III}(CN-Fe^{III}(salpet))_5]Cl_4$ is constructed by a dinuclear unit $[(NC)_5Fe^{II}-CN-Co^{III}(CN)_5]^{6-}$ cyanide-bridged by ten peripheral mononuclear $[Fe^{III}(salpet)]^+$ complexes. Mössbauer measurements show a

completely high spin behaviour at room temperature which corresponds to the maximum spin multiplicity of $S = 50/2$. At 20 K the cluster is partially both in high spin and in low spin state. According to the author, this dodecanuclear star-shaped compound with its ability to switch between ten and fifty unpaired electrons seems to be on top of novel synergisms.[85]

4.2   Reaction Mechanism in Multinuclear Spin Crossover Complexes

In 2012, Renz *et al.* reported a nonanuclear mixed-valence complex $[Mo^{IV}\{(CN)Fe^{III}(saldptm)\}_8]Cl_4$ containing a central octacyano unit $[Mo(CN)_8]^{4-}$, as well as eight peripheral cyanide-bridged mononuclear $[Fe^{III}(saldptm)]^+$ complexes.[86] They proposed a concerted light-induced and a sequential thermal-induced mechanism which is displayed in the following scheme (Figure 7). According to the author, the thermal-induced spin crossover proceeds stepwise while each peripheral Fe^{III} ion changes from low to high spin state with a maximum spin multiplicity of $S = 40/2$. In contrast, the author describes an electron transfer from Mo^{IV} to Fe^{III} induced by light stimulus (514 nm). This leads to a spin transition of seven peripheral Fe^{III} monomers which follow a concerted mechanism. Mössbauer measurements exhibit reversibility for both mechanisms.

Depending on the type of external stimulus a different mechanism can be assumed resulting in stereospecific products. These mechanisms for multinuclear spin crossover compounds can be compared with reaction mechanisms which follow the Woodward-Hoffmann rules for organic molecules.[87] Further investigations will be carried out by the Renz group to verify the suggested mechanisms.
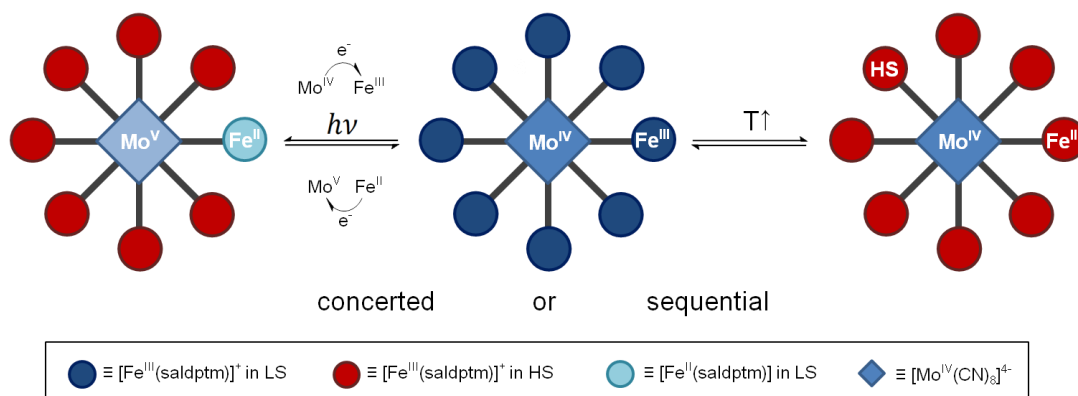
Figure 7. Scheme of a proposed mechanism for a light-induced concerted and thermal-induced sequential spin crossover in a mixed-valence nonanuclear cluster $[Mo^{IV}\{(CN)Fe^{III}(saldptm)\}_8]Cl_4$ according to reference 86.

4.3   Cyanide-Bridged Molecular Square Complexes

Historically, the first cyanide-bridged molecular square complex was published by Schinnerling *et al.* for a Ti_4 square in 1992.[88] Oshio *et al.* found the first iron-copper high spin species in 1999.[15] Since then, a variety of similar homo-, as well as heterometallic structures have been reported.[89] The general design of molecular Prussian blue derivatives comprises a combination of solvated metal cations with cyanometalates. The geometry of the building blocks plays an important role for the cluster formation and the possibility to form cyanide bridges. A number of non-capped cyanometalates are valuable such as $\{[W(CN)_8]^{3-/4}\}$, $\{[Fe(CN)_6]^{3-}\}$, $\{[Ni(CN)_4]^{2-}\}$ and $\{[Pt(CN)_4]^{2-}\}$.[90–98] However, at least one of two sub-units has to be capped to prevent its polymerisation. In addition, the capped metal ions should have at least two available cyanide ligands in cis position with an angle of approximately 90° between the coordination vectors to consider square cyanide-bridged molecules. A general scheme for the synthesis is displayed in Figure 8.
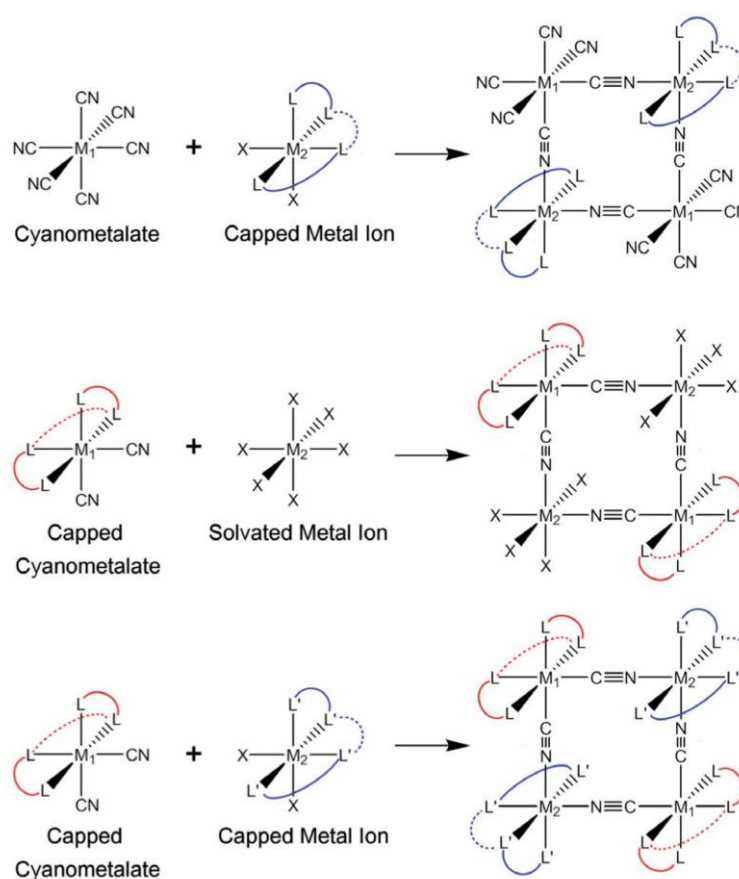
Figure 8. Scheme of three different synthetic methods for cyanide-bridged square complexes. The capping bi- and tridentate ligands are displayed by red and blue lines.[12]

Open-shell transition metal square complexes were reviewed by Oshio *et al.* in 2011 with a particular focus on their synthesis and physical properties.[12] The review deals with a series of bimetallic species such as $[Fe^{II}_2Cu^{II}_2]$ or $[Fe^{III}_2Cu^{II}_2]$ exhibiting a ferromagnetic exchange coupling between Fe^{III}-CN-Cu^{II} across a cyanide bridge. With these two examples Oshio *et al.* proofed at first the isolated controllability of molecular squares by using only bpy[a] as a capping ligand.[15] Square complexes with non capped cyanometalates such as (*meso*-CTH-H_2)[{Ni(*rac*-CTH)}$_2${$Fe^{III}(CN)_6$}$_2$]·$5H_2O$[b] formed by a four-coordinated ligand *rac*-CTH with hexacyanoferrate $[Fe^{III}(CN)_6]^{3+}$ ions have been investigated.[36] Clusters with solvated metal ions have been proven in hetereometallic cyanide-bridged square complexes like {[tp*$Fe^{III}(CN)_3M^{II}(DMF)_4$]$_2(OTf)_2$}·2DMF[c] (M = Mn^{II}, Co^{II}, Ni^{II}).[99,100] Following the scheme of Figure 8, diamagnetic squares containing two capped building blocks {[(bpy)$_2Fe^{II}(CN)_2$]$_2$[M^{II}(bpy)$_2$]$_2$}(PF$_6$)$_4$ with (M = Fe^{II}, Co^{II}, Ru^{II}) have been carried out.[101,102] The first well investigated homometallic spin crossover complex [Fe^{II}_4(μ-CN)$_4$(bpy)$_4$(tpa)$_2$](PF$_6$)$_4$[d] exhibiting a two-step spin transition between LLLL ↔ LLLH ↔ LHLH in the temperature range from 2 to 400 K was published by Oshio *et al.* in 2005.[103] They weakened the ligand field strength of the Fe^{II} centers by replacing the bpy ligand with tpa. As a result, the two opposite Fe^{II} of the [Fe(tpa)(NC)$_2$] unit change their spin state by increasing the temperature.

Within the scope of this thesis, two bimetallic rectangular Ni-Fe clusters with unusual cyanide bridges have been reported by Krüger *et al.* in 2012 (section 6.4).[37] We obtained two types of enantiomeric squares {[Ni(L2$^{R/S}$)]$_2$[Fe^{III}(L1)(CN)$_4$]$_2$}·$6H_2O$·2MeOH in the presence of an asymmetric tetracyanide Fe^{III} complex K_2[Fe^{III}(L1)(CN)$_4$](MeOH)[e], as well as [Ni(L2$^{R/S}$)] involving a chiral bidentate capping ligand L2$^{R/S}$.[f] For both squares ferromagnetic interactions between the nickel and iron ions have been observed. The cyanide-bridge geometry of Ni-N≡C with 104.8° (S-form) and 105.0° (R-form) is unusual and to our knowledge the most acute Ni-N≡C angle observed to date. Ni-N≡C angle in Ni-Fe assemblies are summarised in Table 2. The sharpest angle in any species was in a dinuclear nickel complex displaying angles of 111.2-112.9°.[104]

---

[a] bpy: 2,2´-bipyridine
[b] meso- and racemic-(5,5,7,12,12,14-Hexamethyl-1,4,8,11-tetraazacyclo-tetradecane)Hydrate
[c] tp*: hydrotris(pyrazol-1-yl)borate with dimethyl-derivatised pyrazole groups
[d] tpa: tris(2-pyridylmethyl)amine
[e] HL1: 2,2′-(1H-pyrazole-3,5-diyl)bis-pyridine
[f] L2$^{R/S}$: N-(2-pyridylmethylene)-(R/S)-1-phenylethylamine

Table 2. Comparison of structure properties (∡ of Ni-N≡C) and magnetic coupling constant (J) of cyanide-bridged $Fe^{III}Ni^{II}$ complexes according to reference 105.

Compounds	Ni-N$_{cyano}$ (Å)	Ni-N≡C (°)	J (cm^{-1})	Reference
NiFe-1D	2.103	170.6	3.869	Ni et al.[105]
NiFe-1D-1	2.079	167.5	3.681	Ni et al.[105]
NiFe-1D-2	2.165	163.3	3.641	Ni et al.[105]
NiFe-1D-3	2.096	160	4.244	Ni et al.[105]
NiFe-1D-4	2.11	169.1	9	Atanasov et al.[106]
NiFe-1D-5	2.072	157.7	12.9	Panja et al.[107]
NiFe$_2$-1D-6	2.111	166.8	5.7	Costa et al.[108]
NiFe$_2$-1	2.096	160.2	6.4	Ni et al.[109]
NiFe$_2$-2	2.09	163.2	7.8	Ni et al.[109]
NiFe$_2$-3	2.066	173.2	8.9	Ni et al.[109]
NiFe$_2$-4	2.106	157	6.03	Ni et al.[109]
NiFe$_2$-5	2.039	165.4	2.68	Gu et al.[110]
NiFe$_2$-6	2.096	171.5	17.2	Wang et al.[111]
NiFe$_2$-7	2.096	150	1.3	Li et al.[112]
NiFe$_2$-8	2.049	169.8	7	Li et al.[112]
NiFe$_2$-9	2.156	153.8	1.2	Wang et al.[113]
NiFe$_2$-10	2.1	165.1	2.91	Wang et al.[114]
NiFe$_2$-11	2.054	159.6	4.1	Peng et al.[115]
NiFe$_2$-12	2.173	154.8	0.48	Kang et al.[116]
Ni$_3$Fe$_2$-1	2.05	160.5	5.36	Van Langenberg et al.[117]
Ni$_3$Fe$_2$-2	2.07	157.9	4.3	Berlinguette et al.[118]
Ni$_3$Fe$_2$-3	2.054	164.3	3.3	Berlinguette et al.[118]
Ni$_2$Fe	1.998	176.5	8.62	Panja et al.[107]
Ni$_2$Fe$_3$-1	2.124	148.8	2.1	Kou et al.[119]
Ni$_2$Fe$_3$-2	2.06	168.85	4.84	Gu et al.[120]
Ni$_3$Fe	2.009	171.9	1.2	Yang et al.[32]
Ni$_2$Fe$_2$-1	2.089	156.9	3.06	Panja et al.[107]
Ni$_2$Fe$_2$-2	2.092	167.8	4.52	Liu et al.[121]
Ni$_2$Fe$_2$-3	2.059	170.8	7.36	Liu et al.[121]
Ni$_2$Fe$_2$-4	2.053	169.5	6.5	Li et al.[122]
Ni$_2$Fe$_2$-5	2.053	172.8	10.12	Wu et al.[123]
Ni$_2$Fe$_2$-6	2.074	176.3	4.26	Peng et al.[115]
Ni$_2$Fe$_2$-7	2.073	178.2	4.18	Peng et al.[115]
Ni$_2$Fe$_2$-8	2.075	163.2	6.4	Rodriguez-Dieguez et al.[36]
Ni$_2$Fe$_2$-9	2.105	155.8	8.7	Toma et al.[124]
Ni$_2$Fe$_2$-10	**2.304**	**104.8**	**4.1**	**Krüger et al.[37]**
Ni$_2$Fe$_2$-10	**2.017**	**170.2**	**7.1**	**Krüger et al.[37]**
Ni$_2$Fe$_2$-11	2.035	176.6	5.3	Li et al.[99]
Ni$_4$Fe$_4$-1	2.02	177.4	5.5	Yang et al.[32]
Ni$_4$Fe$_4$-2	2.035	178	6.6	Li et al.[125]
Ni$_4$Fe$_4$-3	2.086	165.7	6.6	Zhang et al.[126]
Ni$_4$Fe$_4$-4	2.068	177.2	6.6	Li et al.[127]

5 Multifunctional Spin Crossover Materials and Potential Applications

The development of multifunctional spin crossover materials is one of the research pursuits nowadays. The focus is particular on the combination of two or more different physical properties involving spin crossover phenomena, even perhaps a synergy between both. The current development of spin crossover applications is multidisciplinary and involves researches from a large number of fields such as inorganic, solid-state and quantum chemistry, condensed matter, statistical and photophysics, as well as nanotechnology.[60] As a result, there are a lot of reviews to this broad topic.[61,128–137] In this part of the thesis, the attention is paid to the combination of spin crossover phenomena with electrical conductivity, liquid crystals and porous materials based partly on the review by Gütlich *et al.* in 2005 and the book by Halcrow in 2013.[5,138]

5.1 Electrical Conductivity and Spin Crossover Properties

The preparation of hybrid materials - displaying metallic conductivity and ferromagnetic properties, as well as field-induced superconducting transitions - is still challenging.[139,140] Those hybrid systems should be sensitive towards external stimuli by using spin crossover phenomena as a function of switching the electrical conductivity.[141–143] For example, Oshio *et al.* presented two novel Fe^{II} complexes containing the neutral and oxidised TTF moieties linked by ethylene bonds.[144] The complex $[Fe^{II}(dppTTF)_2](BPh_4)_2 \cdot Solv^a$ exhibits reversible redox behaviour and thermal spin crossover phenomena. The partial galvanostatic oxidation of $[Fe^{II}(dppTTF)_2]^{2+}$ with $[Ni^{II}(mnt)_2]^-$ leads to the oxidised form $[Fe(dppTTF)_2][Ni(mnt)_2]_2(BF_4) \cdot PhCN^b$. Involving the magnetic and resistivity data, this complex shows an interaction of the spin crossover and conductivity. Djukic and Lemaire reported a spin crossover complex containing $[Fe^{III}(qsal)_2]^c$ which electropolymerises to a hybrid-conducting metallopolythiophene film.[145] The hybrid spin crossover conducting metallopolymer shows temperature variable magnetic and electrical transport properties and displays fascinating variable temperature conductivity profiles.

---

[a] dppTTF: 1-{2-(1,3-dithiol-2ylinene)-1,3-dithiolyl}-2-{2,6-bis(1-pyrazolyl)pyridyl}-ethylene
[b] mnt: maleonitriledithiolate
[c] qsalH: N-(8-quinolyl)salicylaldimine

5.2   Liquid Crystals and Spin Crossover Properties

Strategies to develop multifunctional materials exhibiting interplay between liquid crystal (metallomesogens) transitions and spin crossover have been reviewed by Gütlich *et al.* in 2009.[146] There are two approaches in making metallomesogens: (i) spin crossover centres coordinated by ligands with long alkyl chains and (ii) using 2D cyanide-bridged Hofmann-like clusters with long chain substituents on the pyridine ligands. For (i) non-Hofmann types with a synergy between liquid crystal transitions and spin crossover, Gütlich *et al.* described three classes: (I) metallomesogens with coupling between the spin state and liquid crystal phase transition, (II) metallomesogens with coexisting but uncoupled spin state and liquid crystal phase transition in the same temperature range and (III) metallomesogens with uncoupled spin states in a different temperature range.[146] The latter type of cluster (ii) has been investigated by Gaspar *et al.*,[147] who presented novel 2D heterometallic Fe^{II}-M (M = Ni^{II}, Pd^{II}, Pt^{II}, Ag^{I}, Au^{I}) cyanide-bridged Metal Organic Frameworks (MOFs) exhibiting spin crossover and liquid crystal properties. While some non-alkyl chain compounds exhibit an abrupt hysteretic spin crossover, the substituted analogues (C6, C12, C18) show broad and nonhysteretic magnetic behaviour explained by weaker cooperativity.

5.3   Functional Porous Spin Crossover Materials

According to the latest developments in physico-chemical properties of porous materials, today´s attention focuses on combining these properties with spin crossover effects. An increasing interest especially established in spin crossover MOFs as a promising candidate for chemical sensing devices such as quantitative gas sensors.[6,60,148–150] This type of materials and their synthetic methods offer advantages in tuning of valuable properties like porosity or host-guest chemistry. Recently, Bartual-Murgui *et al.* presented [Fe(bpac)][Pt(CN)$_4$]^a as a spin crossover MOF.[148] They had the ability to measure the absorption of guest molecules in a few hundred ppm by changing the refractive index which is sensitive to the spin state change. The selectivity is linked partly to the spin crossover phenomenon. As a consequence, there is no detection for small molecules with any influence on the ligand field.

---

[a] bpac: bis(4-pyridyl)acetylene

The research is focused on the development of functional porous coordination polymers. Those materials can provide functional microporous frameworks and are able to offer a high degree of selectivity and reversibility in guest-exchange chemistry or heterogeneous catalytic activity.[138] The synthetic method for the construction of such systems is to connect spin crossover units by bridging rigid linear bis-monodentate ligands. The geometry of these units is crucial for the formation of 1D, 2D or 3D polymer systems including solvent molecules within the lattice.[21,151–161] An inclusion or removal of guest molecules such as solvents as a function of the magnetic properties or spin state is one of future research objectives.[138]

5.4   Potential Applications for Spin Crossover Materials

In order of the development of electrical devices and the ongoing scale down process for component sizes, the interest in relevant properties for practical applications of functional molecular materials increased over the last few decades. Highly sensitive and selective molecule-based devices can replace conventional solid-state materials which are limited in size reduction. This is the reason why the reproduction of traditional electronic functions or components such as memories, modulators, rectifiers, transistors, switches and wires on the molecular (or nano) level attracts the attention of researchers today.[162–169]

The application possibilities for functional spin crossover materials were reviewed by Letard *et al.* in 2004,[170] extended by Halcrow in 2013.[5] A critical review was published also by Bousseksou *et al.* in 2011,[60] dealing with chemical synthesis, physical properties, as well as theoretical aspects. Despite the applied development of such functional spin crossover materials there is still a gap towards practical applications. Compared to other classes of functional materials such as organic semiconductors or electro-optical materials, the control of thin film growth and patterning is still limited.[171] Bousseksou *et al.* pointed out that further developments have to be done in (i) techniques for the formation of spin crossover nano-objects and controlling of the crystal growth at the nanoscale, (ii) single-particle spectroscopy for better determination of various properties, (iii) the investigation of the nucleation and growth process during thermal and optical excitation and (iv) addressable nanostructures for applications like gas sensors, displays, nano-thermometers, switchable photonic devices, etc.[60]

Nevertheless, promising materials such as thin films of Fe^{II}tris-triazole 1D chains and 3D Hofmann compounds $[Fe^{II}(pz)[Pt(CN)_4]]^a$ have to be developed further.[172,173] The well investigated mononuclear complex $[Fe^{II}(phen)_2(NCS)_2]^b$ is also still a promising candidate for addressable thin films on a nanoscale.[174–176]

---

[a] pz: pyrazine
[b] phen: 1,10-phenanthroline

References

(1)   Cambi, L.; Szegö, L. *Berichte der Dtsch. Chem. Gesellschaft A B Ser.* **1931**, *64* (10), 2591–2598.

(2)   Cambi, L.; Szegö, L. *Berichte der Dtsch. Chem. Gesellschaft A B Ser.* **1933**, *66* (5), 656–661.

(3)   Cambi, L.; Malatesta, L. *Ber. Dtsch. Chem. Ges.* **1937**, *70* (10), 2067–2078.

(4)   Minkin, V. I. *Pure Applies Chem.* **1999**, *71* (10), 1919–1981.

(5)   Halcrow, M. A. *Spin-Crossover Materials*; Halcrow, M. A., Ed.; John Wiley & Sons Ltd: Oxford, UK, **2013**.

(6)   Gütlich, P.; Gaspar, A. B.; Garcia, Y. *Beilstein J. Org. Chem.* **2013**, *9*, 342–391.

(7)   Gutlich, P.; Goodwin, H. *Spin Crossover in Transition Metal Compounds I-III*; Gutlich, P., Goodwin, H., Eds.; Springer: Berlin, **2004**; Vol. 233-235.

(8)   Krüger, C.; Augustín, P.; Nemec, I.; Trávníček, Z.; Oshio, H.; Boča, R.; Renz, F. *Eur. J. Inorg. Chem.* **2013**, *2013* (5-6), 902–915.

(9)   Krüger, C.; Augustín, P.; Dlháň, L.; Pavlik, J.; Moncol', J.; Nemec, I.; Boča, R.; Renz, F. *Polyhedron* **2015**, *87*, 194–201.

(10)   Krüger, C.; Heyer, L.; Unruh, D.; Preiss, A.; Dlhan, L.; Boca, R.; Renz, F. *Inorganica Chim. Acta* **2016**, submitted.

(11)   Boca, R.; Salitros, I.; Kozísek, J.; Linares, J.; Moncol, J.; Renz, F. *Dalton Trans.* **2010**, *39* (9), 2198–2200.

(12)   Newton, G. N.; Nihei, M.; Oshio, H. *Eur. J. Inorg. Chem.* **2011**, *2011* (20), 3031–3042.

(13)   Ito, A. *J. Chem. Phys.* **1968**, *48* (8), 3597.

(14)   Gunter, M. J.; Berry, K. J.; Murray, K. S. *J. Am. Chem. Soc.* **1984**, *106* (15), 4227–4235.

(15)   Oshio, H.; Tamada, O.; Onodera, H.; Ito, T.; Ikoma, T.; Tero-Kubota, S. *Inorg. Chem.* **1999**, *38* (25), 5686–5689.

(16)   Kou, H.; Gao, S.; Zhang, J.; Wen, G. *Communications* **2001**, *5210* (6), 11809–
         11810.

(17)   Ohba, M.; Usuki, N.; Fukita, N.; Ōkawa, H. *Angew. Chemie* **1999**, *111* (12),
         1911–1914.

(18)   Ohba, M.; Usuki, N.; Fukita, N.; Ōkawa, H. *Angew. Chemie Int. Ed.* **1999**, *38*
         (12), 1795–1798.

(19)   Tanase, S.; Tuna, F.; Guionneau, P.; Maris, T.; Rombaut, G.; Mathonière, C.;
         Andruh, M.; Kahn, O.; Sutter, J. P. *Inorg. Chem.* **2003**, *42* (5), 1625–1631.

(20)   Berlinguette, C. P.; Dragulescu-Andrasi, A.; Sieber, A.; Galán-Mascarós, J.
         R.; Güdel, H.-U.; Achim, C.; Dunbar, K. R. *J. Am. Chem. Soc.* **2004**, *126* (20),
         6222–6223.

(21)   Galet, A.; Niel, V.; Muñoz, M. C.; Real, J. a. *J. Am. Chem. Soc.* **2003**, *125*,
         14224–14225.

(22)   Niel, V.; Thompson, A. L.; Goeta, A. E.; Enachescu, C.; Hauser, A.; Galet, A.;
         Muñoz, M. C.; Real, J. a. *Chem. - A Eur. J.* **2005**, *11* (7), 2047–2060.

(23)   Real, J. A.; Gaspar, A. B.; Niel, V.; Muñoz, M. C. *Coord. Chem. Rev.* **2003**,
         236 (1-2), 121–141.

(24)   Lefebvre, J.; Batchelor, R. J.; Leznoff, D. B. *J. Am. Chem. Soc.* **2004**, *126*
         (49), 16117–16125.

(25)   Rombaut, G.; Golhen, S.; Ouahab, L.; Mathonière, C.; Kahn, O. *J. Chem. Soc.
         Dalt. Trans.* **2000**, *2* (20), 3609–3614.

(26)   Arimoto, Y.; Ohkoshi, S. I.; Zhong, Z. J.; Seino, H.; Mizobe, Y.; Hashimoto,
         K. *J. Am. Chem. Soc.* **2003**, *125* (31), 9240–9241.

(27)   Mathonière, C.; Podgajny, R.; Guionneau, P.; Labrugere, C.; Sieklucka, B.
         Chem. Mater. **2005**, *17* (2), 442–449.

(28)   Herrera, J. M.; Marvaud, V.; Verdaguer, M.; Marrot, J.; Kalisz, M.;
         Mathoniere, C. *Angew. Chemie* **2004**, *116* (41), 5584–5587.

(29)   Herrera, J. M.; Marvaud, V.; Verdaguer, M.; Marrot, J.; Kalisz, M.;
         Mathoniere, C. *Angew. Chemie Int. Ed.* **2004**, *43* (41), 5468–5471.

(30)   Ibrahim, M. S.; Werida, A. H.; Etaiw, S. E. H. *Phosphorus. Sulfur. Silicon
         Relat. Elem.* **2004**, *179* (12), 2441–2451.

(31)   Yoshikawa, H.; Nishikiori, S. *Dalton Trans.* **2005**, 18, 3056–3064.

(32)   Yang, J. Y.; Shores, M. P.; Sokol, J. J.; Long, J. R. *Inorg. Chem.* **2003**, *42* (5), 1403–1419.

(33)   Imai, H.; Inoue, K.; Kikuchi, K.; Yoshida, Y.; Ito, M.; Sunahara, T.; Onaka, S. *Angew. Chemie Int. Ed.* **2004**, *43* (42), 5618–5621.

(34)   Coronado, E.; Giménez-Saiz, C.; Martínez-Agudo, J. .; Nuez, a; Romero, F. .; Stoeckli-Evans, H. *Polyhedron* **2003**, *22* (14-17), 2435–2440.

(35)   Inoue, K.; Ohkoshi, S.-I.; Imai, H. In *Magnetism: Molecules to Materials V*; Wiley-VCH Verlag GmbH & Co. KGaA: Weinheim, FRG, **2005**; pp 41–70.

(36)   Rodriguez-Dieguez, A.; Kivekas, R.; Sillanpaa, R.; Cano, J.; Lloret, F.; Mckee, V.; Stoeckli-Evans, H.; Colacio, E. *Inorg. Chem.* **2006**, *45* (26), 10537–10551.

(37)   Krüger, C.; Sato, H.; Matsumoto, T.; Shiga, T.; Newton, G. N.; Renz, F.; Oshio, H. *Dalt. Trans.* **2012**, *41* (37), 11270.

(38)   Ewald, A. H.; Martin, R. L.; Ross, I. G.; White, A. H. *Proc. R. Soc. A Math. Phys. Eng. Sci.* **1964**, *280* (1381), 235–257.

(39)   Figgis, B. N.; Toogood, G. E. *J. Chem. Soc. Dalt. Trans.* **1972**, *19* (19), 2177.

(40)   Konig, E.; Madeja, K. *Inorg. Chem.* **1967**, *6*, 48–55.

(41)   Ivanov, E. V.; Zelentsov, V. V.; Gerbeleu, N. V.; Ablov, A. V. *Dokl. Akad. Nauk SSSR* **1970**, *191*, 827–830.

(42)   Matsumoto, N.; Ohta, S.; Yoshimura, C.; Ohyoshi, A.; Kohata, S.; Okawa, H.; Maeda, Y. *J. Chem. Soc. Dalt. Trans.* **1985**, *2575* (12), 2575.

(43)   Oshio, H.; Takashima, Y. **1983**, 2684–2689.

(44)   Petty, R. H.; Dose, E. V; Tweedle, M. F.; Wilson, L. J. *Inorg. Chem.* **1978**, *17* (4), 1064–1071.

(45)   Kennedy, B. J.; McGrath, A. C.; Murray, K. S.; Skelton, B. W.; White, A. H. *Inorg. Chem.* **1987**, *26* (4), 483–495.

(46)   Real, A.; Zarembowitch, J.; Kahn, O.; Solanslb, X. *Inorg. Chem.* **1987**, *26*, 2939–2943.

(47)   Vos, G.; De Graaff, R. a. G.; Haasnoot, J. G.; Van der Kraan, A. M.; De Vaal,
       P.; Reedijk, J. *Inorg. Chem.* **1984**, *23* (18), 2905–2910.

(48)   Haasnoot, J. G. *Coord. Chem. Rev.* **2000**, *202*, 131–185.

(49)   Breuning, E.; Ruben, M.; Lehn, J.-M.; Renz, F.; Garcia, Y.; Ksenofontov, V.;
       Gütlich, P.; Wegelius, E.; Rissanen, K. *Angew. Chemie Int. Ed.* **2000**, *39* (14),
       2504–2507.

(50)   Ruben, M.; Breuning, E.; Lehn, J. M.; Ksenofontov, V.; Renz, F.; Gütlich, P.;
       Vaughan, G. B. M. *Chem. - A Eur. J.* **2003**, *9* (18), 4422–4429.

(51)   Duriska, M. B.; Neville, S. M.; Moubaraki, B.; Cashion, J. D.; Halder, G. J.;
       Chapman, K. W.; Balde, C.; Létard, J.-F.; Murray, K. S.; Kepert, C. J.; Batten,
       S. R. *Angew. Chemie Int. Ed.* **2009**, *48* (14), 2549–2552.

(52)   Murray, K. S.; Oshio, H.; Real, J. A. *Eur. J. Inorg. Chem.* **2013**, *2013* (5-6),
       577–580.

(53)   Ozin, G. A.; Arsenault, A.; Cademartiri, L. *Nanochemistry: a chemical
       approach to nanomaterials – 2nd ed.*; **2009**; Vol. 12.

(54)   Volatron, F.; Catala, L.; Rivière, E.; Gloter, A.; Stéphan, O.; Mallah, T. *Inorg.
       Chem.* **2008**, *47* (15), 6584–6586.

(55)   Gaspar, A. B.; Seredyuk, M.; Gütlich, P. *J. Mol. Struct.* **2009**, *924-926* (C), 9–
       19.

(56)   Burda, C.; Chen, X.; Narayanan, R.; El-Sayed, M. A. *Chem. Rev.* **2005**, *105*
       (4), 1025–1102.

(57)   Molnár, G.; Cobo, S.; Real, J. A.; Carcenac, F.; Daran, E.; Vieu, C.;
       Bousseksou, A. *Adv. Mater.* **2007**, *19* (16), 2163–2167.

(58)   Boldog, I.; Gaspar, A. B.; Martínez, V.; Pardo-Ibañez, P.; Ksenofontov, V.;
       Bhattacharjee, A.; Gütlich, P.; Real, J. a. *Angew. Chemie - Int. Ed.* **2008**, *47*
       (34), 6433–6437.

(59)   Niel, V.; Martinez-Agudo, J. M.; Muñoz, M. C.; Gaspar, a. B.; Real, J. a.
       Inorg. Chem. **2001**, *40* (16), 3838–3839.

(60)   Bousseksou, A.; Molnár, G.; Salmon, L.; Nicolazzi, W. *Chem. Soc. Rev.* **2011**,
       40 (6), 3313–3335.

(61)   Bousseksou, A.; Molnar, G.; Matouzenko, G. *Eur. J. Inorg. Chem.* **2004**, *2004* (22), 4353–4369.

(62)   Gütlich, P. *Eur. J. Inorg. Chem.* **2013**, *2013* (5-6), 581–591.

(63)   Šalitroš, I.; Madhu, N. T.; Boča, R.; Pavlik, J.; Ruben, M. *Monatshefte fur Chemie* **2009**, *140* (7), 695–733.

(64)   Boča, R.; Linert, W. In *Molecular Magnets Recent Highlights*; Springer Vienna: Vienna, **2002**; Vol. 1, pp 83–100.

(65)   Boča, R.; Nemec, I.; Šalitroš, I.; Pavlik, J.; Herchel, R.; Renz, F. *Pure Appl. Chem.* **2009**, *81* (8), 1357–1383.

(66)   Pavlik, J.; Nicolazzi, W.; Molnár, G.; Boča, R.; Bousseksou, A. *Eur. Phys. J. B* **2013**, *86* (6), 292.

(67)   Pavlik, J.; Boča, R. *Eur. J. Inorg. Chem.* **2013**, 697–709.

(68)   Boča, R. *Theoretical Foundations of Molecular Magnetism*; Boča, R., Ed.; Elsevier B.V., **1999**.

(69)   Schiff, H. *Justus Liebigs Ann. Chem.* **1864**, *131* (1), 118–119.

(70)   Qin, W.; Long, S.; Panunzio, M.; Biondi, S. *Molecules* **2013**, *18* (10), 12264–12289.

(71)   Abu-Dief, A. M.; Mohamed, I. M. A. *Beni-Suef Univ. J. Basic Appl. Sci.* **2015**, *4* (2), 119–133.

(72)   Koningsbruggen, P. J.; Maeda, Y.; Oshio, H. In *Spin Crossover in Transition Metal Compounds I*; **2004**; Vol. 1, pp 259–324.

(73)   Nihei, M.; Shiga, T.; Maeda, Y.; Oshio, H. *Coord. Chem. Rev.* **2007**, *251* (21-24), 2606–2621.

(74)   Maeda, Y.; Noda, Y.; Oshio, H.; Takashim. *Hyperfine Interact.* **1994**, *84*, 471–476.

(75)   Šalitroš, I.; Boča, R.; Dlháň, L.; Gembický, M.; Kožíšek, J.; Linares, J.; Moncol', J.; Nemec, I.; Perašínová, L.; Renz, F.; Svoboda, I.; Fuess, H. *Eur. J. Inorg. Chem.* **2009**, *2009* (21), 3141–3154.

(76)   Nemec, I.; Herchel, R.; Boča, R.; Trávníček, Z.; Svoboda, I.; Fuess, H.; Linert, W. *Dalton Trans.* **2011**, *40* (39), 10090–10099.

(77)   Herchel, R.; Trávníček, Z. *Dalt. Trans.* **2013**, *42* (46), 16279.

(78)   Masárová, P.; Zoufalý, P.; Moncol, J.; Nemec, I.; Pavlik, J.; Gembický, M.; Trávníček, Z.; Boča, R.; Šalitroš, I. *New J. Chem.* **2015**, *39* (1), 508–519.

(79)   Nemec, I.; Herchel, R.; Trávníček, Z. *Dalt. Trans.* **2015**, *44* (10), 4474–4484.

(80)   Nemec, I.; Boča, R.; Gembický, M.; Dlháň, L.; Herchel, R.; Renz, F. *Inorganica Chim. Acta* **2009**, *362* (13), 4754–4759.

(81)   Nemec, I.; Zoufalý, P.; Herchel, R.; Trávníček, Z. *Inorg. Chem. Commun.* **2013**, *35*, 50–53.

(82)   Renz, F.; Jung, S.; Klein, M.; Menzel, M.; Thünemann, A. F. *Polyhedron* **2009**, *28* (9-10), 1818–1821.

(83)   Renz, F.; Zaba, C.; Roßberg, L.; Jung, S.; Klein, M.; Klingelhöfer, G.; Wünsche, a.; Reinhardt, S.; Menzel, M. *Polyhedron* **2009**, *28* (9-10), 2036–2038.

(84)   Šalitroš, I.; Boča, R.; Herchel, R.; Moncol, J.; Nemec, I.; Ruben, M.; Renz, F. *Inorg. Chem.* **2012**, *51* (23), 12755–12767.

(85)   Renz, F.; Hill, D.; Klein, M.; Hefner, J. *Polyhedron* **2007**, *26* (9–11), 2325–2329.

(86)   Saadat, R.; Renz, F. *Möss. Eff. Ref. Data J.* **2012**, *35* (2), 216–237.

(87)   Woodward, R. B.; Hoffmann, R. *J. Am. Chem. Soc.* **1965**, *87* (1959), 395–397.

(88)   Schinnerling, P.; Thewalt, U. *J. Organomet. Chem.* **1992**, *431* (1), 41–45.

(89)   Shatruk, M.; Avendano, C.; Dunbar, K. R. In *Progress in Inorganic Chemistry*; Kenneth D. Karlin, Ed.; John Wiley & Sons Ltd, **2009**; pp 155–334.

(90)   Wang, Z.-X.; Li; Wang, T.; Li, Y.; Ohkoshi, S.; Hashimoto, K.; Song, Y.; You, X.-Z. *Inorg. Chem.* **2007**, *46* (26), 10990–10995.

(91)   Zhao, H.; Shatruk, M.; Prosvirin, A. V.; Dunbar, K. R. *Chem. - A Eur. J.* **2007**, *13* (23), 6573–6589.

(92)   Venkatakrishnan, T. S.; Desplanches, C.; Rajamani, R.; Guionneau, P.;
       Ducasse, L.; Ramasesha, S.; Sutter, J.-P. *Inorg. Chem.* **2008**, *47* (11), 4854–
       4860.

(93)   Korzeniak, T.; Desplanches, C.; Podgajny, R.; Giménez-Saiz, C.; Stadnicka,
       K.; Rams, M.; Sieklucka, B. *Inorg. Chem.* **2009**, *48* (7), 2865–2872.

(94)   Podgajny, R.; Korzeniak, T.; Przychodzeń, P.; Gimenez-Saiz, C.; Rams, M.;
       Kwaśniak, M.; Sieklucka, B. *Eur. J. Inorg. Chem.* **2010**, *2010* (26), 4166–
       4174.

(95)   Berlinguette, C. P.; Smith, J. a.; Galán-Mascarós, J. R.; Dunbar, K. R.
       Comptes Rendus Chim. **2002**, *5* (10), 665–672.

(96)   Toma, L. M.; Lescouezec, R.; Cangussu, D.; Llusar, R.; Mata, J.; Spey, S.;
       Thomas, J. A.; Lloret, F.; Julve, M. *Inorg. Chem. Commun.* **2005**, *8* (4), 382–
       385.

(97)   Jiang, L.; Lu, T.-B.; Feng, X.-L. *Inorg. Chem.* **2005**, *44* (20), 7056–7062.

(98)   Falvello, L. R.; Tomás, M. *Chem. Commun.* **1999**, 3, 273–274.

(99)   Li, D.; Parkin, S.; Wang, G.; Yee, G. T.; Prosvirin, a. V.; Holmes, S. M.
       Inorg. Chem. **2005**, *44* (14), 4903–4905.

(100) Li, D.; Parkin, S.; Wang, G.; Yee, G. T.; Holmes, S. M. *Inorg. Chem.* **2006**, *45*
       (5), 1951–1959.

(101) Oshio, H.; Onodera, H.; Tamada, O.; Mizutani, H.; Hikichi, T.; Ito, T. *Chem. -
       A Eur. J.* **2000**, *6* (14), 2523–2530.

(102) Oshio, H.; Onodera, H.; Ito, T. *Chemistry (Easton).* **2003**, *9* (16), 3946–3950.

(103) Nihei, M.; Ui, M.; Yokota, M.; Han, L.; Maeda, A.; Kishida, H.; Okamoto, H.;
       Oshio, H. *Angew. Chemie - Int. Ed.* **2005**, *44* (40), 6484–6487.

(104) Meyer, F.; Winter, R. F.; Kaifer, E. *Inorg. Chem.* **2001**, *40* (18), 4597–4603.

(105) Ni, W.-W.; Chen, X.; Cui, A.-L.; Liu, C.-M.; Kou, H.-Z. *Polyhedron* **2014**,
       81, 450–456.

(106) Atanasov, M.; Comba, P.; Förster, S.; Linti, G.; Malcherek, T.; Miletich, R.;
       Prikhod'ko, A. I.; Wadepohl, H. *Inorg. Chem.* **2006**, *45* (19), 7722–7735.

(107) Panja, A.; Guionneau, P.; Jeon, I.-R.; Holmes, S. M.; Clerac, R.; Mathoniere, C. *Inorg. Chem.* **2012**, *51* (22), 12350–12359.

(108) Costa, V.; Lescouëzec, R.; Vaissermann, J.; Herson, P.; Journaux, Y.; Araujo, M. H.; Clemente-Juan, J. M.; Lloret, F.; Julve, M. *Inorganica Chim. Acta* **2008**, *361* (14-15), 3912–3918.

(109) Ni, Z.; Kou, H.; Zhao, Y.; Zheng, L.; Wang, R.; Cui, A.; Sato, O. *Inorg. Chem.* **2005**, *44* (6), 2050–2059.

(110) Gu, J.-Z.; Jiang, L.; Tan, M.-Y.; Lu, T.-B. *J. Mol. Struct.* **2008**, *890* (1-3), 24–30.

(111) Wang, S.; Zuo, J.-L.; Zhou, H.-C.; Song, Y.; Gao, S.; You, X.-Z. *Eur. J. Inorg. Chem.* **2004**, 3681–3687.

(112) Li, D.; Clérac, R.; Parkin, S.; Wang, G.; Yee, G. T.; Holmes, S. M. *Inorg. Chem.* **2006**, *45* (14), 5251–5253.

(113) Wang, S.; Zuo, J.-L.; Zhou, H.-C.; Song, Y.; You, X.-Z. *Inorganica Chim. Acta* **2005**, *358* (6), 2101–2106.

(114) Wang, C. F.; Gu, Z. G.; Lu, X. M.; Zuo, J. L.; You, X. Z. *Inorg. Chem.* **2008**, *47* (18), 7957–7959.

(115) Peng, Y.-H.; Meng, Y.-F.; Hu, L.; Li, Q.-X.; Li, Y.-Z.; Zuo, J.-L.; You, X.-Z. *Inorg. Chem.* **2010**, *49* (4), 1905–1912.

(116) Kang, L.-C.; Chen, X.; Wang, C.-F.; Zhou, X.-H.; Zuo, J.-L.; You, X.-Z. *Inorganica Chim. Acta* **2009**, *362* (15), 5195–5202.

(117) VanLangenberg, K.; VanLangenberg, K.; Batten, S. R.; Batten, S. R.; Berry, K. J.; Berry, K. J.; Hockless, D. C. R.; Hockless, D. C. R.; Moubaraki, B.; Moubaraki, B.; Murray, K. S.; Murray, K. S. *Inorg. Chem.* **1997**, *36* (22), 5006–5015.

(118) Berlinguette, C. P.; Galán-Mascarós, J. R.; Dunbar, K. R. *Inorg. Chem.* **2003**, *42* (11), 3416–3422.

(119) Kou, H. Z.; Zhou, B. C.; Liao, D. Z.; Wang, R. J.; Li, Y. *Inorg. Chem.* **2002**, *41* (25), 6887–6891.

(120) Gu, Z.-G.; Yang, Q.-F.; Liu, W.; Song, Y.; Li, Y.-Z.; Zuo, J.-L.; You, X.-Z. *Inorg. Chem.* **2006**, *45* (22), 8895–8901.

(121) Liu, W.; Wang, C.; Li, Y.; Zuo, J.; You, X. *Inorg. Chem.* **2006**, *45* (25), 10058–10065.

(122) Li, D.; Clérac, R.; Wang, G.; Yee, G. T.; Holmes, S. M. *Eur. J. Inorg. Chem.* **2007**, *2007* (10), 1341–1346.

(123) Wu, D.; Zhang, Y.; Huang, W.; Sato, O. *Dalton Trans.* **2010**, *39* (23), 5500–5503.

(124) Toma, L.; Toma, L. M.; Lescouezec, R.; Armentano, D.; De Munno, G.; Andruh, M.; Cano, J.; Lloret, F.; Julve, M. *Dalt. Trans.* **2005**, No. 8, 1357.

(125) Li, D.; Parkin, S.; Wang, G.; Yee, G. T.; Clérac, R.; Wernsdorfer, W.; Holmes, S. M. *J. Am. Chem. Soc.* **2006**, *128* (13), 4214–4215.

(126) Zhang, Y.; Mallik, U. P.; Rath, N.; Yee, G. T.; Clérac, R.; Holmes, S. M. *Chem. Commun.* **2010**, *46* (27), 4953.

(127) Li, D.; Parkin, S.; Clérac, R.; Holmes, S. M. *Inorg. Chem.* **2006**, *45* (19), 7569–7571.

(128) Real, J. A.; Gaspar, A. B.; Muñoz, M. C. *Dalton Trans.* **2005**, 12, 2062–2079.

(129) Gaspar, A. B.; Munoz, M. C.; Real, J. A. *J. Mater. Chem.* **2006**, *16* (26), 2522–2533.

(130) Browne, W. R.; McGarvey, J. J. *Coord. Chem. Rev.* **2006**, *250*, 1696–1709.

(131) Letard, J.-F. *J. Mater. Chem.* **2006**, *16* (26), 2550.

(132) Sato, O.; Tao, J.; Zhang, Y.-Z. Z. *Angew. Chemie - Int. Ed.* **2007**, *46* (13), 2152–2187.

(133) Halcrow, M. a. *Polyhedron* **2007**, *26* (14), 3523–3576.

(134) Halcrow, M. a. *Chem. Soc. Rev.* **2008**, *37* (2), 278–289.

(135) Murray, K. S. *Eur. J. Inorg. Chem.* **2008**, *2008* (20), 3101–3121.

(136) Brooker, S.; Kitchen, J. A. *Dalt. Trans.* **2009**, *9226* (36), 7331.

(137) Wolny, J. a.; Paulsen, H.; Trautwein, A. X.; Schünemann, V. *Coord. Chem. Rev.* **2009**, *253*, 2423–2431.

(138) Gaspar, A. B.; Ksenofontov, V.; Seredyuk, M.; Gütlich, P. *Coord. Chem. Rev.* **2005**, *249* (23), 2661–2676.

(139) Coronado, E.; Galán-Mascarós, J. R.; Gómez-García, C. J.; Laukhin, V. *Nature* **2000**, *408* (6811), 447–449.

(140) Uji, S.; Shinagawa, H.; Terashima, T.; Yakabe, T.; Terai, Y.; Tokumoto, M.; Kobayashi, a; Tanaka, H.; Kobayashi, H. *Nature* **2001**, *410* (6831), 908–910.

(141) Murata, K.; Kagoshima, S.; Yasuzuka, S.; Yoshino, H.; Kondo, R. *J. Phys. Soc. Japan* **2006**, *75* (5), 1–15.

(142) Hünig, S.; Sinzger, K.; Jopp, M.; Bauer, D.; Bietsch, W.; von Schütz, J. U.; Wolf, H. C. *Angew. Chemie Int. Ed. English* **1992**, *31* (7), 859–862.

(143) Aonuma, S.; Sawa, H.; Kato, R.; Kobayashi, H. *Chem. Lett.* **1993**, 3, 513–516.

(144) Nihei, M.; Takahashi, N.; Nishikawa, H.; Oshio, H. *Dalt. Trans.* **2011**, *40* (10), 2154–2156.

(145) Djukic, B.; Lemaire, M. T. *Inorg. Chem.* **2009**, *48* (22), 10489–10491.

(146) Gaspar, A. B.; Seredyuk, M.; Gütlich, P. *Coord. Chem. Rev.* **2009**, *253* (19-20), 2399–2413.

(147) Seredyuk, M.; Gaspar, a. B.; Ksenofontov, V.; Galyametdinov, Y.; Verdaguer, M.; Villain, F.; Gütlich, P. *Inorg. Chem.* **2010**, *49*, 10022–10031.

(148) Bartual-Murgui, C.; Akou, A.; Thibault, C.; Molnár, G.; Vieu, C.; Salmon, L.; Bousseksou, A. *J. Mater. Chem. C* **2015**, *3* (6), 1277–1285.

(149) Ohba, M.; Yoneda, K.; Kitagawa, S. *CrystEngComm* **2010**, *12* (1), 159.

(150) Kepert, C. J. *Chem. Commun. (Camb).* **2006**, 7, 695–700.

(151) Kahn, O. *Science.* **1998**, *279* (5347), 44–48.

(152) Krober, J.; Audiere, J. P.; Claude, R.; Codjovi, E.; Kahn, O.; Haasnoot, J. G.; Groliere, F.; Jay, C.; Bousseksou, A.; Linares, J.; Varret, F.; Gonthiervassal, A. *Chem. Mater.* **1994**, *6* (8), 1404–1412.

(153) Garcia, Y.; van Koningsbruggen, P. J.; Lapouyade, R.; Rabardel, L.; Kahn, O.; Wieczorek, M.; Bronisz, R.; Ciunik, Z.; Rudolf, M. F. *Comptes Rendus l'Académie des Sci. - Ser. IIC - Chem.* **1998**, *1* (8), 523–532.

(154) Vreugdenhil, W.; Van Diemen, J. H.; De Graaff, R. A. G.; Haasnoot, J. G.; Reedijk, J.; Van Der Kraan, A. M.; Kahn, O.; Zarembowitch, J. *Polyhedron* **1990**, *9* (24), 2971–2979.

(155) Real, J. A.; Andrés, E.; Muñoz, M. C.; Julve, M.; Granier, T.; Bousseksou, A.; Varret, F. *Science.* **1995**, *268* (5208), 265–267.

(156) Halder, G. J.; C.J. Kepert, B. Moubaraki, K.S. Murray, J. D. C. *Science.* **2002**, *298* (5599), 1762–1765.

(157) Moliner, N.; Munoz, C.; Letard, S.; Solans, X.; Menendez, N.; Goujon, a.; Varret, F.; Real, J. a. *Inorg. Chem.* **2000**, *39* (1), 5390–5393.

(158) Garcia, Y.; Kahn, O.; Rabardel, L.; Chansou, B.; Salmon, L.; Tuchagues, J. P. *Inorg. Chem.* **1999**, *38* (21), 4663–4670.

(159) van Koningsbruggen, P. J.; Garcia, Y.; Kooijman, H.; Spek, A. L.; Haasnoot, J. G.; Kahn, O.; Linares, J.; Codjovi, E.; Varret, F. *J. Chem. Soc. Dalt. Trans.* **2001**, 4, 466–471.

(160) Grunert, C. M.; Schweifer, J.; Weinberger, P.; Linert, W.; Mereiter, K.; Hilscher, G.; Muller, M.; Wiesinger, G.; Van Koningsbruggen, P. J. *Inorg. Chem.* **2004**, *43* (1), 155–165.

(161) Niel, V.; Thompson, A. L.; Muñoz, M. C.; Galet, A.; Goeta, A. E.; Real, J. a. *Angew. Chemie - Int. Ed.* **2003**, *42*, 3760–3763.

(162) Aviram, A.; Ratner, M. A. *Chem. Phys. Lett.* **1974**, *29* (2), 277–283.

(163) Chen, J.; Reed, M. A.; Rawlett, A. M.; Tour, J. M. *Science.* **1999**, *286* (5444), 1550–1552.

(164) Metzger, R. M. *Acc. Chem. Res.* **1999**, *32* (11), 950–957.

(165) Balzani, V.; Credi, A.; Raymo, F. M.; Stoddart, J. F. *Artificial Molecular Machines*; **2000**; Vol. 39.

(166) Huang, Y.; Duan, X.; Cui, Y.; Lauhon, L. J.; Kim, K. H.; Lieber, C. M. *Science (80-.).* **2001**, *294* (5545), 1313–1317.

(167) Raymo, F. M. *Adv. Mater.* **2002**, *14* (6), 401–414.

(168) Balzani, V.; Credi, A.; Venturi, M. *Chem. - A Eur. J.* **2002**, *8* (24), 5524–5532.

(169) Carroll, R. L.; Gorman, C. B. *Angew. Chemie - Int. Ed.* **2002**, *41* (23), 4378–4400.

(170) Létard, J.-F.; Guionneau, P.; Goux-Capes, L. In *Spin Crossover in Transition Metal Compounds III*; Gutlich, P., Goodwin, H., Eds.; Springer: Berlin, **2004**; Vol. 1, pp 221–249.

(171) Cavallini, M. *Phys. Chem. Chem. Phys.* **2012**, *14* (34), 11867.

(172) Cobo, S.; Molnár, G.; Real, J. A.; Bousseksou, A. *Angew. Chemie Int. Ed.* **2006**, *45* (35), 5786–5789.

(173) Muñoz, M. C.; Real, J. a. *Coord. Chem. Rev.* **2011**, *255*, 2068–2093.

(174) Cavallini, M.; Bergenti, I.; Milita, S.; Ruani, G.; Salitros, I.; Qu, Z. R.; Chandrasekar, R.; Ruben, M. *Angew. Chemie - Int. Ed.* **2008**, *47* (45), 8596–8600.

(175) Shi, S.; Schmerber, G.; Arabski, J.; Beaufrand, J.-B.; Kim, D. J.; Boukari, S.; Bowen, M.; Kemp, N. T.; Viart, N.; Rogez, G.; Beaurepaire, E.; Aubriet, H.; Petersen, J.; Becker, C.; Ruch, D. *Appl. Phys. Lett.* **2009**, *95* (4), 043303.

(176) Miyamachi, T.; Gruber, M.; Davesne, V.; Bowen, M.; Boukari, S.; Joly, L.; Scheurer, F.; Rogez, G.; Yamada, T. K.; Ohresser, P.; Beaurepaire, E.; Wulfhekel, W. *Nat. Commun.* **2012**, *3*, 938.

6   Results and Discussion

6.1   Spin Crossover in Iron(III) Complexes with Pentadentate Schiff Base Ligands and Pseudohalido Coligands

Christoph Krüger, Peter Augustín, Ivan Nemec, Zdenek Trávnícek, Hiroki Oshio, Roman Boča and Franz Renz

The final publication is available at
http://onlinelibrary.wiley.com/doi/10.1002/ejic.201201038/abstract;jsessionid=118F
C787FFDA2BE1235F91F99162B3CF.f02t02.

Preface

Novel Iron(III) mononuclear complexes involving pentadentate Schiff base ligands and chloride, azide, cyanide, cyanate, thiocyanate or selenocyanate coligands were reported in the present full paper published in the *European Journal of Inorganic Chemistry* in 2013. The obtained results were gained together in cooperation with Prof. Dr. Roman Boča and Peter Augustin from Slovak University of Technology in Bratislava. They designed six novel naphtyl derivative complexes with a pentadentate ligand derived from a Schiff base condensation of 2-hydroxyacetonaphthone analogues (L^1, L^2) whereby two of them, $[Fe(L^1)(NCS)]$ (1a) and α-$[Fe(L^2)(NCS)]$ (2b), show a spin crossover from $S = 3/2 \rightarrow 5/2$ at $T_c = 42$ K (1a) and from $S = 1/2 \rightarrow 5/2$ at $T_c = 114$ K (2b). The author of this thesis designed five novel salicyl derivative complexes with a pentadentate ligand derived from a Schiff base condensation of 5Cl-salicylaldehyde (L^3). $[Fe(L^3)(NCS)]$ (3d) and $[Fe(L^3)(NCSe)]$ (3e) exhibit a spin crossover both from $S = 1/2 \rightarrow 5/2$ at $T_c = 280$ (3d) and $T_c = 293$ K (3e). The results have been partly carried out in the group of Prof. Dr. Hiroki Oshio from Tsukuba University in Japan.

All single-crystal X-ray measurements have been done partly by Prof. RNDr. Zdenek Travnicek and Dr. Ivan Nemec from Palacky University in Czech Republic, by the author of this thesis in the group of Prof. Dr. Hiroki Oshio and with the help of Dr. Michael Wiebcke from Leibniz Universität Hannover.

Prof. Dr. Roman Boča, Dr. Ivan Nemec, Peter Augustin and the author of this thesis wrote the initial manuscript and refined it together with Prof. Dr. Franz Renz.

FULL PAPER

Spin Crossover in Iron(III) Complexes with Pentadentate Schiff Base Ligands and Pseudohalido Coligands

Christoph Krüger,[a] Peter Augustín,[b] Ivan Nemec,[c] Zdeněk Trávníček,[c] Hiroki Oshio,[d] Roman Boča,*[b,e] and Franz Renz*[a]

Iron(III) mononuclear complexes that involve pentadentate Schiff base ligands and chlorido, azido, cyanido, cyanato, thiocyanato, or selenocyanato coligands were synthesized, structurally characterized, and subjected to a magnetochemical investigation. The Schiff bases were derived either from 5-chlorosalicylaldehyde or the 2-hydroxyacetonaphthone analogues by using an asymmetric 1,6-diamino-4-azahexane. A polymorphism that originated from different pentadentate ligand conformations on the iron center or different arrangements of noncovalent contacts was detected for the thiocyanato complexes. The central iron(III) atoms are mostly in the high-spin states, except for that with the coordinated cyanido ligand. Four complexes that contain the thiocyanato or selenocyanato ligand exhibit spin crossover, centered at the critical temperature (T_c) of 42, 114, 282, and 293 K, respectively. The magnetic data of all compounds were analyzed using the spin Hamiltonian formalism including the zero-field splitting (ZFS) term, and in the case of the spin-crossover compounds, the Ising-like model with vibrations was applied.

Introduction

Miniaturization towards the nanoscopic and molecular scales is one of the most pursued targets in modern science and for future developments in the industry. One of the topics might be represented by the molecular switching between physically (e.g., temperature, light, pressure, magnetic and electric field) or chemically (e.g., pH, solvates) induced electronic spin states in coordination compounds, including spin crossover (SC)[1–9] and post-SC effects.[10] Spin crossover is one of the most appealing molecular effects in iron coordination compounds.[1–29]

In iron(III) Schiff base compounds, the pentadentate ligand ^5L forms the pseudo-octahedral building blocks [Fe^{III}(^5L)X] (with X as a monodentate ligand or bridging unit) with a number of interesting electronic and structural

features. This class of compounds often shows a thermally induced transition between the low-spin (LS) $^2T_{2g}$(pseudo-O_h) and high-spin (HS) $^6A_{1g}$(pseudo-O_h) states, but in most cases, the SC behavior of a gradual, weakly cooperative character has been reported so far. Some examples might be as follows: mononuclear,[12–15] binuclear,[11,12,15] trinuclear,[15] tetranuclear,[16] pentanuclear,[23] heptanuclear,[13,17,21,24–28] nonanuclear,[13,17–19] and dodecanuclear.[20] In all these compounds, the selected ligand design allows us to gain a switching effect that follows a sequential or concerted mechanism.[17–19]

The advantage of pentadentate ligand utilizations in octahedral complexes lies in the possibility of a very fine tuning of the SC phenomenon through the substitution of the sixth labile coordination site by a simple monodentate ligand. Then, a shift in the critical temperature (T_c), in accordance with the ligand position in the spectrochemical series, can be expected. Simplicity of such a strategy is in stark contrast to the possibility of tuning the SC phenomenon in the homoleptic Fe^{III} compounds with tridentate, or hexadentate Schiff base ligands, in which the cooperative SC has been observed almost exclusively so far.[30–33] The structural and coordination variabilities of these ligands prevent one from drawing an easy conclusion or of predicting the critical temperature.

The main disadvantage of the pentadentate ligand utilization is, as was outlined above, a lack of highly cooperative SC compounds in the [Fe^{III}(^5L)X] group. However, as has been reported recently, the shortening of the aliphatic part of ^5L implied higher rigidity of the resulting complex, and

_____
[a] Institute of Inorganic Chemistry, Leibniz University Hannover,
    30167 Hannover, Germany
[b] Institute of Inorganic Chemistry, FCHPT, Slovak University of Technology,
    81237 Bratislava, Slovakia
[c] Regional Centre of Advanced Technologies and Materials,
    Department of Inorganic Chemistry, Faculty of Science,
    Palacký University,
    77900 Olomouc, Czech Republic
[d] Graduate School of Pure and Applied Sciences, University of Tsukuba,
    Tennodai 1-1-1, Tsukuba 305-8571, Japan
[e] Department of Chemistry, FPV,
    University of SS Cyril and Methodius,
    91701 Trnava, Slovakia
    Homepage: http://kchem.fpv.ucm.sk/boca/index.html
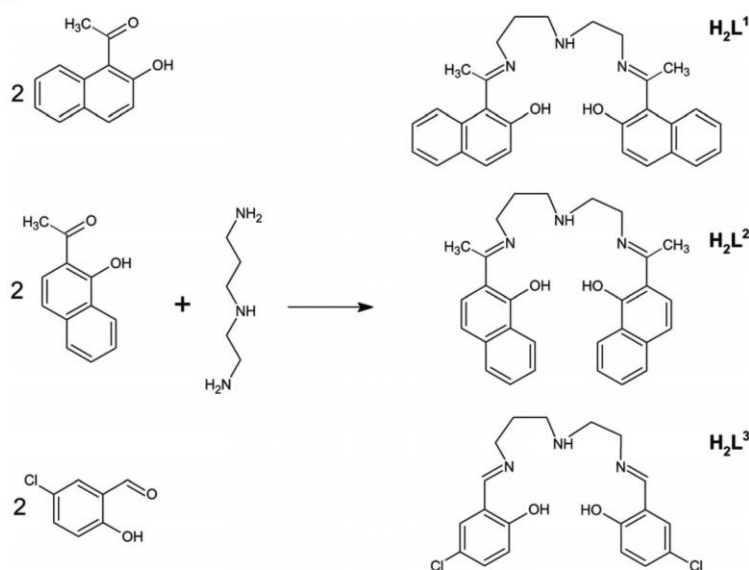   Supporting information for this article is available on the WWW under http://dx.doi.org/10.1002/ejic.201201038.

Figure 1. Synthetic pathways leading to the preparation of the ligands H_2L^1, H_2L^2, and H_2L^3.

consequently, the observation of cooperative SCs for the [Fe(L^0)(N-R)] compounds (L^0 = {1-[2-(2-hydroxynaphth-alen-1-yl)aminoethylamino]propylimino}naphthalene-2-ol, N-R = N-donor pseudohalide).[29] Moreover, for the very first time it was possible to perform fine tuning of the SC by the exchange of the pseudohalide ligand in the Fe^{III} complexes; such a strategy was extraordinarily successful for Fe^{II} SC complexes.[34]

To modify the switching properties, the ligand design plays an important role. This design is a kind of chemical tuning of the electronic and steric properties.[12–29] The main feature of this work is devoted to this chemical tuning. In this report, two groups of Fe^{III} complexes have been studied (Figure 1). The first group contains the Schiff-base pentadentate ligands derived either from 1-hydroxy-2-aceto-naphthone or 2-hydroxy-1-acetonaphthone with asymmet-ric triamine: 1,6-diamino-1,6-dimethyl-4-azahexane (abbr. *pet*); H_2L^2 = (2-{3-[2-(1-hydroxynaphthalen-2-yl)methylen-aminoethylamino]propylimino}methyl)naphthalene-1-ol and H_2L^1 = (1-{3-[2-(2-hydroxynaphthalen-1-yl)methylen-aminoethylamino]propylimino}methyl)naphthalene-2-ol. The second one is based upon the pentadentate ligands H_2L^3 derived from 5-chlorosalicylaldehyde and *pet*. The re-sulting Fe^{III} complexes are abbreviated as [Fe(L^1)(NCS)] (**1a**), [Fe(L^2)(Cl)]·CHCl$_3$ (**2a**), α-[Fe(L^2)(NCS)] (**2b**), β-[Fe(L^2)(NCS)] (**2c**), γ-[Fe(L^2)(NCS)] (**2d**), [Fe(L^2)(N$_3$)] (**2e**), [Fe(L^3)Cl] (**3a**), [Fe(L^3)(CN)] (**3b**), [Fe(L^3)(NCO)] (**3c**), [Fe(L^3)(NCS)] (**3d**), and [Fe(L^3)(NCSe)] (**3e**).

Results and Discussion

Structural Data

Cell parameters of the investigated compounds are listed in Tables 1 and 2.

Table 1. Crystallographic data for the naphthyl derivatives.

	α-[Fe(L^2)(NCS)] **2b** (100 K)	β-[Fe(L^2)(NCS)] **2c** (293 K)	γ-[Fe(L^2)(NCS)] **2d** (130 K)
Crystal system	orthorhombic	triclinic	monoclinic
Space group	*Pbca*	*P*1̄	*P*2$_1$/*c*
a [Å]	24.1948(7)	8.3336(3)	22.8635(8)
b [Å]	16.6835(5)	12.1493(4)	13.4647(5)
c [Å]	26.5952(8)	13.4404(4)	16.9588(7)
α [°]	90.00	100.603(2)	90.00
β [°]	90.00	94.031(2)	94.326(3)
γ [°]	90.00	90.672(2)	90.00
V [Å^3]	10735.3(6)	1333.84(8)	5205.9(3)
Z	8	2	4
R$_1$/wR$_2$ [I > 2σ(I)]	0.0365/0.0664	0.0400/0.0958	0.0406/0.1018

|	[Fe(L^1)(NCS)] **1a** (100 K)	[Fe(L^2)(Cl)]·CHCl$_3$ **2a** (100 K)	[Fe(L^2)(N$_3$)] **2e** (100 K)
Crystal system	monoclinic	monoclinic	orthorhombic
Space group	*P*2$_1$/*c*	*P*2$_1$/*c*	*Pna*2$_1$
a [Å]	10.7551(3)	14.1908(8)	8.2183(13)
b [Å]	13.9689(4)	13.1849(6)	17.158(4)
c [Å]	17.5085(6)	16.5715(9)	18.038(3)
α [°]	90.00	90.00	90.00
β [°]	101.541(3)	107.957(6)	90.00
γ [°]	90.00	90.00	90.00
V [Å^3]	2577.24(14)	2949.6(3)	2543.7(8)
Z	4	4	4
R$_1$/wR$_2$ [I > 2σ(I)]	0.0346/0.0824	0.0359/0.0809	0.0709/0.1468

The overall molecular structure for all the herein re-ported compounds is very similar. The pentadentate Schiff base ligand coordinates to the central iron(III) atom in a chelate manner, in which the oxygen atoms are in the *cis* position; this is typical for the present group of compounds that have a pentadentate ligand that originates in the con-

Table 2. Crystallographic data for the salicyl derivatives.

	[Fe(L³)Cl]·0.25H₂O 3a (213 K)	[Fe(L³)(CN)]·H₂O 3b (273 K)	[Fe(L³)(NCO)] 3c (293 K)	[Fe(L³)(NCS)] 3d (100 K)	[Fe(L³)(NCSe)] 3e (120 K)
Crystal system	triclinic	triclinic	triclinic	monoclinic	monoclinic
Space group	$P\bar{1}$	$P\bar{1}$	$P\bar{1}$	$P2_1/c$	$P2_1/c$
a [Å]	11.8874(1)	11.8244(9)	11.660(4)	8.0659(12)	8.1430(3)
b [Å]	12.9653(1)	13.0878(10)	12.787(4)	12.8301(18)	12.9311(4)
c [Å]	14.8717(1)	14.3632(12)	16.136(5)	20.090(3)	20.0357(6)
α [°]	77.416(1)	78.575(1)	82.321(5)	90	90.00
β [°]	72.755(1)	72.322(1)	69.358(4)	97.635(2)	97.112(3)
γ [°]	66.921(1)	68.257(1)	69.102(5)	90	90.00
V [Å³]	2000.32(59)	1957.9(3)	2103.1(12)	2060.61(76)	2093.50(11)
Z	4	4	4	4	4
R_1/wR_2 [$I>2\sigma(I)$]	0.0500/0.1340	0.0443/0.1165	0.0901/0.2134	0.0259/0.0697	0.0257/0.0560

densation of the aromatic 2-hydroxy-aldehydes/ketones with asymmetric *N*-(2-aminoethyl)propane-1,3-diamine (*pet*).[38] The nitrogen atoms are arranged in the *fac* manner and the remaining coordination site is occupied by the monodentate ligand X = Cl⁻, N₃⁻, CN⁻, NCO⁻, NCS⁻, and NCSe⁻. With respect to the asymmetry of the *pet* amine, two parts of the Schiff base ligand can be recognized: the rigid one that involves the ethylene aliphatic part (henceforth abbreviated as P1), and the more flexible propylene part of the ligand (henceforth abbreviated as P2). As a result of the higher rigidity of P1, the plane formed by the amine nitrogen atom (N_{am}), imine nitrogen atom (N_{im}), and O from the P1 is roughly in plane with the aromatic ring of ligand (P1 part). Furthermore, the monodentate ligand (¹L) always coordinates to the iron atom in the *trans* position to the oxygen atom from P2, which is allowed by the higher flexibility of P2.

Considering the organization of the pentadentate ligand in the vicinity of the central atom, two enantiomers can be distinguished. For their definition, a view down the axis created by the bond between the iron atom and monodentate ligand can be used (Figure 2). When the ligand rotates counterclockwise in the plane of the view, the complex is referred to as the Λ isomer, and the right-rotating variant is therefore the Δ isomer. All the herein reported compounds crystallize in the nonchiral space groups (Tables 1 and 2) and therefore they can be classified as racemic mixtures.

Λ-Isomer   Δ-Isomer
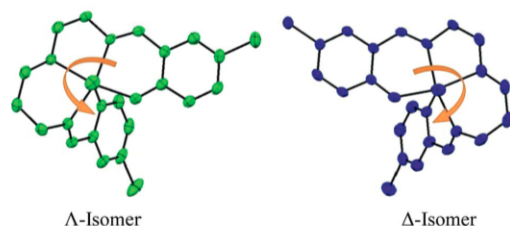
Figure 2. Schematic diagram illustrating two possible enantiomeric pairs of the [Fe^{III}(⁵L)X] complexes.

The metal–ligand bond lengths, typical for both spin states in this group of compounds, were summarized in previous publications.[29,39] The Fe–N_{am} bonds are observed as the longest in both spin forms with typical lengths of approximately 2.21 (HS) and 2.02 Å (LS), Fe–N_{im} bonds are a bit shorter with 2.09 (HS) and 1.93 Å (LS) and Fe–O bonds are the shortest: 1.94 (HS) 1.90 Å (LS). The bond lengths between the monodentate (pseudo)halide ligand and central iron atom Fe–X depend upon the type of X. When X = Cl⁻, the resulting complex is HS only with the Fe–Cl bond length longer than 2.3 Å (compounds **2a** and **3a**). On the other hand, the cyanido complexes have a very short Fe–C bond (below 1.98 Å, **3b**). The remaining pseudohalides (NCS⁻, NCSe⁻, NCO⁻, and N₃⁻) coordinate to the Fe^{III} atom with a greater bond-length variability in the HS state: Fe–X = 2.06–2.13 Å (HS), whereas Fe–X ≈ 1.96 Å (LS).

The X-ray diffraction study of compound **1a** was performed at 100 K, and its molecular structure is shown in Figure 3. The {FeN₃O₂N'} chromophore adopts a distorted octahedral geometry with the angular distortion parameter $\Sigma(1) = 38.5°$. (The parameter Σ is defined as $\Sigma_i = |90 - a_i|$, in which a_i stands for twelve *cis* angles of the coordination polyhedron).[40,41] The average value of the angular distortion for the LS compounds of the [Fe(L⁵)(*N*-R)] composition is $\Sigma(LS)_{avg} = 25.4°$, and for the HS ones it is more than two times larger $\Sigma(HS)_{avg} = 55.4°$.[29] The present value of $\Sigma(1a)$ corresponds to the temperature of measurement at which **1a** is below T_c but still contains a significant amount of the HS molecules. The chromophore bond lengths correspond to this situation as well (Table 3). In the crystal structure of **1a** there are present only very weak intermolecular interactions such as NH···π, CH···π, or very offset π–π stacking interactions and therefore only a weak solid-state cooperativeness is expected.

Compounds **2b**, **2c**, and **2d** are three polymorphs of [Fe(L²)(NCS)] with a considerably different molecular shape (**2b** versus **2c**–**2d**) and different crystal packing. The asymmetric unit of **2b** contains two [Fe(L²)(NCS)] molecules, which do not differ in the orientation of the pentadentate ligand. The most apparent difference between them
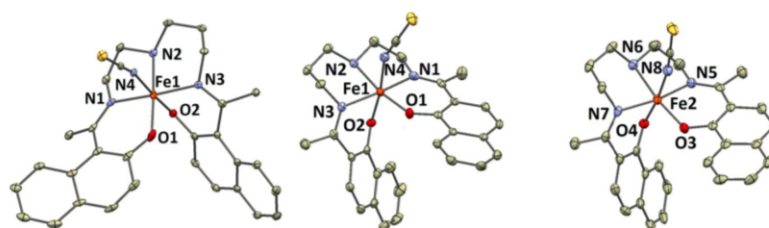
Figure 3. Molecular structures (ORTEP drawing with thermal ellipsoids at the 50% probability level) of **1a** (left) and **2b** (middle and right, two crystallographically independent molecules). Hydrogen atoms are omitted for clarity. Selected bond lengths [Å]: (**1a**) Fe1–N1 2.002(2), Fe1–N2 2.078(2), Fe1–N3 2.013(2), Fe1–N4 2.012(2), Fe1–O1 1.877(2), Fe1–O2 1.931(2); (**2b**) Fe1–N1 2.121(2), Fe1–N2 2.159(2), Fe1–N3 2.090(2), Fe1–N4 2.080(2), Fe1–O1 1.890(2), Fe1–O2 1.965(2), Fe2–O3 1.892(2), Fe2–O4 1.961(2), Fe2–N5 2.094(2), Fe2–N6 2.163(2), Fe2–N7 2.081(2), Fe2–N8 2.073(2).

Table 3. Selected structural parameters for the title compounds.

	Fe–N$_{am}$ [Å]	Fe–X[a] [Å]	Fe–N$_{im}$[b] [Å]	Fe–O[c] [Å]	Σ[d] [°]	a[e] [°]	
1a	2.078	2.012	2.008	1.904	38.5	68.6	this work
2a	2.145	2.409	2.101	1.935	43.0	65.2	this work
2b Fe1	2.159	2.080	2.106	1.927	49.1	63.6	this work
2b Fe2	2.163	2.073	2.088	1.927	51.9	78.4	this work
2c	2.168	2.099	2.115	1.928	56.6	17.7	this work
2d Fe1	2.168	2.133	2.105	1.937	62.8	25.0	this work
2d Fe2	2.168	2.119	2.100	1.936	56.5	19.6	this work
2e	2.165	2.038	2.102	1.932	68.4	66.9	this work
3a Fe1	2.190	2.353	2.093	1.959	66.9	62.2	this work
3a Fe2	2.207	2.368	2.096	1.956	53.1	53.4	this work
3b Fe1	2.010	1.966	1.936	1.903	19.3	65.9	this work
3b Fe2	2.013	1.951	1.932	1.902	28.8	56.0	this work
3c Fe1	2.206	2.007	2.093	1.946	55.4	69.0	this work
3c Fe2	2.204	1.985	2.093	1.960	57.3	61.6	this work
3d	2.000	1.944	1.932	1.879	27.1	84.5	this work
3e	2.001	1.952	1.932	1.881	26.9	85.5	this work
[Fe(L)(NCSe)]·CH$_3$CN (100 K)	2.022	1.964	1.936	1.882	20.5	78.5	[f][29]
[Fe(L)(NCSe)]·CH$_3$CN (300 K)	2.182	2.123	2.072	1.931	52.3	77.6	[f][29]
[Fe(L)(NCSe)]·(CH$_3$)$_2$CO	2.206	2.088	2.077	1.941	60.0	83.2	[f][29]

[a] The bond length between the iron atom and coordinating atom from the monodentate ligand bond. [b] The average value calculated from the iron–imino nitrogen bond lengths. [c] The average value calculated from the Fe–O bond lengths. [d] The octahedral distortion calculated from twelve *cis* angles found in the coordination polyhedron. [e] The dihedral angle (a) between the least-square planes of the aromatic rings. [f] H$_2$**L** = {1-[2-(2-hydroxynaphthalen-1-yl)aminoethylamino]propylimino}naphthalene-2-ol.

is the Fe–N–C angle (N and C atoms from the NCS ligand), which is in one case close to linearity (171.6°, Fe2 molecule) and in the other case it is significantly bent (158.0°, Fe1 molecule). The metal–ligand bond lengths and other parameters are similar to the HS standard at the temperature of measurement (T = 100 K). It must be noted that the Fe–N$_{am}$ bond lengths are rather short relative to previously reported HS compounds, and the same applies for the other compounds (**2a–2e**; Table 3).[29] Therefore, it might be concluded that the shorter Fe–N$_{am}$ bond length is a structural feature of the ferric complexes with the H$_2$**L**^{2} ligand. Only weak intermolecular interactions are present in **2b**, and no aromatic ring–ring stacking is observed.

The important difference between **2c** and **2d** can be recognized in the second coordination sphere. The [Fe(**L**^{2})(NCS)] molecules in **2c** create a 1D supramolecular chain by means of a rather long noncovalent contact between the amine group (donor) and thiocyanato sulfur atom with d(NH···S) = 3.439(3) Å, whereas in **2d** the amine

group is involved in the creation of the supramolecular dimer with the phenolic oxygen atom from the neighboring complex molecule with d(NH···O) = 3.449(3) and 3.540(2) Å (Figure 4).

Compound **2e** has in the asymmetric unit one [Fe(**L**^{2})(N$_3$)] molecule with the HS bond lengths close to those observed for **2b–2d**, thus underlining its HS character. The crystal packing of **2e** does not show any significant intermolecular interaction.

Compounds **3a–3e** can be divided into two isostructural subgroups: triclinic ($P\bar{1}$), which involves **3a–3c**, and monoclinic ($P2_1/c$) with **3d** and **3e**. The compounds in the triclinic series contain in their asymmetric units two [Fe(**L**^{3})(X)] molecules that differ in ligand orientation (Λ, Δ), whereas the compounds from the monoclinic series have only one [Fe(**L**^{3})(X)] symmetry-independent molecule.

A general feature found in compounds **3a–3c** is the presence of a cocrystallized water molecule in their crystal structures. However, it is apparent that all samples undergo
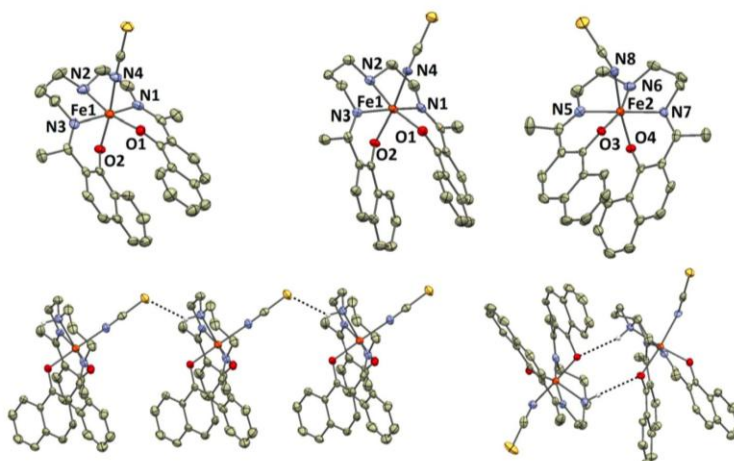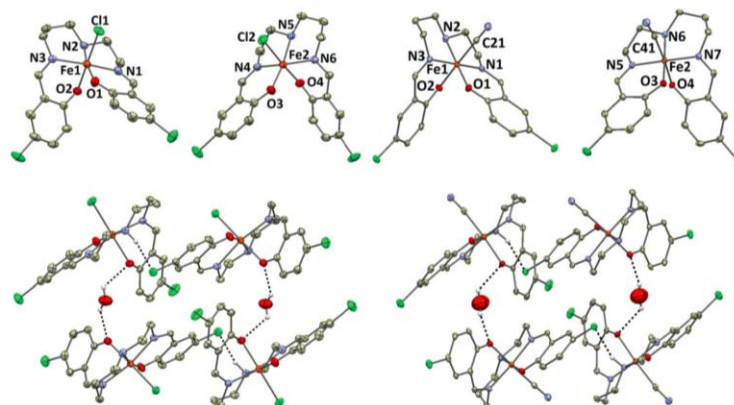
Figure 4. Molecular structures (ORTEP drawing with thermal ellipsoids at the 30% probability level) of **2c** (top left) and **2d** (top, middle, and right; two crystallographically independent molecules). A perspective view of the 1D chain fragment in **2c** (bottom left) and supramolecular dimer in **2d** (bottom right). Hydrogen atoms are omitted for clarity except those involved in hydrogen bonding. Selected bond lengths [Å]: (**2c**) Fe1–N1 2.114(2), Fe1–N2 2.168(2), Fe1–N3 2.116(2), Fe1–N4 2.099(2), Fe1–O1 1.905(2), Fe1–O2 1.951(1); (**2d**) Fe1–N1 2.112(2), Fe1–N2 2.168(2), Fe1–N3 2.096(2), Fe1–N4 2.133(2), Fe2–N5 2.112(2), Fe2–N6 2.168(2), Fe2–N7 2.088(2), Fe2–N8 2.119(3), Fe1–O1 1.909(2), Fe1–O2 1.965(2), Fe2–O3 1.913(2), Fe2–O4 1.959(2).

a solvent loss that affects the composition (e.g., the occupation factor of water molecule in **3a** is 0.25; Figure 5). The water molecule interconnects two adjacent $[Fe(L^3)(X)]$ molecules by a hydrogen bond that involves the phenolate oxygen atoms from their P2 parts: $d(OH\cdots O) = 2.585(3)$, 2.842(2) Å in **3a**; 2.645(2), 2.799(2) Å in **3b**; and 2.529(3),

2.784(3) Å in **3b**. The amine groups create rather long hydrogen bonds to the chloride atoms from the L^3 ligand: $d(NH\cdots Cl) = 3.457(3)$ Å in **3a**, 3.466(3) Å in **3b**, and 3.434(8) Å in **3c**. The other noncovalent contacts (which involve $Cl\cdots Cl$, $CH\cdots O$, and $CH\cdots Cl$) are also of a weak nature.

Figure 5. Molecular structures (ORTEP drawing with thermal ellipsoids at the 50% probability level) of **3a** (top left) and **3b** (top right; two crystallographically independent molecules). A perspective view on the noncovalent contacts (highlighted by dashed lines) in the crystal structure of **3a** (bottom left) and **3b** (bottom right). Hydrogen atoms are omitted for clarity. Selected bond lengths of compounds **3a** and **3b** [Å]: (**3a**) Fe1–N1 2.092(3), Fe1–N2 2.190(3), Fe1–N3 2.094(3), Fe2–N4 2.104(3), Fe2–N5 2.207(3), Fe2–N6 2.086(3), Fe1–O1 1.906(2), Fe1–O2 2.012(2), Fe2–O3 1.914(2), Fe2–O4 1.998(2), Fe1–Cl1 2.353(1) Fe2–Cl2 2.368(1); (**3b**) Fe1–N1 1.917(3), Fe1–N2 2.010(3), Fe1–N3 1.954(3), Fe2–N5 1.910(3), Fe2–N6 2.013(3), Fe2–N7 1.954(3), Fe1–O1 1.886(2), Fe1–O2 1.920(2), Fe2–O3 1.878(2), Fe2–O4 1.926(2), Fe2–C41 1.951(4), Fe1–C21 1.966(4).
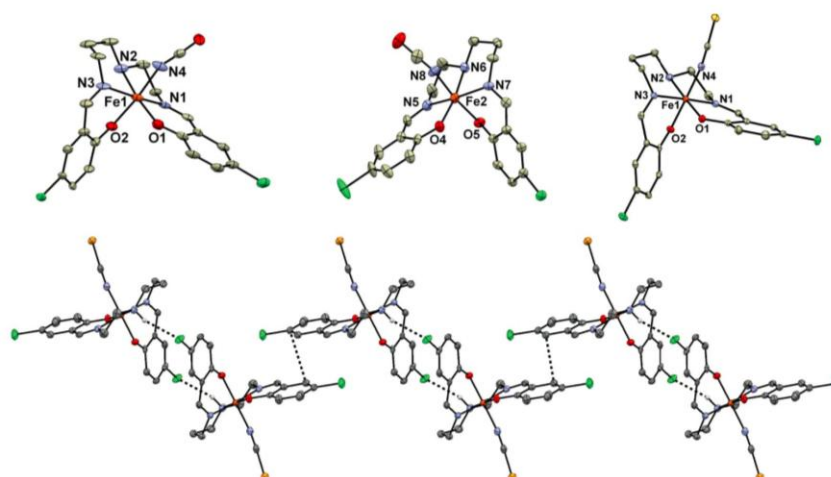
Figure 6. Molecular structure of **3c** (ORTEP drawing with thermal ellipsoids at the 50% probability level) Fe1 (top left; two crystallo-graphically independent molecules), **3c** Fe2 (top middle) and **3e** (top right). A perspective view on the noncovalent contacts (highlighted by dashed lines) in the crystal structure of **3d** and **3e** (bottom). Hydrogen atoms are omitted for clarity. Selected bond lengths of compounds **3c–3e** [Å]: (**3c**) Fe1–N1 2.100(8), Fe1–N2 2.206(7), Fe1–N3 2.085(9), Fe1–N4 2.007(9), Fe2–N5 2.090(7), Fe2–N6 2.204(7), Fe2–N7 2.095(7), Fe2–N8 1.985(8), Fe1–O1 1.916(7), Fe1–O2 1.976(6), Fe2–O3 1.926(6), Fe2–O4 1.993(6); (**3d**) Fe1–N1 1.916(2), Fe1–N2 2.000(2), Fe1–N3 1.948(2), Fe1–N4 1.944(2), Fe1–O1 1.889(2), Fe1–O2 1.869(1); (**3e**) Fe1–N1 1.916(2), Fe1–N2 2.001(2), Fe1–N3 1.948(2), Fe1–N4 1.952(2), Fe1–O1 1.890(2), Fe1–O2 1.871(2).

The metal–ligand bond lengths in **3a–3c** depend upon the type of the ligand X: HS complexes **3a** and **3c** have these bond lengths similar to those observed for the HS structures of compounds **2b–2e**, except for the Fe–N$_{am}$ bond length, which is significantly longer than in **2b–2e**. The bond lengths and structural parameters found for **3b**
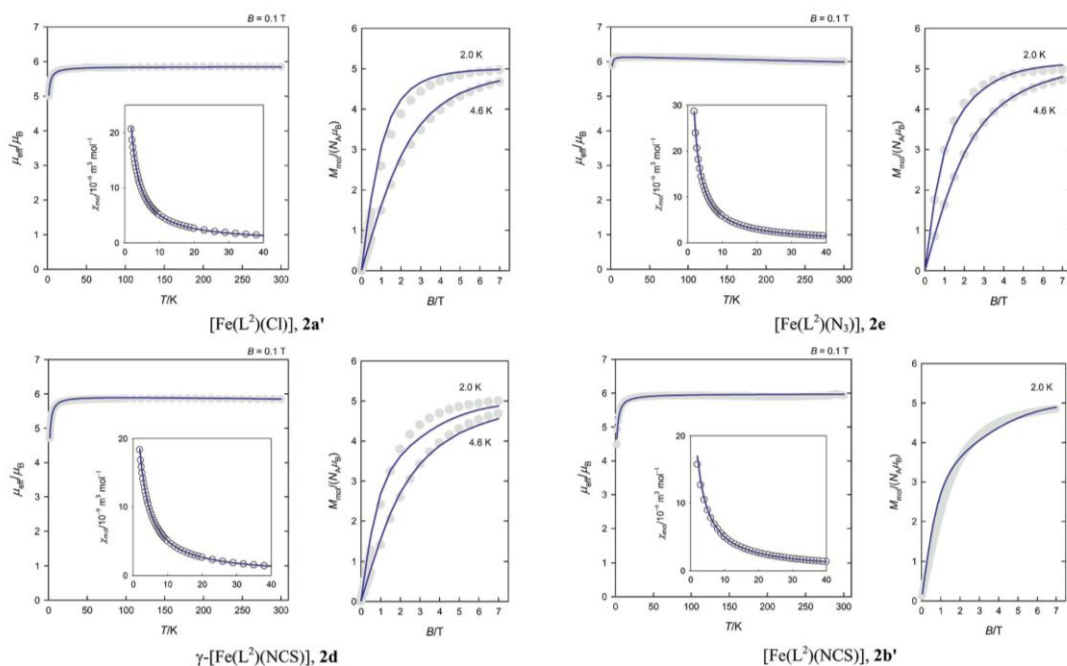
Figure 7. Magnetic functions for naphthyl-derivative complexes. Circles: experimental; lines: fitted data.

match the previously reported structures of the cyanido complexes with pentadentate Schiff base ligands.

Compounds **3d**–**3e** are isomorphous and this causes a high degree of similarity of their crystal structures. As can be seen from Table 3, the bond lengths correspond well to the low-spin state. Remarkably, the shape of the coordinated L^3 ligand differs in **3d** and **3e** significantly relative to **3a**–**3c**; the α parameter is much larger and adopts values close to 85°, whereas this parameter is 10–20° smaller in **3a**–**3c** (Table 3). The metal–ligand bond lengths and the Σ parameters are typical for LS complexes, and these match the magnetic data (see below). The second coordination sphere in **3d** and **3e** is created by supramolecular dimers held by the slightly offset aromatic ring–ring stacking with centroid–centroid distances of 3.649(2) Å in **3d** and 3.695(2) Å in **3e**. This stack is supported by the weak hydrogen bond between the amine group and chloride atom from the pentadentate ligand of the adjacent $[Fe(L^3)(X)]$ molecule $[d(NH\cdots Cl) = 3.418(2)$ Å in **3d** and 3.437(2) Å in **3e**; Figure 6]. The adjacent supramolecular dimers are interconnected by offset π–π stacking [centroid–centroid distances: 4.094(2) Å in **3d**, 4.156(3) Å in **3e**]. The other present noncovalent interactions (which involve $CH\cdots O$, $CH\cdots Cl$, and $CH\cdots S/Se$) are of a weak character.

Magnetic Data for Naphthyl Derivative Complexes

The molar magnetic susceptibility has been corrected for the underlying diamagnetism and converted into the effective magnetic moment; its temperature evolution is shown in Figure 7 for four Fe^{III} compounds. Complexes **2a′**, **2b′**, **2d**, and **2e** are high spin; their effective magnetic moment on cooling from room temperature stays constant down to $T = 20$ K, which reflects the Curie law. Below this temperature the magnetic moment drops, which is an indication of the zero-field splitting (ZFS). The magnetization per formula unit for these complexes saturates to a value of $M_1 = M_{mol}/N_A = 5\ \mu_B$ at $T = 2.0$ K, which indicates that the axial ZFS parameter D is rather low. The magnetic data were fitted with g_H close to 2.0 and $|D| < 1$ cm^{-1}. Some minor corrections are achieved by using the temperature-independent term α and the molecular-field correction zj (see Table 4).

From Figure 8 it can be seen that for **1a**, which contains the thiocyanato ligand, μ_{eff} at the lowest temperature ($T = 2$ K) adopts a value of $\mu_{eff} = 2.51\ \mu_B$. Upon heating, the effective magnetic moment stays almost constant until $T = 40$ K. This reflects a Curie law for the low-spin Fe^{III} complex with the magnetogyric factor $g \approx 2.89$ since $\mu_{eff}/\mu_B = g[S(S+1)]^{1/2}$. Such a result matches the magnetization data taken at $T = 2.0$ K, which at $B = 7$ T saturates to $M_1 = gS = 1.39\ \mu_B$ so that $g \approx 2.78$. Upon further heating, the effective magnetic moment rises gradually until $\mu_{eff} = 5.76\ \mu_B$ at $T = 350$ K (above 200 K it is almost constant). This is an indication of the spin crossover between $S_L = 1/2$ and $S_H = 5/2$.

In fitting the magnetic data, three assumptions have been made: (i) The low-spin state of Fe^{III} is thoroughly described by the Curie–Weiss law enlarged by the temperature-inde-

Table 4. Review of magnetic behavior of Fe^{III} complexes with pentadentate Schiff base ligands.

		Spin	T_c [K]	Magnetic parameters
Naphthyl derivatives				
2a′	$[Fe(L^2)Cl]$	HS		$g_H = 2.00$, $D_H = -0.20$ cm^{-1}, $zj = -0.040$ cm^{-1}
2e	$[Fe(L^2)N_3]$	HS		$g_H = 2.058$, $D_H = 0.69$ cm^{-1}, $\alpha_H = -10.0\times10^{-9}$ m^{3}mol^{-1}
2d	γ-$[Fe(L^2)(NCS)]$	HS		$g_H = 2.00$, $D_H = 1.00$ cm^{-1}, $\alpha_H = -5.00\times10^{-9}$ m^{3}mol^{-1}, $zj = -0.055$ cm^{-1}
2b′[a]	$[Fe(L^2)(NCS)]$	HS		$g_H = 2.02$, $D_H = \pm1.0$ cm^{-1}, $zj = -0.064$ cm^{-1}
2b	α-$[Fe(L^2)(NCS)]$	SC	44, 40	$g_T = 2.395$, $\Theta_T = -0.50$ K, $g_H = 2.005$, $\Delta_{eff}/k = 190$ K, $J/k = 82$ K,
		3/2–5/2		$\nu_T = 174$ cm^{-1}, $\nu_H = 158$ cm^{-1}; $\Delta H = 1.66$ kJ mol^{-1}, $\Delta S = 3.69$ J K^{-1} mol^{-1}
1a	$[Fe(L^1)(NCS)]$	SC	114	$g_L = 3.00$, $\Theta_L = -0.25$ K, $g_H = 2.0$, $\Delta_{eff}/k = 193$ K, $J/k = 52$ K, ν_L
		1/2–5/2		$= 267$ cm^{-1}, $\nu_H = 209$ cm^{-1}; $\Delta H = 1.61$ kJ mol^{-1}, $\Delta S = 14.0$ J K^{-1} mol^{-1}
Salicyl derivatives				
3a	$[Fe(L^3)Cl]\cdot xH_2O$	HS		$g_H = 1.93$, $D_H = 2.2$ cm^{-1}, $\alpha_H = -5.0\times10^{-9}$ m^{3}mol^{-1}, $zj = -0.11$ cm^{-1}
3c	$[Fe(L^3)(NCO)]$	HS		$g_H = 1.96$, $D_H = 0.06$ cm^{-1}, $\alpha_H = -2.5\times10^{-9}$ m^{3}mol^{-1}, $zj = -0.052$ cm^{-1}
3d	$[Fe(L^3)(NCS)]$	SC	280	$g_L = 2.38$, $\Theta_L = -0.91$ K, $\alpha_L = +5.0\times10^{-9}$ m^{3}mol^{-1}, $g_H = 2.0$,
		1/2–5/2		$\Delta_{eff}/k = 694$ K, $J/k = 180$ K, $\nu_L = 306$ cm^{-1}, $\nu_H = 250$ cm^{-1}; $\Delta H = 5.77$ kJ mol^{-1}, $\Delta S = 20.6$ J K^{-1} mol^{-1}
3e	$[Fe(L^3)(NCSe)]$	SC	293	$g_L = 2.20$, $\Theta_L = -0.20$ K, $\alpha_L = +2.6\times10^{-9}$ m^{3}mol^{-1}, $g_H = 2.0$, $\Delta_{eff}/k = 787$ K, J/k
		1/2–5/2		$= 197$ K, $\bar{\nu}_L/c = 320$ cm^{-1}, $\bar{\nu}_H/c = 254$ cm^{-1}; $\Delta H = 6.54$ kJ mol^{-1}, $\Delta S = 22.3$ J K^{-1} mol^{-1}
3b	$[Fe(L^3)(CN)]$	LS		$g_L = 2.36$, $\alpha_L = +5.7\times10^{-9}$ m^{3}mol^{-1}, $zj = -0.166$ cm^{-1}

[a] Compound **2b** recrystallized from acetonitrile.

pendent (van Vleck) term. The free parameters are the g_L factor, the Weiss constant Θ_L, and α_L. (ii) The same holds true for the high-spin state; however, one can safely fix $g_H = 2.0$ and omit Θ_H and α_H. (iii) There is nothing like a paramagnetic impurity for the Fe^{III} complex (as opposed to it being a frequent occurrence for Fe^{II} ones).

The fourth assumption postulates a model of the spin crossover. From a large and varied menu we selected the Ising-like model with vibrations.[42,43] This model contains

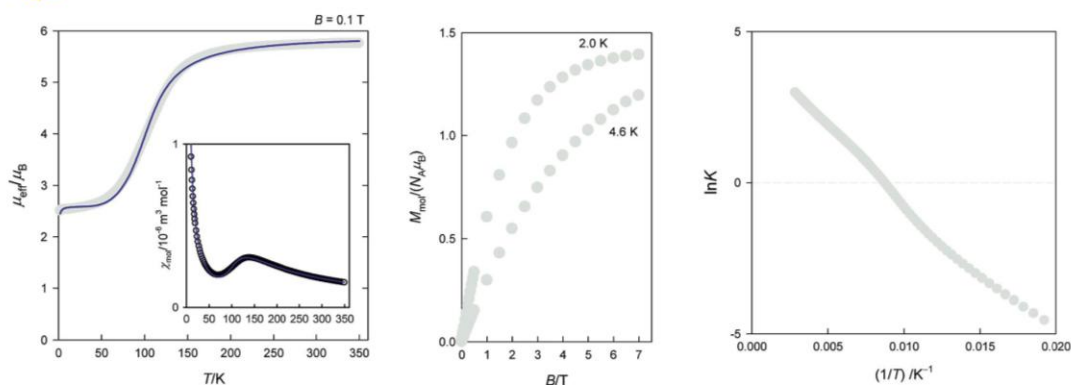www.eurjic.org   **FULL PAPER**

Figure 8. Magnetic data for **1a**. Left: effective magnetic moment; center: magnetization; right: van 't Hoff plot. Circles: experimental; lines: fitted data.

four parameters: (i) the energy difference between LS and HS state Δ_{eff} that is proportional to the enthalpy of the spin transition $\Delta H = R\Delta_{eff}$; (ii) the solid-state cooperativeness J (not to be confused with the exchange coupling constant); and (iii) two averaged vibrational frequencies (in fact, the Einstein modes) that enter the vibrational partition function. In such a model, Equations (1) and (2) were iterated to achieve self-consistency.

$$\langle\sigma\rangle_T = \frac{F-1}{F+1} \quad (1)$$

$$F = \exp[-(\Delta_{eff} - kT\ln r_{eff}^T - 2J\langle\sigma\rangle_T)/kT] \quad (2)$$

The high-spin mole fraction is related to a "fictitious spin" through $x_H = (1 + \langle\sigma\rangle_T)/2$; the entropic factor is given through Equation (3) for $m = 15$ active modes in a hexaco-ordinate complex, $h\bar{v}_H$- and $h\bar{v}_L$-averaged vibration energies. The transition entropy is then $\Delta S = Rr_{eff}^T|_{x_H = 1/2}$. To this end, the equilibrium constant is calculated as $K =$

$x_H(1 - x_H)$, and this is used in generating the van 't Hoff plot: $\ln K$ versus T^{-1}.

$$r_{eff}^T = \frac{g_H^{el}}{g_H^{el}}\left[\frac{1-\exp(h\bar{v}_L/kT)}{1-\exp(h\bar{v}_H/kT)}\right]^m \quad (3)$$

An advanced fitting procedure converged to the following set of parameters for **1a**: $g_L = 3.00$, $\Theta_L = -0.25$ K, $\Delta_{eff}/k = 193$ K, $J/k = 52.4$ K, $\bar{v}_L/c = 267$ cm^{-1}, and $\bar{v}_H/c = 209$ cm^{-1}; the discrepancy factor $R = 0.029$. The fitted data are shown as lines in Figure 8, and one can conclude that the fit is almost perfect. The reconstructed thermodynamic quantities are $\Delta H = 1.61$ kJ mol^{-1}, $\Delta S = 14.0$ J K^{-1} mol^{-1}, and their ratio $\Delta H/\Delta S = 114.8$ K matches the value of $T_c = 114.0$ K obtained from $x_H = 1/2$. This test confirms that the model is self-consistent.

The van 't Hoff plot (Figure 8, right) shows a small non-linearity around $\ln K = 0$, which reflects an effect of the solid-state cooperativeness. Indeed $J/k < T_c$ in the present case, so that a thermal hysteresis is absent. Another effect is seen at the end of the $1/T$ plot in which another nonline-
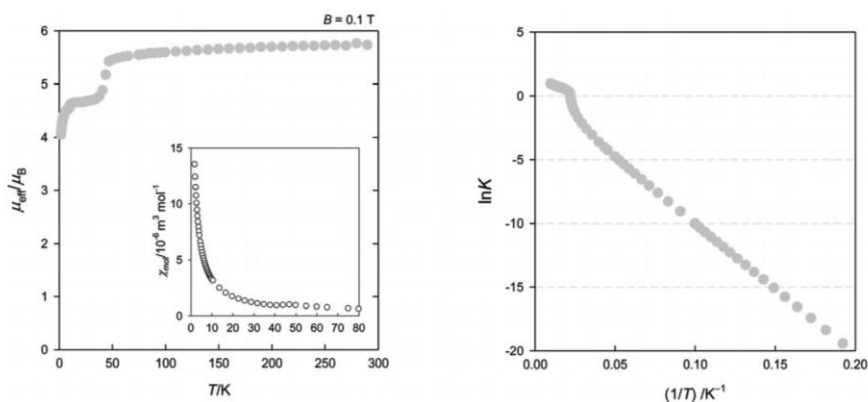
Figure 9. Magnetic data for **2b**, α-[Fe(L^2)(NCS)]. Left: effective magnetic moment; right: van 't Hoff plot.
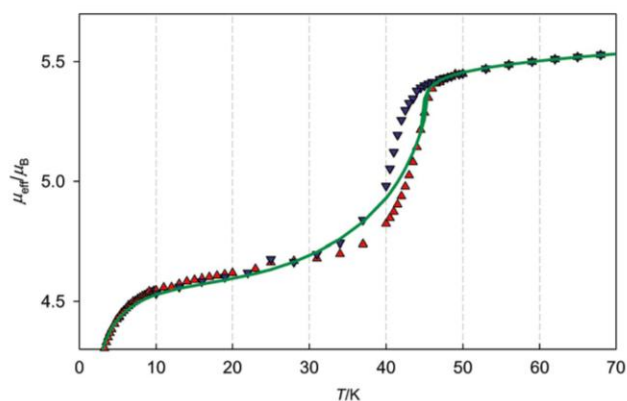
Figure 10. Zoomed transition area for **2b** on heating mode (triangles up), cooling mode (triangles down), and fitted lines.

arity appears. This reflects the effect of the temperature-variable entropy that has roots in the thermal population of vibrational levels.

Complex **2b**, which also contains the isothiocyanato ligand, shows features of the spin crossover, but contrary to previous cases, the transition starts from the intermediate spin state $S_I = 3/2$ (Figure 9). Such a situation occurs, for instance, in [Fe(saldptn-5Cl)py]BPh$_4$ (saldptn = N,N'-bis(1-hydroxy-2-benzylidene)-1,7-diamino-4-azaheptane; py = pyridine).[12] Complex **2b** exhibits a small hysteresis of the width $\Delta T = 4$ K centered at $T_c = 42$ K. As the walls of the hysteresis loop are angled instead of rectangular ones, the Gaussian distribution model has been applied for the data fitting.[44] It differs from the previously described Ising-like model with vibrations in the feature in that the cooperativeness J is no longer a constant parameter but it decays according to the normal distribution $J_i = n_i J$ for a number of grids ($i = 50$). The fitting procedure gave: $g_I = 2.395$, $\Theta_I = -0.50$ K, $g_H = 2.005$, $\Delta_{eff}/k = 190$ K, $J/k = 82$ K, $\nu_I = 174$ cm^{-1}, and $\nu_H = 158$ cm^{-1}; in addition, the distribution

parameters are $\sigma = 0.00211$ and $X_{opt} = 0.52$. The thermodynamic quantities are $\Delta H = 1.66$ kJ mol^{-1}, $\Delta S = 3.69$ J K^{-1} mol^{-1}, and their ratio is $\Delta H/\Delta S = 45$ K. The fitting is of a good quality (see Figure 10 for the fitted line), though not perfect ($R = 0.022$). The van 't Hoff plot shows a strong nonlinearity around $\ln K = 0$.

Magnetic Data for Salicyl Derivative Complexes

Of the studied complexes, compound **3b**, which contains the cyanido ligand, is low spin (Figure 11) with parameters $g_L = 2.36$, $a_L = +5.7 \times 10^{-9}$ m^3 mol^{-1}, and $zj = -0.166$ cm^{-1} ($R = 0.019$). On the contrary, compound **3c**, which contains the cyanato ligand, is high spin: $g_H = 1.96$, $D_H = 0.06$ cm^{-1}, $a_H = -2.5 \times 10^{-9}$ m^3 mol^{-1}, $zj = -0.052$ cm^{-1} ($R = 0.003$). By analogy with other Cl-containing complexes, complex **3a** [Fe(L^3)Cl]·xH$_2$O is expected to be high spin, which was confirmed by magnetic data (Figure 12).

The magnetic behavior for compound **3d** that contains the thiocyanato ligand shows the spin crossover that is
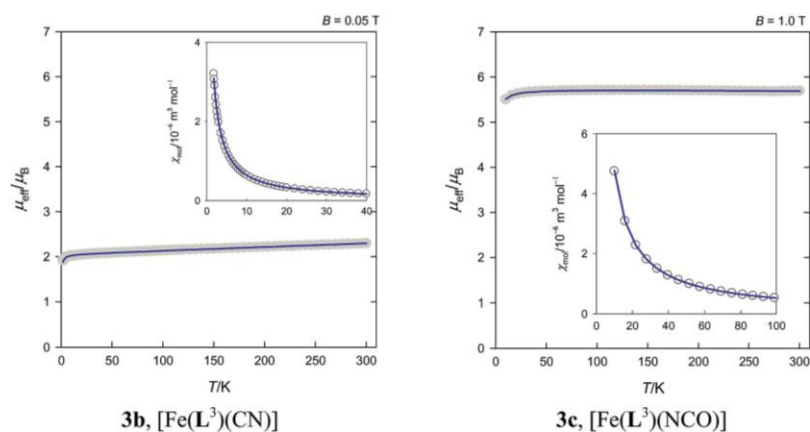
Figure 11. Magnetic functions for salicyl derivative complexes. Dark points: experimental data; solid line: fitted.
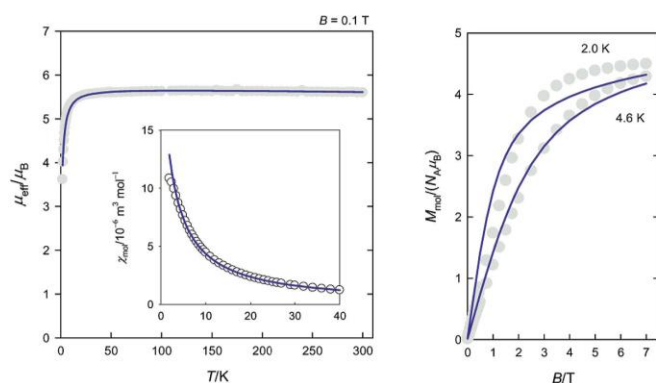
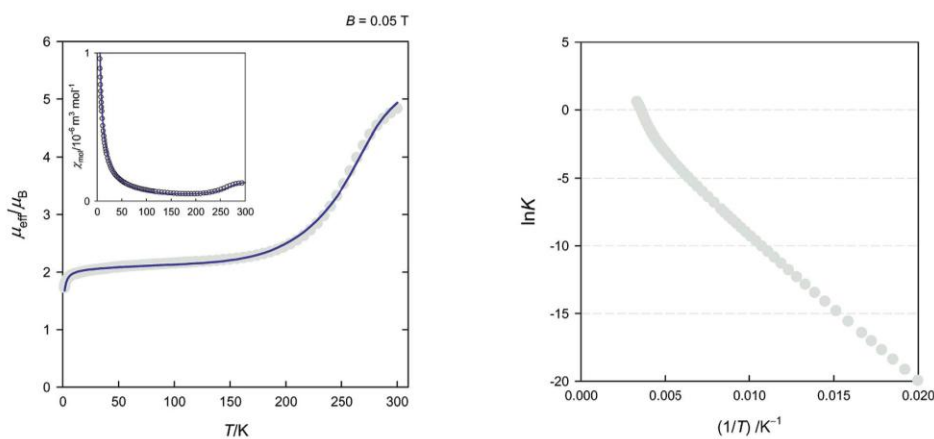Figure 12. Magnetic functions for **3a**, $[Fe(L^3)Cl] \cdot xH_2O$. Dark points: experimental data; solid line: fitted.

Figure 13. Magnetic data for **3d**, $[Fe(L^3)(NCS)]$. Left: effective magnetic moment; right: van 't Hoff plot.

somehow similar to that of **1a**; however, the transition temperature is shifted to the room-temperature region (Figure 13). The fitting procedure gave the following set of mag-

netic and spin-crossover parameters: $g_L = 2.38$, $\Theta_L = -0.91$ K, $a_L = +5.0 \times 10^{-9}$ $m^3 mol^{-1}$, $\Delta_{eff}/k = 694$ K, $J/k = 180$ K, $\bar{\nu}_L/c = 306$ cm^{-1}, $\bar{\nu}_H/c = 250$ cm^{-1} ($R = 0.037$). The
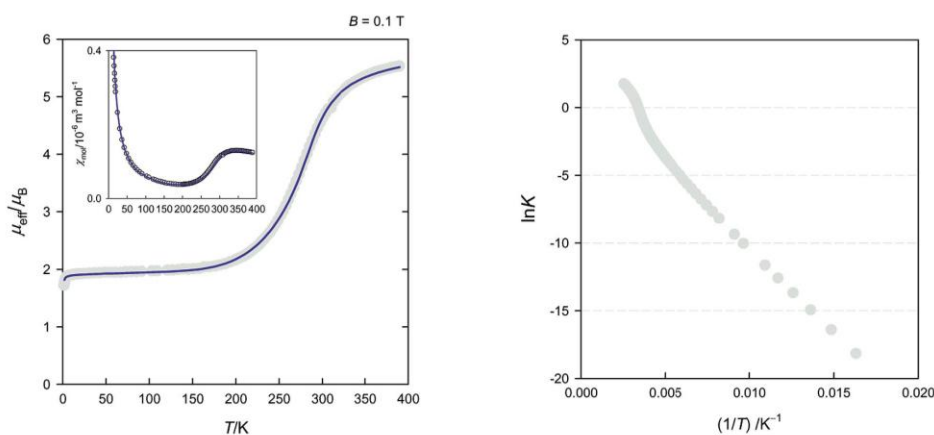
Figure 14. Magnetic data for **3d**, $[Fe(L^3)(NCSe)]$. Left: effective magnetic moment. Right: van 't Hoff plot.

fitted data are shown as lines in Figure 13, and one can conclude that the fit again is almost perfect. The reconstructed thermodynamic quantities are $\Delta H = 6.81$ kJ mol^{-1}, $\Delta S = 24.4$ J K^{-1} mol^{-1}, and their ratio $\Delta H/\Delta S = 279$ K matches the value of $T_c = 282$ K obtained from $x_H = 1/2$. Note that there are not many compounds that show spin crossover around room temperature.[45]

The substitution of the thiocyanato ligand for the selenocyanato one brings some effect to the transition temperature which rises from $T_c = 280$ K to 293 K (Figure 14). The fitted parameters are $g_L = 2.20$, $\Theta_L = -0.20$ K, $\alpha_L = +2.6 \times 10^{-9}$ m^3 mol^{-1}, $\Delta_{eff}/k = 787$ K, $J/k = 197$ K, $\bar{v}_L/c = 320$ cm^{-1}, $\bar{v}_H/c = 254$ cm^{-1} ($R = 0.061$); $\Delta H = 6.54$ kJ mol^{-1}; and $\Delta S = 22.3$ J K^{-1} mol^{-1}.

Discussion

A recent report focused on a series of analogous Fe^{III} complexes with pentadentate Schiff base ligands (*salpet* is derived from the salicylaldehyde; 3MeO/3EtO represents the methoxy/ethoxy group at the third position of aromatic ring; 3Bu5Me represents the *tert*-butyl at the third and the methyl group at the fifth positions):[29]

(a) [Fe(3MeO-*salpet*)(N$_3$)], [Fe(3MeO-*salpet*)(NCO)]·CH$_3$OH, and [Fe(3Bu5Me-*salpet*)(NCS)] are high spin;

(b) [Fe(3MeO-*salpet*)(CN)]·CH$_3$OH and [Fe(3EtO-*salpet*)(CN)]·H$_2$O are low spin.

(c) complexes [Fe(L^0)(NCO)], [Fe(L^0)(NCS)]·CH$_3$CN, and [Fe(L^0)(NCSe)]·CH$_3$CN show a gradual spin crossover with the transition temperature varying as $T_c = 155$, 151, 170 K.

(d) complex [Fe(L^0)(N$_3$)] exhibits a small thermal hysteresis ($T_{1/2}\uparrow = 122$ K, $T_{1/2}\downarrow = 117$ K).

We have seen that the iron(III) complexes under study, which contain the pentadentate Schiff base ligands and a pseudohalide coligand, can be classified into four groups: (i) the high-spin complexes, which are [Fe(L^2)Cl], [Fe(L^2)-N$_3$], [Fe(L^3)Cl]·xH$_2$O, [Fe(L^3)(NCO)], and two polymorphs of [Fe(L^2)(NCS)]; (ii) compounds [Fe(L^1)(NCS)], [Fe(L^3)(NCS)], and [Fe(L^3)(NCSe)], which exhibit spin crossover from the $S_L = 1/2$ to $S_H = 5/2$ state; (iii) one compound that shows spin transition between the $S_I = 3/2$ to $S_H = 5/2$ state {i.e., the polymorph α-[Fe(L^2)(NCS)]}; and (iv) the low-spin complex is [Fe(L^3)(CN)].

The stabilization of the low-spin state by the CN$^-$ ligand correlates with its strong crystal-field strength as opposed to the stabilization of the high-spin state with weak-field Cl$^-$, NCO$^-$, and N$_3^-$ ligands. The NCS$^-$ ligand stabilizes either the high-spin state or causes a bistability that manifests itself in the spin crossover. The unusual behavior of α-[Fe(L^2)(NCS)] is attributed to a fine balance of the crystal-field strength and the pairing energy along with a structural distortion within the chromophore and the specific crystal packing.[46]

Of great interest is the increase of the transition temperature in the series of [Fe(L^1)(NCS)], [Fe(L^3)(NCS)], and [Fe(L^3)(NCSe)] complexes: $T_c = 114$, 280, and 293 K,

respectively. This order correlates with the transition enthalpy (derived from the magnetic data fitting): $\Delta H = 1.61$, 5.77, and 6.54 kJ mol^{-1}. The transition enthalpy originates in the energy gap between the low-spin and the high-spin state that can be influenced by the crystal-field strength. Note that the averaged Fe–X (X = N) bond lengths at room temperature for high-spin Fe^{III} complexes under study are close or over 2 Å (Table 5). They vary between 2.013 (after spin crossover) and 1.994 Å (at the spin crossover) for **1a** and **3d** complexes that contain the same NCS$^-$ ligand, respectively. It is likely that the increase of the crystal-field strength of the ligand will result in an increase of ΔH and consequently also in T_c; the f_L increment of the crystal field strength $\Delta = g_M f_L$ varies from Cl$^-$ (0.78) < N$_3^-$ (0.83) < NCS$^-$ (1.02) < NCSe$^-$ (1.05) < CN$^-$ (1.7). This could be understood on the basis of the constraint $T_c = \Delta H/\Delta S$ when the transition entropy is constant. In fact, ΔS also varies within this series: $\Delta S = 14.0$, 20.6, and 22.3 J K^{-1} mol^{-1}. Moreover, there is some solid-state cooperativeness at play that has been established as $J/k = 52$, 180, and 197 K, or in the units of molar energy $J' = R(J/k) = 0.43$, 1.50, and 1.64 kJ mol^{-1}.

Table 5. Averaged metal–ligand distances in Fe^{III} complexes {FeN$_3$O$_2$X}.

	Complex	d(Fe–N)$_{av}$	d(Fe–O)$_{av}$	d(Fe–X)	Spin state
3a	[Fe(L^3)Cl]·xH$_2$O	2.129	1.975	Cl, 2.361	HS
2a′	[Fe(L^2)Cl]	missing structure			HS
2a	[Fe(L^2)Cl]·CHCl$_3$	2.115	1.934	Cl, 2.408	HS
2e	[Fe(L^2)N$_3$]	2.122	1.931	2.038	HS
2d	γ-[Fe(L^2)(NCS)]	2.124	1.936	2.126	HS
3c	[Fe(L^3)(NCO)]	2.134	1.954	1.998	HS
2b′	[Fe(L^2)(NCS)]	missing structure			HS
2c	β-[Fe(L^2)(NCS)]	2.131	1.929	2.103	–
2b	α-[Fe(L^2)(NCS)]	2.118	1.972	2.077 (HS)	SC, 42
1a	[Fe(L^1)(NCS)], 100 K	2.031	1.904	2.013 (HS)	SC, 114
3d	[Fe(L^3)(NCS)]	1.955	1.878	1.944	SC, 280
3e	[Fe(L^3)(NCSe)], 120 K	1.955	1.880	1.952	SC, 293
3b	[Fe(L^3)(CN)]	1.961	1.901	C, 1.955	LS

Conclusion

The spin state of the Fe^{III} complexes that contain the pentadentate Schiff base ligands **L** derived either from salicylaldehyde or acetonaphthone can be tuned by the sixth (pseudo)halide ligand X = Cl$^-$, N$_3^-$, NCO$^-$, NCS$^-$, NCSe$^-$, and CN$^-$. Whereas the weak-field ligands stabilize the high-spin state, the cyanido ligand stabilizes the low-spin state of the [Fe(^{5}L)X] complex. The thiocyanato complexes are either high spin or they exhibit, along with the selenocyanato analogue, spin crossover. The transition temperature varies within the series of α-[Fe(L^2)(NCS)], [Fe(L^1)(NCS)], [Fe(L^3)(NCS)], and [Fe(L^3)(NCSe)] in the range of $T_c = 42$, 114, 280, and 293 K, respectively. The solid-state cooperativeness is rather small in this class of complexes.

Experimental Section

[Fe(L^1)(NCS)] (1a): The Schiff condensation of 2-hydroxy-1-acetonaphthone (2.22 mmol) with aliphatic amine 1,6-diamino-4-aza-

hexane, $H_2N(CH_2)_3NH(CH_2)_2NH_2$ (1.11 mmol), in a ratio of 2:1 in a mixture of methanol (15 cm^3) and acetonitrile (15 cm^3) resulted in a pentadentate Schiff base ligand H_2L^1 (yellow oil). The reaction mixture was stirred at the boiling temperature for 30 min (mixture 1). Meanwhile, a solution of potassium thiocyanate in acetonitrile (2.22 mmol in 10 cm^3) was added to a solution of $FeCl_3\cdot6H_2O$ in methanol (1.11 mmol in 10 cm^3), and the color of the solution changed to dark violet (mixture 2). Both mixtures were combined, and the resulting solution was stirred at its boiling temperature for 15 min. In the end, triethylamine (2.11 mmol) in methanol (5 cm^3) was added dropwise to the final solution. The mixture was stirred at its boiling temperature for 45 min. The precipitate was separated by filtration, then washed with cold methanol and diethyl ether. The filtrate was left to evaporate spontaneously, yield 33%. $C_{30}H_{29}FeN_4O_2S$: m/z = 565.5; calcd. C 63.7, H 5.17, N 9.91; found C 63.5, H 5.05, N 9.88. IR spectra can be found in the Supporting Information.

Ligand H_2L^2: The Schiff condensation of 1-hydroxy-2-acetonaphthone with an asymmetric triamine, 1,6-diamino-4-azahexane [$H_2N(CH_2)_3NH(CH_2)_2NH_2$] in a ratio of 2:1 resulted in a pentadentate Schiff base ligand (bright yellow powder) according to Figure 1.

[Fe(L^2)(Cl)] (2a') and [Fe(L^2)(Cl)]·CHCl$_3$ (2a): A solution of H_2L^2 in methanol (1.11 mmol in 20 cm^3) was combined with a solution of $FeCl_3\cdot6H_2O$ in methanol (1.11 mmol in 15 cm^3) accompanied by a color change to dark green. Then, triethylamine (2.11 mmol) was added by adding methanol (5 cm^3) dropwise. After 50 min of stirring at the boiling temperature, the precipitate from the reaction mixture was separated by filtration, then washed with cold methanol and diethyl ether. Then, the chlorido precursor **2a'** was recrystallized from chloroform, and the crystals were collected as **2a**. $C_{30}H_{30}Cl_4FeN_3O_2$: m/z = 662.2; calcd. C 54.4, H 4.57, N 6.35; found C 54.9, H 4.13, N 5.98.

α-[Fe(L^2)(NCS)] (2b): A solution of $FeCl_3\cdot6H_2O$ in methanol (1.11 mmol in 10 cm^3) was combined with a solution of potassium thiocyanate in methanol (2.22 mmol in 10 cm^3), and the color of the solution changed to dark violet. The resulting solution was stirred for 10 min. The ligand H_2L^2 (1.11 mmol in methanol/acetonitrile, 20 cm^3/20 cm^3) was added to this solution and stirred for 15 min. Then potassium hydroxide (2.22 mmol) was added in two portions, and the solution was stirred at its boiling temperature for 1 h. The precipitate was separated by filtration and washed with cold methanol and diethyl ether. The filtrate was left to evaporate spontaneously for 1 d when the crystals were formed and separated, yield 15%. $C_{30}H_{29}FeN_4O_2S$: m/z = 565.5; calcd. C 63.7, H 5.17, N 9.91; found C 63.2, H 4.87, N 9.73.

β-[Fe(L^2)(NCS)] (2c): A solution of [Fe(L^2)Cl] in acetone (0.184 mmol, 20 cm^3) was combined with a solution of potassium thiocyanate in acetone (0.202 mmol in 10 cm^3), and the mixture was stirred for 40 min at the boiling temperature. The prepared dark green solution was filtered immediately, washed with cold methanol and diethyl ether, and the filtrate was left for evaporation. The next day the crystals were isolated, yield 46%. $C_{30}H_{29}FeN_4O_2S$: m/z = 565.5; calcd. C 63.7, H 5.17, N 9.91; found C 64.0, H 5.03, N 10.08.

γ-[Fe(L^2)(NCS)] (2d): A solution of $FeCl_3\cdot6H_2O$ in acetone (0.252 mmol in 5 cm^3) was combined with a solution of potassium thiocyanate in acetone (0.378 mmol in 5 cm^3), and it was stirred for 10 min. The ligand H_2L^2 in acetone (0.252 mmol, 15 cm^3) was added to this solution, and it was stirred for 15 min. Finally, triethylamine (0.495 mmol, in 5 cm^3 of acetone) was added dropwise. The solution was stirred at its boiling temperature for 2 h. The

precipitate was separated by filtration, then washed with cold methanol and diethyl ether. The filtrate was left to evaporate spontaneously. Two days later, the crystals were isolated, yield 34%. $C_{30}H_{29}FeN_4O_2S$: m/z = 565.5; calcd. C 63.7, H 5.17, N 9.91; found C 63.3, H 5.55, N 9.38.

[Fe(L^2)(NCS)] (2b'): Compound **2b'** was prepared by recrystallization of **2b** from acetonitrile. $C_{30}H_{29}FeN_4O_2S$: m/z = 565.5; calcd. C 63.7, H 5.17, N 9.91; found C 64.3, H 5.53, N 9.86. The X-ray structure is missing but magnetic data were collected.

[Fe(L^2)(N$_3$)] (2e): A solution of $FeCl_3\cdot6H_2O$ in methanol (1.11 mmol in 10 cm^3) was combined with a solution of sodium azide in methanol (2.22 mmol in 10 cm^3), and the resulting solution was stirred for 10 min. The ligand H_2L^2 (1.11 mmol in methanol/acetonitrile, 20 cm^3/20 cm^3) was added to this solution and stirred for 15 min. Then, potassium hydroxide (2.22 mmol) was added in two portions, and the solution was stirred at its boiling temperature for 1 h. The precipitate was separated by filtration, then washed with cold methanol and diethyl ether. The filtrate was left to evaporate spontaneously for 1 d when the crystals were formed and separated, yield 52%. $C_{29}H_{29}FeN_6O_2$: m/z = 549.4; calcd. C 63.4, H 5.32, N 15.3; found C 63.3, H 5.25, N 15.2.

[Fe(L^3)Cl] (3a): A solution (100 cm^3) of N-(2-aminoethyl)-1,3-propanediamine (1.17 g, 10 mmol) in methanol was combined with 5-chlorosalicylaldehyde (3.13 g, 20 mmol) in methanol (25 cm^3). The solution was heated to reflux for 15 min, and afterwards $FeCl_3\cdot6H_2O$ (2.7 g, 10 mmol) in methanol (25 cm^3) was added. Then Et_3N (2.2 g, 22 mmol) was added, and the mixture was heated to reflux for 1 h. After cooling in the fridge for 24 h, the product was filtered, washed with cooled methanol, and dried under vacuum, yield 4.11 g (85%). $C_{19}H_{19}FeN_3O_2Cl_3$: m/z = 483.58; calcd. C 47.2, H 3.96, N 8.69, C/N 5.43; found C 46.0, H 4.36, N 9.07, C/N 5.07. IR (ATR): $\tilde{v}$ = 3268 (N–H), 2902 (C–H) (m), 1616 (C=N) cm^{-1}. All theoretical compositions for **3a–3e** were calculated as solvent-free.

[Fe(L^3)(CN)] (3b): A solution (80 cm^3) of **3a** (0.2 g, 0.4 mmol) in methanol was combined with KCN (0.027 g, 0.42 mmol) in methanol/acetonitrile (20 cm^3, 1:1). The solution was stirred and filtered. Turquoise single crystals were obtained by slow evaporation at room temperature. $C_{20}H_{19}FeN_4O_2Cl_2$: m/z = 474.15; calcd. C 50.7, H 4.04, N 11.8, C/N 4.29; found C 50.0, H 4.00, N 11.2, C/N 4.46. IR (ATR): $\tilde{v}$ = 3241 (N–H), 2923 (C–H) (m), 2051 (NC), 1621 (C=N) cm^{-1}.

[Fe(L^3)(NCO)] (3c): A solution (80 cm^3) of **3a** (0.2 g, 0.4 mmol) in methanol was combined with KNCO (0.034 g, 0.42 mmol) in methanol (20 cm^3). The solution was stirred and filtered. Black single crystals were obtained by slow evaporation. $C_{20}H_{19}FeN_4O_3Cl_2$: m/z = 490.15; calcd. C 49.0, H 3.91, N 11.4, C/N 4.29; found C 47.5, H 3.88, N 10.4, C/N, 4.57. IR (ATR): $\tilde{v}$ = 3258 (N–H), 2933 (C–H) (m), 2186 (NCO), 1621 (C=N) cm^{-1}.

[Fe(L^3)(NCS)] (3d): A solution (80 cm^3) of **3a** (0.2 g, 0.4 mmol) in methanol was combined with KSCN (0.041 g, 0.42 mmol) in methanol (20 cm^3). The solution was stirred and filtered. Black single crystals were obtained by slow evaporation at room temperature. $C_{20}H_{19}FeN_4O_2Cl_2S_1$: m/z = 506.22; calcd. C 47.4, H 3.78, N 11.1, S 6.33, C/N 4.29; found C 46.2, H 3.72, N 11.0, S 6.50, C/N 4.20. IR (ATR): $\tilde{v}$ = 3248 (N–H), 2927 (C–H) (m), 2101 (NCS), 2061 (NCS), 1610 (C=N) cm^{-1}.

[Fe(L^3)(NCSe)] (3e): A solution (80 cm^3) of **3a** (0.2 g, 0.4 mmol) in methanol was combined with KSCN (0.061 g, 0.42 mmol) in methanol (20 cm^3). The solution was stirred and filtered. Black single crystals were obtained by slow evaporation at room temperature.

$C_{20}H_{19}FeN_4O_2Cl_2Se_1$: m/z = 553.11; calcd. C 43.4, H 3.46, N 10.1, C/N 4.29; found C 41.5, H 3.39, N, 9.64, C/N 4.30. IR (ATR): $\tilde{v}$ = 3233 (N–H), 2927 (C–H) (m), 2101 (NCSe), 2071 (NCSe), 1610 (C=N) cm^{-1}.

X-ray Diffraction: Single-crystal X-ray diffraction data were collected with an Oxford Xcalibur2 diffractometer with the Sapphire CCD detector and fine-focused sealed tube (Mo-K_α radiation, λ = 0.71073 Å) source and equipped with an Oxford Cryosystem nitrogen gasflow apparatus. All structures were solved by direct methods using SHELXS97[35] incorporated into the WinGX program package.[36] For each structure its space group was checked by the AD-SYMM procedure of the PLATON software.[37] All structures were refined using full-matrix least-squares on $F_o^2 - F_c^2$ with SHELXTL-97 with anisotropic displacement parameters for all non-hydrogen atoms.[35] The hydrogen atoms were placed into the calculated positions and they were included into the riding model approximation, with U_{iso} = 1.2/1.5 U_{eq}.

CCDC-900755 (for **1a**), -900756 (for **2a**), -900757 (for **2b**), -900758 (for **2c**), -900759 (for **2d**), -900760 (for **2e**), -900761 (for **3a**), -900762 (for **3b**), -900763 (for **3c**), -900764 (for **3d**), and -900765 (for **3e**) contain the supplementary crystallographic data for this paper. These data can be obtained free of charge from The Cambridge Crystallographic Data Centre via www.ccdc.cam.ac.uk/data_request/cif.

Magnetic Data: The magnetic data were performed with the SQUID apparatus (MPMS-XL7, Quantum Design) using the RSO mode of detection with the sample (ca. 20 mg) encapsulated in a gelatin-made sample holder. The susceptibility recorded at B = 0.1 T was corrected for the underlying diamagnetism and converted into the effective magnetic moment. The magnetization was measured at two temperatures, T = 2.0 and 4.6 K. Some magnetic data were recorded with SQUID (MPMS-5, Quantum Design) in the DC mode of detection.

Supporting Information (see footnote on the first page of this article): IR spectra of **1a**, **2a′**, **2b**, **2b′**, **2c**, **2d**, **2e**.

Acknowledgments

[1] H. A. Goodwin, *Coord. Chem. Rev.* **1976**, *18*, 293.
[2] P. Gütlich, *Struct. Bonding (Berlin)* **1981**, *44*, 83.
[3] E. König, *Struct. Bonding (Berlin)* **1991**, *76*, 51.
[4] P. Gütlich, A. Hauser, H. Spiering, *Angew. Chem.* **1994**, *106*, 2109.
[5] P. Gütlich, Y. Garcia, H. A. Goodwin, *Chem. Soc. Rev.* **2000**, *29*, 419.
[6] P. Gütlich, Y. Garcia, P. J. van Koningsbruggen, F. Renz, *Introduction to Physical Techniques in Molecular Magnetism*, part 1: *Structural and Magnetic Methods* (Eds.: F. Palacio, J. Schweizer, E. Ressouche), University Press, Zaragoza, **2000**.
[7] A. Hauser, J. Jeftic, H. Romstedt, R. Hinek, H. Spering, *Coord. Chem. Rev.* **1999**, *190–192*, 471.
[8] P. Gütlich, H. A. Goodwin (Eds.), *Spin Crossover in Transition Metal Compounds I, II, III*, in: *Topics in Current Chemistry*, Springer, Berlin, **2004**, vol. 233–235.
[9] P. Gütlich, P. van Koningsbruggen, F. Renz, *Struct. Bonding (Berlin)* **2004**, *107*, 27–75.
[10] S. Jung, F. Renz, M. Klein, M. Menzel, R. Boča, R. Stösser, *J. Phys. Conf., Ser.* **2010**, *217*, 012027.
[11] I. Nemec, R. Boča, R. Herchel, Z. Trávníček, M. Gembický, W. Linert, *Monatsh. Chem.* **2009**, *140*, 815–828.
[12] R. Boča, Y. Fukuda, M. Gembický, R. Herchel, R. Jaroščiak, W. Linert, F. Renz, J. Yuzurihara, *Chem. Phys. Lett.* **2000**, *325*, 411–419.
[13] F. Renz, P. Kerep, D. Hill, M. Klein, *Hyperfine Interact.* **2007**, *168*, 981–987.
[14] R. Boča, I. Nemec, I. Šalitroš, J. Pavlik, R. Herchel, F. Renz, *Pure Appl. Chem.* **2009**, *81*, 1357.
[15] I. Šalitroš, R. Boča, Ľ. Dlháň, M. Gembický, J. Kožíšek, J. Linares, J. Moncoľ, I. Nemec, L. Perašínová, F. Renz, I. Svoboda, H. Fuess, *Eur. J. Inorg. Chem.* **2009**, 3141.
[16] R. Herchel, R. Boča, M. Gembický, J. Kožíšek, F. Renz, *Inorg. Chem.* **2004**, *43*, 4103.
[17] F. Renz, P. Kerep, *Polyhedron* **2005**, *24*, 2849.
[18] F. Renz, P. Kerep, *Hyperfine Interact.* **2004**, *156/157*, 371.
[19] F. Renz, M. Klein, S. Jung, P. Homenya, R. Saadat, D. Nariaki, *Unimagazin*, Leibniz Universität Hannover, **2011**, *1–2*, 24.
[20] F. Renz, D. Hill, M. Klein, J. Hefner, *Polyhedron* **2007**, *26*, 2325.
[21] R. Boča, I. Šalitroš, J. Kožíšek, J. Linares, J. Moncoľ, F. Renz, *Dalton Trans.* **2010**, *39*, 2198.
[22] R. Saadat, F. Renz, *Moessbauer Eff. Ref. Data J.* **2012**, 1–25, in press.
[23] F. Renz, S. Jung, M. Klein, M. Menzel, A. F. Thünemann, *Polyhedron* **2009**, *28*, 1818.
[24] F. Renz, C. Zaba, L. Rossberg, S. Jung, M. Klein, G. Klingelhöfer, A. Wünsche, S. Reinhardt, M. Menzel, *Polyhedron* **2009**, *28*, 2036.
[25] F. Renz, P. Kerep, D. Hill, R. Müller-Seipel, M. Klein, *Hyperfine Interact.* **2006**, *168*, 1051.
[26] M. Gembický, R. Boča, F. Renz, *Inorg. Chem. Commun.* **2000**, *3*, 662.
[27] F. Renz, V. Martinez, M. Klein, *Hyperfine Interact.* **2008**, *184*, 251.
[28] F. Renz, V. Martinez, M. Klein, M. Schott, T. Hoffmann, M. Blumers, I. Fleischer, G. Klingelhöfer, R. Boča, M. Menzel, *Hyperfine Interact.* **2008**, *184*, 259.
[29] I. Nemec, R. Herchel, R. Boča, Z. Trávníček, I. Svoboda, H. Fuess, W. Linert, *Dalton Trans.* **2011**, *40*, 10090.
[30] S. Hayami, Z. Z. Gu, H. Yoshiki, A. Fujishima, O. Sato, *J. Am. Chem. Soc.* **2001**, *123*, 11644.
[31] J. K. Tang, J. S. Costa, S. Smulders, G. Molnar, A. Bousseksou, S. J. Teat, Y. G. Li, G. A. van Albada, P. Gamez, J. Reedijk, *Inorg. Chem.* **2009**, *48*, 2128.
[32] S. Dorbes, L. Valade, J. A. Real, C. Faulmann, *Chem. Commun.* **2005**, 69.
[33] M. S. Haddad, W. D. Federer, M. W. Lynch, D. N. Hendrickson, *Inorg. Chem.* **1981**, *20*, 131.
[34] P. Guionneau, M. Marchivie, G. Bravic, J. F. Letard, D. Chasseau, in *Spin Crossover in Transition Metal Compounds II*, Springer, Berlin, **2004**, vol. 234, pp. 97–128.
[35] G. M. Sheldrick, *Acta Crystallogr., Sect. A* **2008**, *64*, 112.
[36] L. J. Farrugia, *J. Appl. Crystallogr.* **1999**, *32*, 837.
[37] a) A. L. Speck, *PLATON, A Multipurpose Crystallographic Tool*, Utrecht University, The Netherlands, **2001**; b) *MISSYM*, v.1.1, a flexible new release, see: Y. Le Page, *J. Appl. Crystallogr.* **1988**, *21*, 983.
[38] I. Nemec, R. Boča, M. Gembický, Ľ. Dlháň, R. Herchel, F. Renz, *Inorg. Chim. Acta* **2009**, *362*, 4754.

[39] P. J. van Koningsbruggen, Y. Maeda, H. Oshio, in: *Spin Cross-over in Transition Metal Compounds I*, Springer, Berlin, **2004**, vol. 233, pp. 259–324.

[40] M. Marchivie, P. Guionneau, J. F. Letard, D. Chasseau, *Acta Crystallogr., Sect. B* **2005**, *61*, 25.

[41] R. Pritchard, S. A. Barrett, C. A. Kilner, M. A. Halcrow, *Dalton Trans.* **2008**, 3159.

[42] R. Boča, *A Handbook of Magnetochemical Formulae*, Elsevier, Amsterdam, **2012**.

[43] R. Boča, W. Linert, *Monatsh. Chem.* **2003**, *134*, 199.

[44] R. Boča, M. Boča, L. Dlháň, K. Falk, H. Fuess, W. Haase, R. Jaroščiak, B. Papánková, F. Renz, M. Vrbová, R. Werner, *Inorg. Chem.* **2001**, *40*, 3025.

[45] I. Šalitroš, N. T. Madhu, R. Boča, J. Pavlik, M. Ruben, *Monatsh. Chem.* **2009**, *140*, 695.

[46] T. Ikeue, Y. Ohgo, T. Yamaguchi, M. Takahashi, M. Takeda, M. Nakamura, *Angew. Chem.* **2001**, *113*, 2687; *Angew. Chem. Int. Ed.* **2001**, *40*, 2617.

6.2   Iron(III) Complexes with Pentadentate Schiff-Base Ligands: Influence of Crystal Packing Change and Pseudohalido Coligand Variations on Spin Crossover

Christoph Krüger, Peter Augustín, Lubor Dlhán, Ján Pavlik, Ján Moncol, Ivan Nemec, Roman Boča and Franz Renz

The final publication is available at

http://www.sciencedirect.com/science/article/pii/S0277538714007219.

Preface

This work has been published as a full paper in *Polyhedron* in 2015. It deals with two novel iron(III) complexes, $[Fe(L^{Br})(L^1)]$, which show a temperature induced incomplete spin crossover. The pentadentate ligand L^{Br} is gained from a Schiff base reaction and the coligand L^1 varies from chloride, thiocyanate, selenocyanate and azide. While for $L^1 = NCSe^-$ as a coligand the transition temperature (326 K or 317 K) is above room temperature and for the coligand N_3^- at 143 K or 140 K (two values were obtained by different models) The two analogous complexes with Cl^- and NCS^- coligands remain in the high spin state over the whole temperature range. The complex $[Fe(L^{Br})(NCS)]$ exhibit high spin behaviour whereas $[Fe(L^{Br})(NCSe)]$ and previously reported $[Fe(L^{Cl})(NCS)]$ and $[Fe(L^{Cl})(NCSe)]$ show a spin crossover (section 6.1). By comparison, $[Fe(L^{Br})(NCS)]$ crystallises in a different crystal structure.

The complexes $[Fe(L^{Br})(N_3)]$ and $[Fe(L^{Br})(Cl)]$ were synthesised by Peter Augustin and his colleagues Dr. Jan Pavlik, as well as Jan Moncol. The preparation of $[Fe(L^{Br})(NCS)]$ and $[Fe(L^{Br})(NCSe)]$ were performed by the author of this thesis. Single-crystal X-ray diffraction measurements were carried out with the help of Fabian Kempf from Leibniz Universität Hannover and Dr. Ivan Nemec from Palacky University in Czech Republic. Magnetic measurements were carried out and analysed by Dr. Lubor Dlhan and fitted by Prof. Dr. Roman Boča.

Prof. Dr. Roman Boča, Dr. Jan Pavlik and the author of this thesis wrote the initial manuscript which was refined together with Prof. Dr. Franz Renz.

Contents lists available at ScienceDirect

Polyhedron

journal homepage: www.elsevier.com/locate/poly

CrossMark

Iron(III) complexes with pentadentate Schiff-base ligands: Influence of crystal packing change and pseudohalido coligand variations on spin crossover

Christoph Krüger [a], Peter Augustín [b], L'ubor Dlháň [b], Ján Pavlik [b,*], Ján Moncol' [b], Ivan Nemec [c], Roman Boča [b,d], Franz Renz [a]

[a] Institute of Inorganic Chemistry, Leibniz University Hannover, D-30167 Hannover, Germany
[b] Institute of Inorganic Chemistry, FCHPT, Slovak University of Technology, SK-812 37 Bratislava, Slovakia
[c] Regional Centre of Advanced Technologies and Materials, and Department of Inorganic Chemistry, Faculty of Science, Palacký University, CZ-779 00 Olomouc, Czech Republic
[d] Department of Chemistry, FPV, University of SS Cyril and Methodius, SK-917 01 Trnava, Slovakia

ARTICLE INFO

ABSTRACT

Two novel iron(III) complexes involving pentadentate Schiff-base ligands, $[Fe(L^{Br})(L^1)]$, show temperature induced incomplete spin crossover of a gradual nature. While for the $L^1 = NCSe^-$ coligand the transition temperature (326 K or 317 K) lies above room temperature, the N_3^- coligand causes its drop down to 143 K or 140 K (two values were obtained by different models). This shift is associated with a significant decrease of the enthalpy of the transition from about $\Delta H = 6.1$ kJ mol^{-1} to ca. $\Delta H = 1.7$ kJ mol^{-1}, while the entropy of the transition is about $\Delta S = 19$ J K^{-1} mol^{-1} and $\Delta S = 12$ J K^{-1} mol^{-1}, respectively. Two analogous complexes with Cl$^-$ and NCS$^-$ coligands remain high-spin over the whole temperature range.

© 2014 Elsevier Ltd. All rights reserved.

1. Introduction

Spin crossover (SCO) is one of the most fascinating phenomena occurring in coordination compounds of transition-metal ions and has gained more and more interest during the last decades. Already in the early 1930s Cambi and his co-workers first reported on dithiocarbamato complexes of iron(III) with unusual magnetic properties [1–3]. Since that time a lot of iron(III) SCO systems have been published and the achievements in this research were reviewed and categorized by Van Koningsbruggen et al. in 2003 or recently, by Bruker et al. or Murray in 2013 [4]. Nowadays, these types of molecular switches seem to be very attractive for potential applications such as switching devices or sensors [5].

There is a plethora of mononuclear iron(III) SCO compounds of the general composition $[Fe(X-L^5)L^1]$ involving pentadentate N_3O_2-donating Schiff-base ligands H_2X-L^5, originating in the condensation of derivatives of salicylaldehydes and aliphatic triamines; X denotes the substitution of the aromatic rings. The sixth coordination site of iron can be occupied by various monodentate organic or inorganic ligands [6–11]. The pentadentate H_2X-L^5 together with

the monodentate ligands form a distorted octahedral coordination environment, which is a usual condition for the occurrence of SCO in Fe(III) compounds, but it should be noted, that SCO has been observed also for pentacoordinate Fe(III) compounds [12]. Furthermore, the monodentate ligand can be replaced by a bridging ligand/complex to build polynuclear complexes which often exhibit SCO [6,10,13–17,7,18–26].

Previous studies have established that ligand design is crucial for the possibility of fine tuning the SCO properties, especially, by increasing the ligand rigidity, modification of the intermolecular interactions between the SCO molecules [9,11] or just by the substitution at the variable sixth coordination site [27–30].

The six-coordinate iron(III) compounds exhibit SCO from the low-spin (LS) to high-spin (HS) state ($S = 1/2 \rightarrow S = 5/2$), while SCO from the intermediate state ($S = 3/2 \rightarrow S = 5/2$) is observed typically for the five-coordinate complexes [12,31]. The spin transition can be induced physically (such as temperature, light or pressure change) as well as chemically (such as a solvate, ligand or pH change) [32–40].

Herein, we report on four novel mononuclear iron(III) complexes $[Fe(L^{Br})(L^1)]$ involving a pentadentate Schiff-base ligand H_2L^{Br} and Cl$^-$, N_3^-, NCS$^-$ and NCSe$^-$ as L^1 coligands. The pentadentate ligand H_2L^{Br} was prepared by the condensation of 5-bromosalicylaldehyde with an asymmetric triamine –

---

* Corresponding author.
  E-mail address: jan.pavlik@stuba.sk (J. Pavlik).
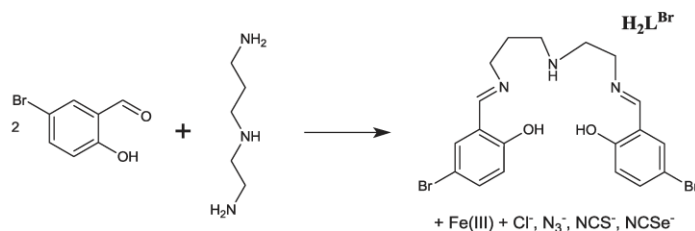
Scheme 1. Synthetic route for the preparation of the complexes [Fe(L^{Br})Cl]·0.5H$_2$O (**1**), [Fe(L^{Br})N$_3$]·CH$_3$OH (**2**), [Fe(L^{Br})NCS] (**3**) and [Fe(L^{Br})NCSe] (**4**) using the Schiff-base ligand H$_2$L^{Br}.

1,6-diamino-4-azahexane (Scheme 1). The complexes [Fe(L^{Br})(-Cl)]·0.5H$_2$O (**1**), [Fe(L^{Br})(N$_3$)]·CH$_3$OH (**2**), [Fe(L^{Br})(NCS)] (**3**), and [Fe(L^{Br})(NCSe)] (**4**) have been characterized by single-crystal X-ray diffraction, elemental analysis, IR spectroscopy and magnetic measurements. In our previous work we reported on two isostructural compounds with a general formula [Fe(L^{Cl})(NCS/Se)], which exhibit rather gradual SCO near room temperature with T_C = 280 (NCS$^-$) and 293 K (NCSe$^-$). In this study, the effect of the peripheral substitution of Cl by the Br atom is examined in terms of the crystal packing and intermolecular interactions, and magnetic properties of the compounds lie in the center of interest.

2. Results and discussion

2.1. Structural data

Cell parameters of the investigated compounds are listed in Table 1; the remaining crystallographic data are deposited in Supplementary material and they can be retrieved from the Cambridge Crystallographic Data Centre.

The molecular structures of the compounds **1**–**4** are very similar to the structures of the [Fe(L^X)(L^1)] compounds (where L^1 = Cl$^-$, N$_3^-$, NCS$^-$, NCSe$^-$; X marks the substitutions by functional groups on the aromatic rings of the primary ligand H$_2$L = N,N′-bis(1-hydroxy-2-benzyliden)-1,6-diamino-4-azahexane) reported previously [9–11,14]. The pentadentate Schiff base ligand (L^{Br})$^{2-}$ chelates the central iron(III) atom by three nitrogen atoms (one amine (N$_{am}$), two imine (N$_{im}$)) and two oxygen atoms.

The nitrogen atoms are arranged in a *fac* manner while the oxygen atoms are in the *cis* positions. The sixth coordination site of the central atom is occupied by the monodentate chlorido or pseudohalido ligand with the donor atom (Cl or N$_{term}$) in the *trans* position to the oxygen atom from the more flexible "propyl" part of the pentadentate ligand. The metal–ligand bond lengths of the compounds under study are summarized in Table 2.

The compound [Fe(L^{Br})(Cl)]·0.5H$_2$O (**1**) is isostructural with the previously reported [Fe(L^{Cl})(Cl)]·0.5H$_2$O and [Fe(L^{Cl})(CN)]·0.5H$_2$O complexes [9]. The asymmetric unit contains two complex molecules and one molecule of the crystal water. The chromophore bond lengths and angular distortion parameter, Σ,[1] correspond to the HS state of the complex molecule (Σ(**1**) = 62.3 and 52.3°) and they are similar to those observed for other iron(III) chlorido complexes with pentadentate Schiff base ligands with the longest Fe–Cl bond (2.3458(6) and 2.3569(6) Å). The Fe–N$_{am}$ bond lengths are a bit shorter (2.178(2) and 2.198(3) Å) and the Fe–N$_{im}$ and Fe–O are the shortest bond lengths (Fig. 1 and Table 2). The crystal water is involved in the hydrogen bonding pattern including four [Fe(L^{Br})

[1] The angular distortion from the ideal octahedron Σ is calculated as sum of the absolute values of the deviations of the twelve cis chromophore angles from the ideal value 90°.

(Cl)] molecules non-covalently bridged (O–H···O hydrogen bonding) by two water molecules and N–H···Br (Fig. 1). The water molecules provide hydrogen bonding of significant strength with d(O···O) = 2.657(4) and 2.868(6) Å, while N–H···Br contacts are much weaker: d(N···Br) = 3.499(2) Å.

The bond lengths in the chromophore of [Fe(L^{Br})(N$_3$)] CH$_3$OH (**2**) correspond to the HS state of the metal center (Fig. 2): the Fe–N$_{am}$ bonds are the longest with d(Fe–N$_{am}$) = 2.183(4) Å, while the Fe–N$_{im}$ bonds are significantly shorter (2.109(4), 2.117(4) Å) and the Fe–N$_{term}$ bond is the shortest one (2.048(3) Å). The Fe–O bond lengths do not differ significantly from those observed for the LS structure of **1** and they amount to 1.916(3) and 1.968(3) Å. Remarkably, the dihedral angle (previously correlated to the occurrence of SCO in Fe(III) compounds with hexadentate ligands [41]) between the least-square planes of the aromatic rings is very narrow (α = 35.0°) in comparison with the other compounds reported in this article (Table 2). Also the angular distortion parameter (Σ(**2**) = 72.3°) is very large for the HS structure of this type of compounds (typical values for [Fe(X-L^5)L^1] HS compounds are close to 60°).

The structure of **2** is formed of the [Fe(L^{Br})(N$_3$)] molecules aligned in supramolecular chains and held by the N–H···N hydrogen bonds between the nitrogen atoms from the amine and azido groups of the adjacent complex molecules with d(N···N) = 3.036(6) Å. The crystal structure contains methanol molecules coupled with the [Fe(L^{Br})(N$_3$)] molecules by a relatively short hydrogen bond between the methanol oxygen atom and phenolato group of the complex molecule (Fig. 2): d(O···O) = 2.781(6) Å.

The compound [Fe(L^{Br})(NCS)] (**3**) crystallizes in the monoclinic space group Pn. The chromophore bond lengths and angular distortion parameter (Σ(**3**) = 56.3°) refer to the HS state (Table 2).

The crystal structure is formed of the chains of the [Fe(L^{Br})(NCS)] molecules interconnected by weak NH···S hydrogen bonds between the nitrogen atoms from the amine groups and sulfur atoms of the thiocyanato ligand from the adjacent complex molecules (d(N···S) = 3.323(7) Å). The thiocyanato sulfur atoms are further involved in other non-covalent interactions – the supramolecular [Fe(L^{Br})(NCS)]$_n$ chains are mutually interlocked by weak Br···S non-covalent contacts (Fig. 3) with d(Br···S) = 3.481(3) and 3.564(4) Å (sum of the van der Waals radii of the Br···S pair is 3.650 Å).

The bond lengths (Fig. 4) within the chromophore of [Fe(L^{Br})(NCSe)] (**4**) at T = 193 K are close to the typical LS values with the longest bond between the iron atom and the amine nitrogen atom: d(Fe–N$_{am}$) = 2.013(7) Å. The Fe–N$_{im}$, Fe–N$_{term}$ and Fe–O bond lengths are significantly shorter: d(Fe–N$_{im}$) = 1.937(7), 1.967(7); d(Fe–N$_{term}$) = 1.944(6); d(Fe–O) = 1.896(6), 1.872(5) Å. The N–Fe–N and N–Fe–O bond angles of the *trans* bonds in the chromophore are close to linearity and their values range from 174.9° to 177.6°. Also, the *cis* chromophore angles adopt values close to the right angle (ideal octahedron): from 84.4° to 94.4°. This causes a

Table 1
Crystallographic data for compounds **1–4**.

	1	2	3	4
	[Fe(L^{Br})Cl]·0.5H$_2$O	[Fe(L^{Br})(N$_3$)]·CH$_3$OH	[Fe(L^{Br})(NCS)]	[Fe(L^{Br})(NCSe)]
M/g mol^{-1}	581.49	611.09	595.11	642.01
T/K	90(1)	293(1)	100(1)	193(1)
Crystal system	triclinic	monoclinic	monoclinic	monoclinic
Space group	$P\bar{1}$	$P2_1/c$	Pn	$P2_1/c$
a (Å)	12.1643(7)	12.6077(3)	12.1647(6)	8.31180(10)
b (Å)	12.9750(7)	15.7666(4)	7.9347(4)	12.99640(10)
c (Å)	14.8456(8)	12.7549(4)	12.4122(6)	20.23030(10)
α (°)	77.065(3)	90	90	90
β (°)	72.484(2)	112.623(3)	115.540(2)	97.503(3)
γ (°)	66.470(2)	90	90	90
V (Å)^3	2034.22(19)	2340.34(11)	1081.00(9)	2166.64(3)
Z	2	4	2	4
$R_{int}/R_1/wR_2(I > 2\sigma(I))$	0.0272/0.0259/0.0613	0.0281/0.0500/0.1102	0.0717/0.0472/0.1257	0.0629/0.0782/0.2352
CCD deposit number	998903	998904	998905	998906

Table 2
Selected structural parameters for the title compounds.

Compound	Behavior	Fe–N$_{am}$ (Å)	Fe–X (Å)[a]	Fe–N$_{im}$ (Å)[b]	Fe–O (Å)[c]	Σ[d](°)	α[e](°)	Ref.
[Fe(L^{Br})(Cl)]·0.5H$_2$O (**1**)	HS	2.188[f]	2.352[f]	2.088	1.959	62.3/52.3	63.1/54.2	This work
[Fe(L^{Br})(NCS)] (**3**)	HS	2.207	2.111	2.099	1.927	56.3	67.7	This work
[Fe(L^{Br})(N$_3$)]·CH$_3$OH (**2**)	SCO	2.183	2.048	2.113	1.942	72.3	35.0	This work
[Fe(L^{Br})(NCSe)] (**4**)	SCO	2.013	1.944	1.952	1.884	27.8	85.9	This work
[Fe(L^{Cl})(Cl)]·0.25H$_2$O	HS	2.199[f]	2.361[f]	2.095	1.958	66.9/53.1	62.2/53.4	[9]
[Fe(L^{Cl})(NCO)]	HS	2.205[f]	1.996[f]	2.093	1.954	55.4/57.3	69.0/61.6	[9]
[Fe(L^{Cl})(NCS)]	SCO	2.000	1.944	1.932	1.879	27.1	84.5	[9]
[Fe(L^{Cl})(NCSe)]	SCO	2.001	1.952	1.932	1.881	26.9	85.5	[9]
[Fe(L^{Cl})(CN)]·H$_2$O	LS	2.012[f]	1.959[f]	1.934	1.903	19.3/28.8	65.9/56.0	[9]
[Fe(L)(CN)]·CH$_3$OH	LS	2.000	1.962	1.922	1.880	24.6	76.0	[10]
[Fe(3^{t}Bu5Me-L)(NCS)]	HS	2.191	2.100	2.096	1.916	56.0	75.6	[11]
[Fe(3MeO-L)(NCO)]·CH$_3$OH	HS	2.218[f]	2.081[f]	2.078	1.946	54.0[f]	73.3/82.8	[11]
[Fe(3MeO-L)(N$_3$)]	HS	2.211	2.085	2.085	1.936	57.4	58.1	[11]
[Fe(3MeO-L)(CN)]·CH$_3$OH	LS	2.028[f]	1.971[f]	1.935	1.904	26.0[f]	69.1/71.5	[11]
[Fe(3EtO-L)(CN)]·H$_2$O	LS	2.010	1.975	1.944	1.904	20.8	66.4	[11]

[a] The bond length between the iron atom and the donor atom of the monodentate ligand.

[b] The average value calculated from the iron-imino nitrogen bond lengths.

[c] The average value calculated from the Fe–O bond lengths.

[d] The angular distortion from the ideal octahedron Σ is calculated as sum of the absolute values of the deviations of the twelve *cis* chromophore angles from the ideal value 90°.

[e] The dihedral angle (α) between the least-square planes of the aromatic rings.

[f] The average value calculated from two bond lengths/parameters. Ligand abbreviations: H$_2$L = N,N'-bis(1-hydroxy-2-benzyliden)-1,6-diamino-4-azahexane, H$_2$L^{Br} = N,N'-bis(1-hydroxy-4-bromo-2-benzyliden)-1,6-diamino-4-azahexane, H$_2$L^{Cl} = N,N'-bis(1-hydroxy-4-chloro-2-benzyliden)-1,6-diamino-4-azahexane, H$_2$3MeO-L = N,N'-bis(1-hydroxy-6-methoxy-2-benzyliden)-1,6-diamino-4-azahexane, H$_2$3EtO-L = N,N'-bis(1-hydroxy-6-ethoxy-2-benzyliden)-1,6-diamino-4-azahexane, H$_2$3^{t}Bu5Me-L = N,N'-bis(1-hydroxy-4-methyl-6-tert-buthyl-2-benzyliden)-1,6-diamino-4-azahexane.
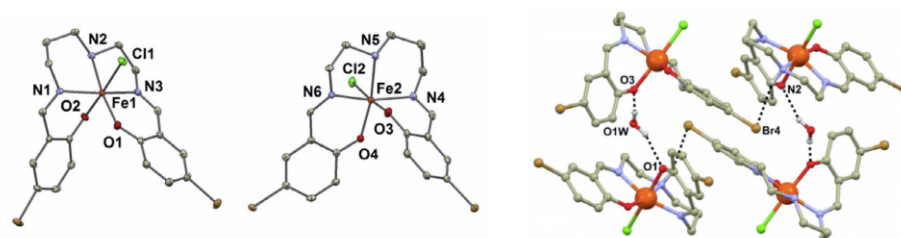
Fig. 1. Molecular structure of **1** (ORTEP drawing with thermal ellipsoids at the 50% probability level). Selected bond lengths (Å): Fe1–O2 = 1.8986(19), Fe1–O1 = 2.0246(18), Fe1–N3 = 2.087(2), Fe1–N1 = 2.091(3), Fe1–N2 = 2.178(2), Fe2–O4 = 1.9097(19), Fe2–O3 = 2.0012(18), Fe2–N4 = 2.081(2), Fe2–N6 = 2.094(2), Fe2–N5 = 2.198(3), Fe2–Cl2 = 2.3569(6). Right – the crystal packing in **1**. Hydrogen atoms are omitted for clarity except for those involved in the hydrogen bonds (dashed lines).

low-value of the spin dependent parameter of the angular distortion from the ideal octahedron: Σ(**4**) = 27.8°. The compound **4** is isostructural with [Fe(L^{Cl})(NCR)] complexes [9] (R = S and Se) and

consists of supramolecular dimers linked by rather weak non-covalent N–H···Br interactions with d(N···Br) = 3.506(6) Å. This alignment is supported by π–π stacking interactions of the
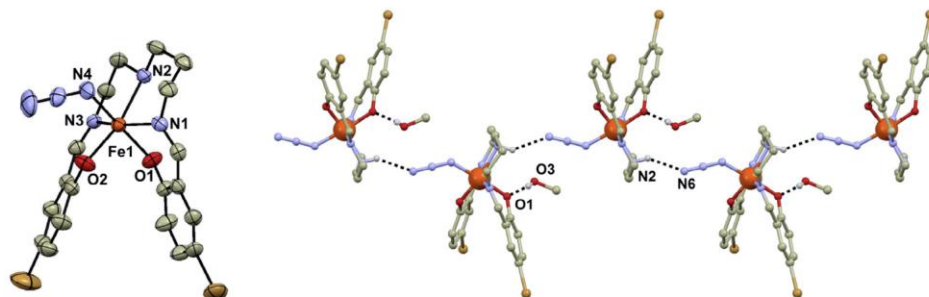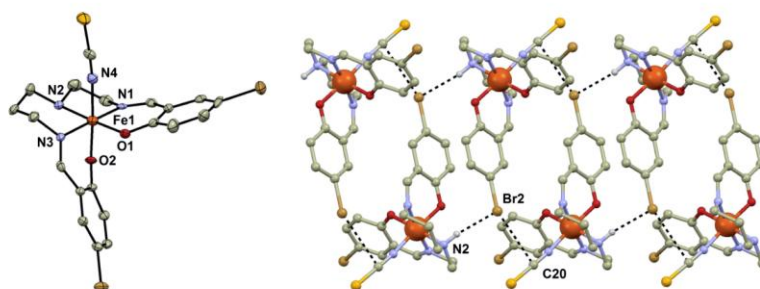
Fig. 2. Molecular structure of **2** (ORTEP drawing with thermal ellipsoids at the 50% probability level. Selected bond lengths (Å): Fe1–N1 = 2.117(4), Fe1–N3 = 2.109(4), Fe1–N2 = 2.183(4), Fe1–N4 = 2.048(3), Fe1–O1 = 1.968(3), Fe1–O2 = 1.916(3). Right – the crystal packing in **2**. Hydrogen atoms are omitted for clarity except for those involved in the hydrogen bonds (dashed lines).
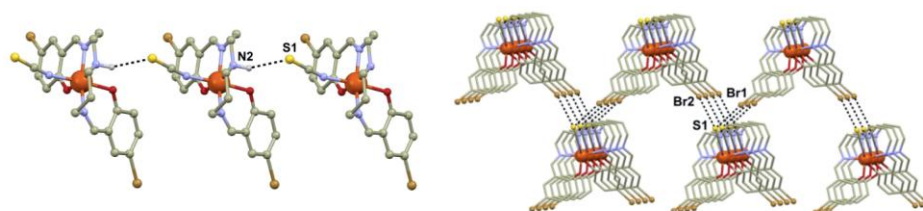
Fig. 3. The supramolecular chains [Fe(L^{Br})(NCS)]$_n$ in **3**. Right: Interconnection of the chain substructures by Br$\cdots$S non-covalent contacts (dashed lines) in **3**. Hydrogen atoms are omitted for clarity (except for those involved in the hydrogen bonds). Selected bond lengths (Å): Fe1–N1 = 2.099(5), Fe1–N2 = 2.207(9), Fe1–N3 = 2.099(5), Fe1–N4 = 2.111(7), Fe1–O1 = 1.905(7), Fe1–O2 = 1.948(5).


Fig. 4. Molecular structure of **4** (ORTEP drawing with thermal ellipsoids at the 50% probability level). Right: The crystal packing in **4**. Hydrogen atoms are omitted for clarity except for those involved in the hydrogen bonds (dashed lines). Selected bond lengths (Å) in **4**: Fe1–O1 = 1.896(6), Fe1–O2 = 1.872(5), Fe1–N1 = 1.937(7), Fe1–N4 = 1.944(6), Fe1–N3 = 1.967(7), Fe1–N2 = 2.013(7).

neighboring complex molecules with the centroid–centroid distance of 3.700(5) Å and by short C$\cdots$Br contacts with d(C$\cdots$Br) = 3.474(8) Å (sum of the van der Waals radii of the C$\cdots$Br pair is 3.650 Å, Fig. 4).

2.2. Magnetic data

The magnetic functions of complexes **1–4** are shown in Fig. 5. The complex **1**, [Fe(L^{Br})Cl]$_2$·H$_2$O, is high-spin in the whole temperature interval ($S = 5/2$), however, the structural data show that there are two units bridged by a rather strong hydrogen bond (*vide supra*) therefore the value of the magnetic moment is higher than in the case of the monomeric complex **2**. The model of exchange

coupled dimers combined with the zero field splitting (abbr. ZFS) was employed in the data analysis (for more details, see ESI) [42]. The temperature dependence of the magnetic susceptibility and the field dependence of the magnetization (ESI, Fig. S1) are fitted simultaneously thus allowing more reliable determination of the sign and value of independent parameters, namely the isotropic exchange coupling constant J, the axial zero-field splitting parameter D, the isotropic gyromagnetic factor g, the Weiss constant Θ and the temperature-independent susceptibility α_{TIM} (not to be confused with the dihedral angle where no lower index is used). Their optimum values were found as: $J/hc = -0.145$ cm^{-1}, $g = 1.984$, $\alpha_{TIM} = 4.76 \times 10^{-9}$ m^3 mol^{-1}, $D/hc = -1.02$ cm^{-1}, $\Theta = -0.130$ K; the corresponding discrepancy factors are
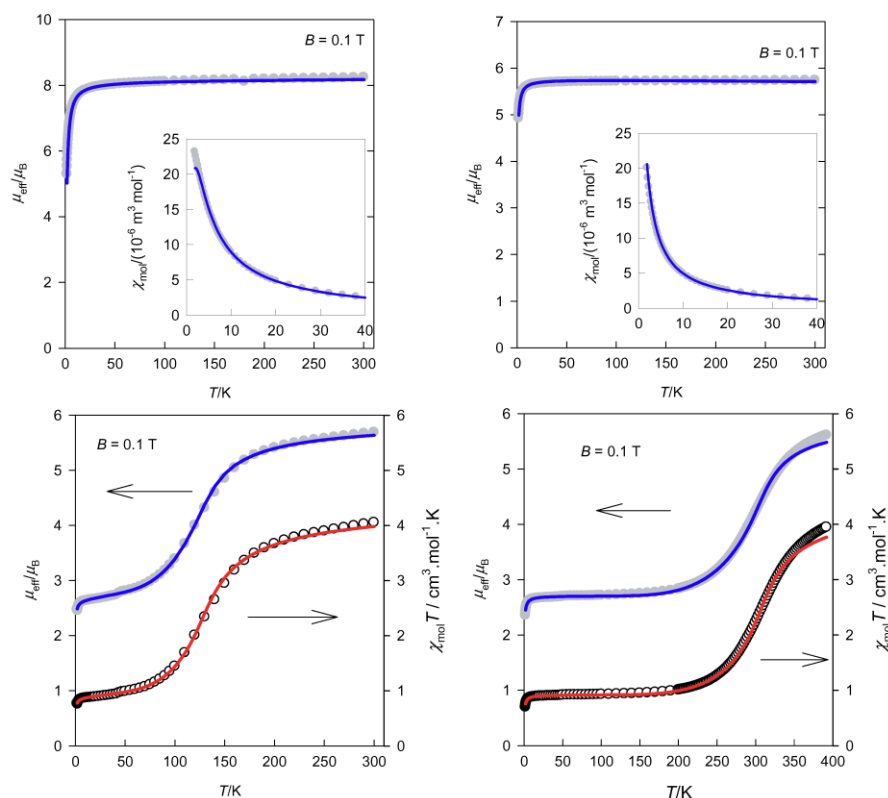
Fig. 5. Effective magnetic moment for **1** (up left), **2** (bottom left), **3** (up right) and **4** (bottom right). The inset for **1** and **3** shows the low temperature fit of the magnetic susceptibility. The empty circles for **2** and **4** show the $\chi_m T$ product which is directionally proportional to the high spin fraction. Circles – experimental data, solid lines – fitted.

$R(\chi) = 0.039$ and $R(M) = 0.042$ for the susceptibility and magnetization, respectively. Here; J is too small in order to cause a maximum at the susceptibility curve above 1.9 K, nevertheless, it is responsible for a rapid drop of the effective magnetic moment at the lowest temperatures (Fig. 5).

Also the complex **3**, [Fe(L^{Br})(NCS)], is high-spin in the whole temperature range and the same approach can be used as for **1** except that no magnetic exchange is present. The data fitting gave the following set of optimum parameters: $g = 1.926$, $\alpha_{TIM} = -2.98 \times 10^{-9}$ m^3 mol^{-1}, $D/hc = -0.53$ cm^{-1}, $\Theta = -0.130$ K; $R(\chi) = 0.011$, $R(M) = 0.015$. In this case the drop of the effective magnetic moment at low temperature originates in the zero-field splitting of the HS state and the molecular field effect (Fig. 5).

For the complexes **2**, [Fe(L^{Br})(N$_3$)] and **4**, [Fe(L^{Br})(NCSe)] gradual SCO between $S_L = 1/2$ and $S_H = 5/2$ is visible. For **4**, the effective magnetic moment stays almost constant between 5 and 200 K; below 5 K its decrease is registered. Above $T > 200$ K gradual SCO proceeds and it is not complete until $T = 390$ K when $\mu_{eff} = 5.61$ μ_B; $S_H = 5/2$ assumes $\mu_{eff} = 5.92$ μ_B. For both complexes the magnetization per formula unit at $M_1 = M_{mol}/N_A\mu_B = 1.5$ is much higher than $M_1 = 1.0$ expected for the $S_L = 1/2$ and $g_L = 2$ system (ESI, Fig. S1). This fact was modeled by two approaches: (i) the model A assumes a rather large magnetogyric factor $g_L > 3$ owing to the presence of low-lying excited states belonging to the high-spin state; (ii) the model B assumes a presence of a "frozen" high spin state, i.e. by
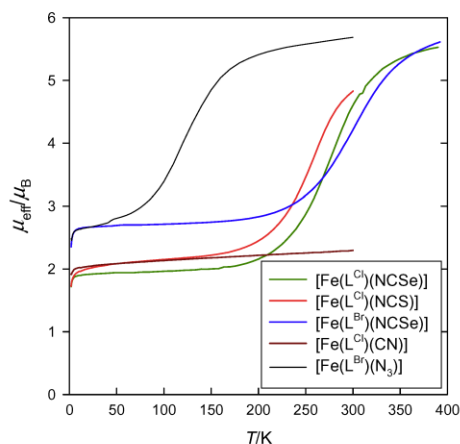
Fig. 6. Comparison of the spin crossover behavior for related complexes (including compounds from [9]).

Table 3
Review of spin crossover parameters in Fe(III) complexes with pentadentate Schiff-base ligands.

Compound	Model	S_L–S_H	T_c (K)	Magnetic parameters	Ref.
[Fe(L^{Br})(N_3)]·CH$_3$OH (**2**)	A	1/2–5/2	143	g_L = 2.95, Θ_L = −0.09 K, $\alpha_{TIM,L}$ = 36.8 × 10^{-9} m^3 mol^{-1}, g_H = 2.02, $\alpha_{TIM,H}$ = 0.0 × 10^{-9} m^3 mol^{-1}, E/k_B = 197 K, Γ/k_B = 76.0 K, $\bar{\nu}_L$ = 336 cm^{-1}, $\bar{\nu}_H$ = 292 cm^{-1}; $R(\chi)$ = 0.028 and $R(M)$ = 0.048; ΔH = 1.64 kJ mol^{-1}, ΔS = 11.5 J K^{-1} mol^{-1}	This work
	B	1/2–5/2	140	g_L = 2.12, Θ_L = −0.00 K, $\alpha_{TIM,L}$ = 30.0 × 10^{-9} m^3 mol^{-1}, g_H = 2.00, Θ_H = 0.46 K, $\alpha_{TIM,H}$ = 0.0 × 10^{-9} m^3 mol^{-1}, E/k_B = 203 K, Γ/k_B = 84.0 K, $\bar{\nu}_L$ = 302 cm^{-1}, $\bar{\nu}_H$ = 263 cm^{-1}, x_{frz} = 0.11; $R(\chi)$ = 0.021 and $R(M)$ = 0.031; ΔH = 1.69 kJ mol^{-1}, ΔS = 12.1 J K^{-1} mol^{-1}	This work
[Fe(L^{Cl})(NCS)]	A	1/2–5/2	280	g_L = 2.38, Θ_L = −0.91 K, $\alpha_{TIM,L}$ = +5.0 × 10^{-9} m^3 mol^{-1}, g_H = 2.0, E/k_B = 694 K, Γ/k_B = 180 K, $\bar{\nu}_L$ = 306 cm^{-1}, $\bar{\nu}_H$ = 250 cm^{-1}; ΔH = 5.77 kJ mol^{-1}, ΔS = 20.6 J K^{-1} mol^{-1}	[9]
[Fe(L^{Cl})(NCSe)]	A	1/2–5/2	293	g_L = 2.20, Θ_L = −0.20 K, $\alpha_{TIM,L}$ = +2.6 × 10^{-9} m^3 mol^{-1}, g_H = 2.0, E/k_B = 787 K, Γ/k_B = 197 K, $\bar{\nu}_L$ = 320 cm^{-1}, $\bar{\nu}_H$ = 254 cm^{-1}; ΔH = 6.54 kJ mol^{-1}, ΔS = 22.3 J K^{-1} mol^{-1}	[9]
[Fe(L^{Br})(NCSe)] (**4**)	A	1/2–5/2	326	g_L = 3.11, Θ_L = −0.48 K, g_H = 2.14, $\alpha_{TIM,H}$ = 0.41 × 10^{-9} m^3 mol^{-1}, E/k_B = 725 K, Γ/k_B = 215 K, $\bar{\nu}_L$ = 275 cm^{-1}, $\bar{\nu}_H$ = 239 cm^{-1}; $R(\chi)$ = 0.020 and $R(M)$ = 0.036; ΔH = 6.03 kJ mol^{-1}, ΔS = 18.5 J K^{-1} mol^{-1}	This work
	B	1/2–5/2	317	g_L = 2.20, Θ_L = 0.00 K, $\alpha_{TIM,L}$ = 0.00 × 10^{-9} m^3 mol^{-1}, g_H = 2.05, Θ_H = −0.90 K, $\alpha_{TIM,H}$ = 0.00 × 10^{-9} m^3 mol^{-1}, E/k_B = 743 K, Γ/k_B = 226 K, $\bar{\nu}_L$ = 224 cm^{-1}, $\bar{\nu}_H$ = 195 cm^{-1}, x_{frz} = 0.11; $R(\chi)$ = 0.039 and $R(M)$ = 0.040; ΔH = 6.18 kJ mol^{-1}, ΔS = 19.5 J K^{-1} mol^{-1}	This work
[Fe(L^{Cl})(CN)]		1/2	–	g_L = 2.36, Θ_L = −0.060 K, α_{TIM} = +5.7 × 10^{-9} m^3 mol^{-1}	[9]

cooling down, not all molecules switch their state (ESI, Fig. S2). The obtained value of the transition enthalpy is ΔH = 6.03 kJ mol^{-1} and 6.18 kJ mol^{-1}, the transition entropy ΔS = 18.5 J K^{-1} mol^{-1} and 19.5 J K^{-1} mol^{-1} and the characteristic temperature T_c = 326 K and 317 K for the model A and B, respectively. In both models $\Gamma/k_B < T_c$ so that a thermal hysteresis is absent. The optimum parameters resulting from the fitting procedure are collected in Table 3 and the fitted data are displayed as solid lines in Fig. 5 for the case of model B.

Substitution of the NCSe$^-$ ligand for N_3^- led to significant lowering of the transition temperature, but the complex **2** still shows SCO (Fig. 5). The same fitting procedure was applied with the results ΔH = 1.64 kJ mol^{-1} and 1.69 kJ mol^{-1}, ΔS = 11.5 J K^{-1} mol^{-1} and 12.1 J K^{-1} mol^{-1} and T_c = 143 K and 140 K, for models A and B, respectively. The cooperativeness is again below the limiting value for the hysteresis.

Thermal evolution of the effective magnetic moment for [Fe($L^{Cl/Br}$)X] complexes is compared in Fig. 6. The quantitative characteristics, as they result from the fitting procedure are listed in Table 3. It can be concluded that SCO centered near the room temperature is associated with a considerable transition enthalpy of the order of $\Delta H \sim$ 5.8–6.5 kJ mol^{-1}. The transition entropy varies as ΔS = 18.5–22.3 J K^{-1} mol^{-1}, which means that a considerable contribution from molecular vibrations assists.

3. Discussion

A detailed analysis of the crystal and molecular structures reveals that the occurrence of SCO in the series of the [Fe($L^{Cl/Br}$)(L^1)] compounds is influenced by a number of factors. First, the expected isostructurality of the isothiocyanato and isoselenocyanato compounds is not preserved within these two series: only the compounds [Fe(L^{Cl})(NCS)], [Fe(L^{Cl})(NCSe)] and [Fe(L^{Br})(NCSe)] (**4**) are isostructural ($P2_1/c$, Fig. 6) and they exhibit SCO. The [Fe(L^{Br})(NCS)] compound (**3**) possesses different crystal packing (Pn, Fig. 4) and it stays HS over the whole temperature range (Fig. 5).

When inspecting their molecular structures at the chromophore level (compounds **3** and **4**), it is apparent that they do not differ in bond lengths or bond angles significantly from the typical LS/HS forms of the SCO compounds, or from pure HS compounds reported for this type of complexes previously [9,12]. Thus there is no evidence that there exists any structural difference in the

[Fe(L^{Br})(NCS)] complex molecule, which would lead to lowering of the overall ligand-field strength resulting in stabilization of the HS state. Only a very slight difference between the ligand field strengths of the L^{Cl} and L^{Br} ligands can be deduced from the transition temperatures of the SCO compounds: T_c([Fe(L^{Cl})(NCSe)]) = 293 K and T_c([Fe(L^{Br})(NCSe)]) ≈ 320 K. The alteration of the L^1 ligand from NCSe$^-$ to NCS$^-$ does not lead to a sizable decrease of the increment to the crystal-field strength ($\Delta = g_M f_L$); f_L(NCS$^-$) = 1.02 while f_L(NCSe$^-$) = 1.05 (f_L(Cl) = 0.78).

When inspecting the topology of the complex molecule, a significant difference can be found: the α parameter describing the dihedral angle between the planes of the aromatic rings differs significantly when comparing three SCO compounds (α = 84.5–85.9°) with compound **3** (α = 67.7°, Table 2). This difference opens a question if the molecular shape can play a dominant role in hindering the SCO behavior in **3** as it was observed previously for a group of [Fe^{III}(R-L^6)]$^+$ complexes [41] (H$_2$R-L^6 = variously substituted H$_2$ sal$_2$trien). In these compounds the purely LS or HS complexes prefer different molecular shapes (α is significantly larger for HS compounds) [44]. However, this might not be the case for **3** and it can be documented by the example of compound **2**, which has a very low value of the α parameter (α = 35.0°, Table 2) but still exhibits SCO (Fig. 6). Furthermore, there are several examples of purely HS [Fe(L^a)(NCS)] compounds [12] (H$_2$L^a stands for 2-{3-[2-(1-hydroxynaphthalen-2-yl)methylenaminoethylaminopropylimino]methyl}naphthalene-1-ol) with very low α values ranging from 17° to 25°; this is in a clear contradiction with the magneto-structural correlation found for the [Fe^{III}(R-L^6)]$^+$ complexes.

Remarkably, the crystal structure of **2** consists of the supramolecular chains of the [Fe(L^{Br})(N_3)] molecules held by N–H⋯N hydrogen bonds. It must be noted that such structural motif (i.e. assembly to chain supramolecular structure by NH⋯N/O hydrogen bonding) was observed for similar SCO compounds [Fe(L^n)(NCO)] and [Fe(L^n)(N_3)] previously [11] (H$_2$L^n stands for N,N'-bis(2-hydroxy-naphthylidene)-1,6-diamino-4-azahexane); however, in the case of **2** an additional methanol molecule is found in the crystal structure (Fig. 2). On the other hand, the previously reported compound with similar composition, [Fe(3MeO-L)(N_3)], does not possess the above mentioned structural motif and it does not exhibit SCO.[11] This brings discussion back to the importance of the isostructurality, or in other words, of preservation of the SCO molecular packing motifs and it underlines the importance of molecular organization in the solid state for the occurrence and character of SCO [45].

4. Conclusion

In this work we reported on a series of Fe(III) complexes of the general formula [Fe(L^{Br})(L^1)] involving the pentadentate Schiff-base ligand (L^{Br})$^{2-}$ and (pseudo)halide coligands L^1 = Cl$^-$ (**1**), N$_3^-$ (**2**), NCS$^-$ (**3**) and NCSe$^-$ (**4**). These compounds were characterized by single-crystal X-ray diffraction and by magnetic measurements, which revealed that two of them, [Fe(L^{Br})(N$_3$)]·CH$_3$OH and [Fe(L^{Br})(NCSe)], exhibit weakly cooperative incomplete SCO with T_c = 143 K or 140 K (**2**) and 326 K or 317 K (**4**) (modelled by two different approaches), while compounds **1** and **3** are purely HS.

In the case of the compound **1**, the non-occurrence of SCO was explained on the basis of low ligand-field strength arising from the weak π-donor chlorido ligand. Furthermore, this compound exhibits weak intermolecular magnetic exchange coupling (J/hc = 0.145 cm^{-1}) mediated by a water molecule involved in hydrogen bonds interconnecting phenolato oxygen atoms from the neighboring [Fe(L^{Br})(Cl)] molecules. The stabilization of the HS state in the [Fe(L^{Br})(NCS)] compound was explained on the basis of the different crystal packing motif in comparison with the herein reported [Fe(L^{Br})(NCSe)] compound or previously reported [Fe(L^{Cl})(NCS)] and [Fe(L^{Cl})(NCSe)], which all exhibit SCO and they are mutually isostructural.

5. Experimental

5.1. Synthesis

5.1.1. [Fe(L^{Br})Cl]·0.5H$_2$O, **1**

The Schiff-condensation of 5-bromo-2-hydroxybenzaldehyde (2.0 mmol) with an asymmetric triamine, 1,6-diamino-4-azahexane, H$_2$N(CH$_2$)$_3$NH(CH$_2$)$_2$NH$_2$ in the ratio of 2:1 in 30 cm^3 of methanol resulted in a pentadentate Schiff-base ligand (bright yellow solution) according to Scheme 1. The reaction mixture was stirred at 55 °C for 30 min. This mixture was combined with a methanol solution of FeCl$_3$·6H$_2$O (2.0 mmol in 10 cm^3) at 55 °C for 15 min. Then, the solution of triethylamine (3.8 mmol in 5 cm^3 of methanol) was added drop wise. After 40 min of stirring at the boiling temperature, the black powder was separated by filtration on a fritted funnel, washed with cold methanol and diethyl ether (yield 36%). The filtrate was left to evaporate spontaneously. A few days later, black crystals were separated. Yield: 37%. C$_{19}$H$_{20}$Br$_2$FeClN$_3$O$_{2.5}$ (M = 581.49). *Anal.* Calc.: C, 39.25; H, 3.47; N, 7.23. Found: C, 39.06; H, 3.57; N, 7.32%.

5.1.2. [Fe(L^{Br})(N$_3$)] CH$_3$OH, **2**

A methanol solution of **1** (8.734.10^{-2} mmol, 20 cm^3) was combined with a methanol solution of NaN$_3$ (9.61·10^{-2} mmol in 10 cm^3) and the mixture was stirred for 60 min at the boiling temperature. The prepared solution was filtered and the filtrate was left for evaporation. The next day black crystals were isolated. Yield: 35%. C$_{20}$H$_{23}$Br$_2$FeN$_6$O$_3$ (M = 611.09). *Anal.* Calc.: C, 39.31; H, 3.79; N, 13.75. Found: C, 39.66; H, 3.56; N, 14.07%.

5.1.3. [Fe(L^{Br})(NCS)], **3**

Compound **1** (0.2 g, 0.4 mmol) was dissolved in 80 cm^3 methanol and combined with 0.041 g (0.42 mmol) KNCS in 20 cm^3 of methanol. Then, the solution was stirred for 60 min and filtered. Black single crystals were obtained by slow evaporation at room temperature. C$_{20}$H$_{19}$FeN$_4$O$_2$Br$_2$S$_1$ (M = 595.11). *Anal.* Calc.: C, 40.37; H, 3.22; N, 9.41. Found: C, 39.98; H, 3.21; N, 9.30; IR (ATR): $\tilde{v}$(N–H) = 3166 cm^{-1}, $\tilde{v}$(C–H) = 2913 cm^{-1} (m), $\tilde{v}$(NCS) = 2052 cm^{-1}, $\tilde{v}$(C=N) = 1616 cm^{-1}.

5.1.4. [Fe(L^{Br})(NCSe)], **4**

Compound **1** (0.2 g, 0.4 mmol) was dissolved in 80 cm^3 of methanol and combined with 0.061 g (0.42 mmol) KNCSe in 20 cm^3 of methanol. Then, the solution was stirred for 60 min and filtered. Black single crystals were obtained by slow evaporation at room temperature. C$_{20}$H$_{19}$FeN$_4$O$_2$Br$_2$Se$_1$ (M = 642.01). *Anal.* Calc.: C, 37.42; H, 2.98; N, 8.73. Found: C, 37.32; H, 2.93; N, 8.43, IR (ATR): $\tilde{v}$(N–H) = 3219 cm^{-1}, $\tilde{v}$(C–H) = 2921 cm^{-1} (m), $\tilde{v}$(NCSe) = 2061 cm^{-1}, $\tilde{v}$(C=N) = 1616 cm^{-1}.

5.2. X-ray structure analysis

Single crystal X-ray diffraction data were collected on diffractometers Bruker X8 APEX-II or Oxford Diffraction Xcalibur with the Sapphire CCD detector and fine-focused sealed tube (Mo Kα radiation, λ = 0.71073 Å or Cu Kα radiation, λ = 1.54184 Å). All structures were solved by direct methods using SHELXS-97 [46] incorporated into the WINGX program package [47]. For each structure its space group was checked by the ADSYMM procedure of the PLATON software [48]. All structures were refined using full-matrix least-squares on Fo^2-Fc^2 with SHELXL-2014 or SHELXL-97 with anisotropic displacement parameters for all non-hydrogen atoms [46]. The hydrogen atoms were placed into the calculated positions and they were included into the riding model approximation, with U_{iso} = 1.2/1.5 U_{eq}. The structure were drawn by MERCURY software [49].

5.3. Magnetic data

The magnetic data were taken with the SQUID apparatus (MPMS-XL7, Quantum Design) using the RSO mode of detection with ca 20 mg of the sample encapsulated in a gelatin-made sample holder. The magnetic susceptibility taken at B = 0.1 T was corrected for the underlying diamagnetism and converted to the effective magnetic moment. The magnetization was measured at two temperatures: T = 2.0 and T = 4.6 K.

Appendix A. Supplementary data

CCDC 998903–998906 contain the supplementary crystallographic data for complexes **1**–**4**, respectively. These data can be obtained free of charge via http://www.ccdc.cam.ac.uk/conts/retrieving.html, or from the Cambridge Crystallographic Data Centre, 12 Union Road, Cambridge CB2 1EZ, UK; fax: (+44) 1223-336-033; or e-mail: deposit@ccdc.cam.ac.uk. Supplementary data associated with this article can be found, in the online version, at http://dx.doi.org/10.1016/j.poly.2014.11.014.

References

[1] L. Cambi, L. Szegö, Ber. Dtsch. Chem. Ges. (A and B Series) 64 (1931) 2591.
[2] L. Cambi, L. Szegö, Ber. Dtsch. Chem. Ges. (A and B Series) 66 (1933) 656.
[3] L. Cambi, L. Malatesta, Ber. Dtsch. Chem. Ges. (A and B Series) 70 (1937) 2067.
[4] (a) P.J. van Koningsbruggen, Y. Maeda, H. Oshio, Top. Curr. Chem. 233 (2004) 259;
   (b) M. Nihei, T. Shiga, Y. Maeda, H. Oshio, Coord. Chem. Rev. 251 (2007) 2606;
   (c) J. Olguin, S. Brooker, Spin-Crossover in Discrete Polynuclear Complexes, in: Malcolm A. Halcrow (Ed.), Spin-Crossover Materials: Properties and Applications, Wiley, 2013;
   (d) K.S. Murray, The Development of Spin-Crossover Research, in: Malcolm A. Halcrow (Ed.), Spin-Crossover Materials: Properties and Applications, Wiley, 2013;

(e) P.N. Martinho, C. Rajnák, M. Ruben, Nanoparticles, Thin Films and Surface Patterns From Spin Crossover Materials and Electrical Spin State Control, in: Malcolm A. Halcrow (Ed.), Spin-Crossover Materials: Properties and Applications, Wiley, 2013.

[5] (a) P. Gütlich, A.B. Gaspar, Y. Garcia Beilstein, J. Org. Chem. 9 (2013) 342;
(b) A. Bousseksou, G. Molnár, L. Salmon, W. Nicolazzi, Chem. Soc. Rev. 40 (2011) 3313;
(c) G. Molnár, L. Salmon, W. Nicolazzi, F. Terki, A. Bousseksou, J. Mater. Chem. C 2 (2014) 1360.

[6] R. Boča, Y. Fukuda, M. Gembický, R. Herchel, R. Jaroščiak, W. Linert, F. Renz, J. Yuzurihara, Chem. Phys. Lett. 325 (2000) 411.

[7] F. Renz, P. Kerep, D. Hill, M. Klein, Hyperfine Interact. 168 (2007) 981.

[8] R. Boča, I. Nemec, I. Šalitroš, J. Pavlik, R. Herchel, F. Renz, Pure Appl. Chem. 81 (2009) 1357.

[9] C. Krüger, P. Augustín, I. Nemec, Z. Trávníček, H. Oshio, R. Boča, F. Renz, Eur. J. Inorg. Chem. 5–6 (2013) 902.

[10] I. Šalitroš, R. Boča, Ľ. Dlháň, M. Gembický, J. Kožíšek, J. Linares, J. Moncoľ, I. Nemec, L. Perašínová, F. Renz, I. Svoboda, H. Fuess, Eur. J. Inorg. Chem. (2009) 3141.

[11] I. Nemec, R. Herchel, R. Boča, Z. Trávníček, I. Svoboda, H. Fuess, W. Linert, Dalton Trans. 40 (2011) 10090.

[12] S. Mossin, B.L. Tran, D. Adhikari, M. Pink, F.W. Heinemann, J. Sutter, R.K. Szilagyi, K. Meyer, D.J. Mindiola, J. Am. Chem. Soc. 134 (2012) 13651.

[13] I. Nemec, R. Boča, R. Herchel, Z. Trávníček, M. Gembický, W. Linert, Monatsh. Chem. 140 (2009) 815.

[14] I. Šalitroš, R. Boča, R. Herchel, J. Moncoľ, I. Nemec, M. Ruben, F. Renz, Inorg. Chem. 51 (2012) 12755.

[15] R. Herchel, R. Boča, M. Gembický, J. Kožíšek, F. Renz, Inorg. Chem. 43 (2004) 4103.

[16] F. Renz, P. Kerep, Polyhedron 24 (2005) 2849.

[17] F. Renz, P. Kerep, Hyperfine Interact. 156/157 (2004) 371.

[18] F. Renz, M. Klein, S. Jung, P. Homenya, R. Saadat, D. Nariaki, Unimagazin (Leibniz Universität Hannover) 1–2 (2011) 24.

[19] F. Renz, D. Hill, M. Klein, J. Hefner, Polyhedron 26 (2007) 2325.

[20] R. Boča, I. Šalitroš, J. Kožíšek, J. Linares, J. Moncoľ, F. Renz, Dalton Trans. 39 (2010) 2198.

[21] F. Renz, S. Jung, M. Klein, M. Menzel, A.F. Thünemann, Polyhedron 2009 (1818) 28.

[22] F. Renz, C. Zaba, L. Rossberg, S. Jung, M. Klein, G. Klingelhöfer, A. Wünsche, S. Reinhardt, M. Menzel, Polyhedron 28 (2009) 2036.

[23] F. Renz, P. Kerep, D. Hill, R. Müller-Seipel, M. Klein, Hyperfine Interact. 168 (2006) 1051.

[24] M. Gembický, R. Boča, F. Renz, Inorg. Chem. Commun. 3 (2000) 662.

[25] F. Renz, V. Martinez, M. Klein, Hyperfine Interact. 184 (2008) 251.

[26] F. Renz, V. Martinez, M. Klein, M. Schott, T. Hoffmann, M. Blumers, I. Fleischer, G. Klingelhöfer, R. Boča, M. Menzel, Hyperfine Interact. 184 (2008) 259.

[27] S. Hayami, Z.Z. Gu, H. Yoshiki, A. Fujishima, O. Sato, J. Am. Chem. Soc. 123 (2001) 11644.

[28] J.K. Tang, J.S. Costa, S. Smulders, G. Molnár, A. Bousseksou, S.J. Teat, Y.G. Li, G.A. van Albada, P. Gamez, J. Reedijk, Inorg. Chem. 48 (2009) 2128.

[29] S. Dorbes, L. Valade, J.A. Real, C. Faulmann, Chem. Commun. (2005) 69.

[30] M.S. Haddad, W.D. Federer, M.W. Lynch, D.N. Hendrickson, Inorg. Chem. 20 (1981) 131.

[31] P. Gütlich, Eur. J. Inorg. Chem. (2013) 581.

[32] H.A. Goodwin, Coord. Chem. Rev. 18 (1976) 293.

[33] P. Gütlich, Struct. Bonding 44 (1981) 83.

[34] E. König, Struct. Bonding 76 (1991) 51.

[35] P. Gütlich, A. Hauser, H. Spiering, Angew. Chem. 106 (1994) 2109.

[36] P. Gütlich, Y. Garcia, H.A. Goodwin, Chem. Soc. Rev. 29 (2000) 419.

[37] P. Gütlich, Y. Garcia, P.J. van Koningsbruggen, F. Renz, in: F. Palacio, J. Schweizer, E. Ressouche (Eds.), Introduction to Physical Techniques in Molecular Magnetism, Part 1 – Structural and Magnetic Methods, University Press, Zaragoza, 2000.

[38] A. Hauser, J. Jeftić, H. Romstedt, R. Hinek, H. Spering, Coord. Chem. Rev. 190–192 (1999) 471.

[39] Spin crossover in transition metal compounds I, II, IIIP. Gütlich, H.A. Goodwin (Eds.), Topics in Current Chemistry, 233, Springer, Berlin, 2004.

[40] P. Gütlich, P. van Koningsbruggen, F. Renz, Struct. Bonding 107 (2004) 27.

[41] M.A. Halcrow, Chem. Soc. Rev. 40 (2011) 4119.

[42] R. Boča, Handbook of Magnetochemical Formulae, Elsevier, Amsterdam, 2012.

[43] I. Nemec, R. Herchel, I. Šalitroš, Z. Trávníček, J. Moncoľ, H. Fuess, M. Ruben, W. Linert, CrystEngComm 14 (2012) 7015.

[45] J. Tao, R.-J. Wei, R.-B. Huang, L.-S. Zheng, Chem. Soc. Rev. 41 (2012) 703.

[46] G.M. Sheldrick, Acta Crystallogr., Sect. A 64 (2008) 112.

[47] L.J. Farrugia, J. Appl. Crystallogr. 45 (2012) 849.

[48] (a) A.L. Speck, Acta Crystallogr., Sect. D. Biol. Crystallogr. 65 (2009) 148;
(b) Y. Le Page, MISSYM1.1 – a flexible new release, J. Appl. Crystallogr. 21 (1988) 983.

[49] C.F. Macrae, P.R. Edgington, P. McCabe, E. Pidcock, G.P. Shields, R. Taylor, M. Towler, J. van de Streek, J. Appl. Crystallogr. 39 (2006) 453.

6.3 Hysteretic Spin Crossover in a Mononuclear Iron(III) Complex with a Pentadentate Schiff Base Ligand and NCSe⁻ Coligand

Christoph Krüger[‡], Lars Heyer[‡], Daniel Unruh, Annika Preiss, Ľubor Dlháň, Roman Boča, Franz Renz

‡ These two authors contributed equally to this study.

The revised manuscript has been already under submission and will be published in the early 2016.

Revised manuscript for Inorganica Chimica Acta, Christoph Krüger, Lars Heyer, Daniel Unruh, Annika Preiss, Ľubor Dlháň, Roman Boča, Franz Renz, Hysteretic Spin crossover in a Mononuclear Iron(III) Complex with a Pentadentate Schiff Base Ligand and NCSe⁻ Coligand, submitted and will be published approximately early 2016.

Preface

The present paper "Hysteretic Spin crossover in a Mononuclear Iron(III) Complex with a Pentadentate Schiff Base Ligand and NCSe⁻ Coligand" has been submitted already and will be published in the journal *Inorganica Chimica Acta* in early 2016. The publication deals with an extension of previous results. Eight novel Fe^{III} complexes with the general formula [Fe(3,5-X-salpet)(anion)] containing an asymmetric pentadentate N_3O_2 Schiff base ligand with anion = Cl, NCS, NCSe, N_3 and X = Cl or Br are presented. All complexes exhibit high spin behaviour except [Fe(3,5-Cl-salpet)(NCSe)] which shows a cooperative spin crossover process in the range 70-130 K, with a hysteresis of ca. 24 K. Within the class of complexes including salpet ligands in mononuclear Fe^{III} spin crossover compounds with a pseudo-octahedral sphere, the observed loop is the widest so far.

The complexes were synthesised by the author of this thesis, as well as partly analysed by A. Preiss, D. Unruh. Magnetic measurements have been carried out and fitted by Prof. Dr. Roman Boča and Dr. Lubor Dlhan.

The manuscript has been written by Prof. Dr. Roman Boča, Dipl.-Chem. Lars Heyer and the author of this thesis. The refinements have been done together with Prof. Dr. Franz Renz.

Hysteretic Spin-Crossover in a Mononuclear Iron(III) Complex with a Pentadentate Schiff Base Ligand and NCSe[-] Coligand

Christoph Krüger [1,‡], Lars Heyer [1,‡], Daniel Unruh [1], Annika Preiss [1], Ľubor Dlháň [2], Roman Boča [3], Franz Renz [1]

[1] Institute of Inorganic Chemistry, Leibniz University Hannover, 30167 Hannover, Germany

[2] Institute of Inorganic Chemistry, FCHPT, Slovak University of Technology 81237 Bratislava, Slovakia

[3] Department of Chemistry, FPV, University of SS Cyril and Methodius, 91701 Trnava, Slovakia

‡ These two authors contributed equally to this study.

Abstract

Novel iron(III) mononuclear complex [Fe(3,5-Cl-*salpet*)(NCSe)] with a pentadentate Schiff base ligand 3,5-Cl-*salpet* and NCSe[-] as a coligand shows a thermally induced spin crossover between 123 K (warming) and 99 K (cooling) with hysteresis width of 24 K. Other complexes of [Fe(3,5-X-*salpet*)(Y)] type with X = Cl^{-} or Br^{-} and Y = NCS[-], NCSe[-] and N_3^- are high-spin over the whole temperature region.

1. Introduction

Stimuli-responsive spin state switching of complex compounds – referred to as spin crossover (SCO) – has been a broad topic in the field of coordination chemistry [1-9]. First discovered by Cambi et al. in 1930 [10-12], this fascinating phenomenon gathered increasing interest over the last decades due to its potential for the miniaturization of electronic devices. In this case, the bottom-up approach of nanoscopic applications based on stimuli-responsive complexes has been discussed [13].

The spin crossover effect mainly occurs in 3d-transition metal coordination compounds with d^4-d^7 configuration. For example, iron(III) complexes in an (pseudo-)octahedral ligand sphere exhibit a spin transition from its ground low-spin state (LS, $S = 1/2$) to an excited metastable high-spin state (HS, $S = 5/2$). This transition is followed by changes of the macroscopic material properties (e.g. color, magnetism, volume, etc.) and could be triggered chemically (e.g. solvents, ligand exchange, isomerization, etc.) as well as physically (e.g. temperature, light, pressure) [14]. The spin state switching can take place either gradually or abruptly. In addition, in some complexes intermolecular interactions lead to appearance of thermal hysteresis. As thermal propagation has been the most observed stimulus a transition temperature $T_{1/2}$ with a LS/HS-ratio of 0.5 is defined as a significant parameter in spin crossover research [8].

The spin transition characteristics are influenced by modification of the coordination sphere (e.g. ligand-changes, chemical substitutions, etc.). Good examples of such modifications have been observed in iron(III) coordination compounds containing pentadentate N_3O_2-donating Schiff base ligands (L^{XY}) and a monodentate ligand (L^1) [15-22]. A great variety of those complexes of the general composition [$Fe^{III}(L^{XY})L^1$] has been discussed in recent years. Alongside a great number of mononuclear compounds multinuclear complexes containing up to twelve metal-centers have been investigated [15-35].

In this work, we are reporting about mononuclear compounds of the type [Fe(3,5-X-*salpet*)(Y)] with X = Cl$^-$ or Br$^-$ and Y = NCS$^-$, NCSe$^-$ or N$_3^-$ with a novel pentadentate Schiff base ligand. The magnetic susceptibility is recorded, analyzed, and compared with the [Fe(5-X-*salpet*)(Y)] type complexes reported earlier [18, 21, 22, 36].

2. Experimental

The synthesis part is summarized with X = Cl or Br and Y = NCS, NCSe or N_3. IR measurements in transmission were made with a Tensor-27 device from BRUKER. The magnetic data (temperature dependence of the magnetic susceptibility, and field dependence of the magnetization) was taken with a SQUID magnetometer (Quantum Design, MPMS-XL7) in the RSO mode of the data acquisition at $B_{DC} = 0.1$ T. Raw data were corrected for the underlying diamagnetism and presented in the form of the temperature evolution of the effective magnetic moment, and the field dependence of the magnetization per formula unit.

2.1. [Fe(3,5-X-*salpet*)(Cl)]:

N-(2-aminoethyl)-1,3-propanediamine (10 mmol) and 3,5-dichlorosalicylaldehyde/ 3,5-Dibromosalicylaldehyde (20 mmol) were dissolved in 120 cm^3 methanol. The solution was boiled under reflux for 15 min, $FeCl_3·6H_2O$ (10 mmol) in 25 cm^3 methanol was added and further boiled for 1 h. After cooling in a fridge for 24 h, the product was filtered off and dried at room temperature.

2.1.1. [Fe(3,5-Cl-*salpet*)(Cl)]:

$C_{19}H_{17}FeN_3O_2Cl_5$ yield 4.2 g (76 %), (M = 552.48 g/mol) Calculated: C, 41.31 %; H, 3.10 %; N, 7.61 %; C/N, 5.43. ESI-MS: [Fe(3,5-Cl-*salpet*)]$^+$: Calculated = 516.9389 g/mol; Found: 516.8966 g/mol. IR (Tr): v(N-H) = 3260 cm^{-1}, v(C-H) = 2901 cm^{-1}, v(C=N) = 1638, 1610 cm^{-1}.

2.1.2. [Fe(3,5-Br-*salpet*)(Cl)]:

$C_{19}H_{17}FeN_3O_2ClBr_4$ yield 3.72 g (51 %), (M = 730.28 g/mol) Calculated: C, 31.25 %; H, 2.35 %; N, 5.75 %; C/N, 5.43. ESI-MS: [Fe(3,5-Br-*salpet*)]$^+$: Calculated = 694.7357 g/mol; Found: 694.6833 g/mol. (IR (Tr): v(N-H) = 3050 cm^{-1}, v(C=N) = 1633, 1609 cm^{-1}.

2.2. [Fe(3,5-X-*salpet*)(Y)]:

KY/NaN$_3$ (0.42 mmol) was dissolved in 30 cm^3 methanol and added to a solution of [Fe(3,5-X-*salpet*)(Cl)] (0.4 mmol) in 100 cm^3 methanol. The mixture was stirred in an ultrasonic bath for 5 minutes and filtered afterwards. Single crystals were obtained by slow evaporation in a beaker at room temperature.

2.2.1. [Fe(3,5-Cl-*salpet*)(NCS)]:

$C_{20}H_{17}FeN_4O_2Cl_4S$ yield 0.2 g (85 %), (M = 575.11 g/mol) Calculated: C, 41.77 %; H, 2.98 %; N, 9.74 %; C/N, 4.29. Found: C, 41.49 %; H, 2.91 %; N, 9.56 %; C/N, 4.34. IR (Tr): v(N-H) = 3265 cm^{-1}, v(C-H) = 2902 cm^{-1}, v(NCS) = 2036 cm^{-1}, v(C=N) = 1639,1618 cm^{-1}.

2.2.2. [Fe(3,5-Cl-*salpet*)(NCSe)]:

$C_{20}H_{17}FeN_4O_2Cl_4Se$ yield 0.2 g (82 %), (M = 621.99 g/mol) Calculated: C, 38.62 %; H, 2.75 %; N, 9.01 %; C/N, 4.29. Found: C, 38.71 %; H, 2.64; N, 9.05 %; C/N, 4.78. IR (Tr): v(N-H) = 3266 cm^{-1}, v(C-H) = 2904 cm^{-1}, v(NCSe) = 2037 cm^{-1}, v(C=N) = 1640, 1619 cm^{-1}.

2.2.3. [Fe(3,5-Cl-*salpet*)(N$_3$)]:

$C_{19}H_{17}FeN_6O_2Cl_4$ yield 0.19 g (83 %), (M = 559.03 g/mol) Calculated: C, 40.82 %; H, 3.07 %; N, 15.03 %; C/N, 2.72. Found: C, 40.77 %; H, 2.96 %; N, 14.91 %; C/N, 2.73. IR (Tr): v(N-H) = 3244 cm^{-1}, v(C-H) = 2903 cm^{-1}, v(N$_3$) = 2085 cm^{-1}, v(C=N) = 1632, 1610 cm^{-1}.

2.2.4. [Fe(3,5-Br-*salpet*)(NCS)]:

$C_{20}H_{17}FeN_4O_2Br_4S$ yield 0.13 g (42 %), (M = 752.91 g/mol) Calculated: C, 31.91 %; H, 2.28 %; N, 7.44 %; C/N, 4.29. Found: C, 31.51 %; H, 2.23 %; N, 7.03 %; C/N, 4.48. IR (Tr): v(N-H) = 3243 cm^{-1}, v(C-H) = 2926 cm^{-1}, v(NCS) = 2036 cm^{-1}, v(C=N) = 1637, 1616 cm^{-1}.

2.2.5. [Fe(3,5-Br-*salpet*)(NCSe)]:

$C_{20}H_{17}FeN_4O_2Br_4Se$ yield 0.13 g (40 %), (M = 799.80 g/mol) Calculated: C, 30.03 %; H, 2.14 %; N, 7.01 %; C/N, 4.28. Found: C, 30.25 %; H, 2.18 %; N, 6.35 %; C/N, 4.76. IR (Tr): v(N-H) = 3246 cm^{-1}, v(C-H) = 2909 cm^{-1}, v(NCSe) = 2038 cm^{-1}, v(C=N) = 1637, 1616 cm^{-1}.

2.2.6. [Fe(3,5-Br-*salpet*)(N₃)]:

$C_{19}H_{17}FeN_6O_2Br_4$ yield 0.13 g (44 %), (M = 736.85 g/mol) Calculated: C, 30.97 %; H, 2.33 %; N, 11.41 %; C/N, 2.71. Found: C, 30.88 %; H, 2.41 %; N, 11.41 %; C/N, 2.71. IR (Tr): v(N-H) = 3241 cm^{-1}, v(C-H) = 2928 cm^{-1}, v(N₃) = 2084 cm^{-1}, v(C=N) = 1631, 1609 cm^{-1}.
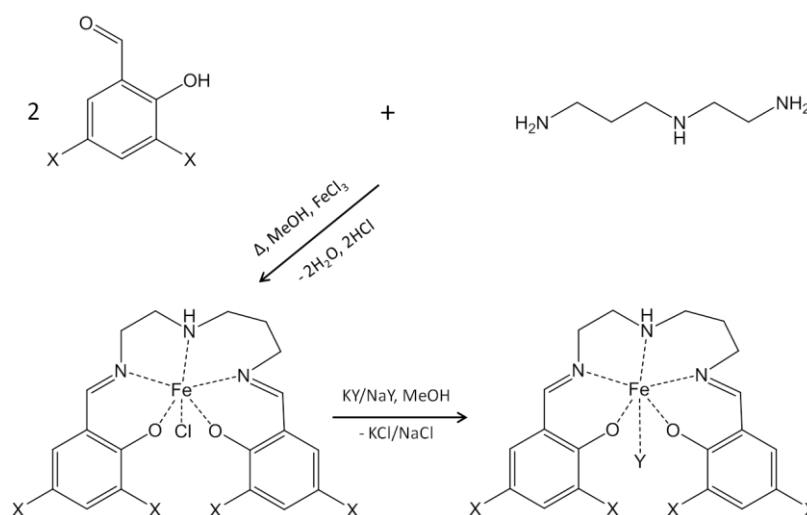
Fig. 1. Sketch of the pentadentate ligands 3,5-Cl-*salpet*, 3,5-Br-*salpet* (X = Cl or Br) and their complexes (Y = NCS, NCSe or N₃).

3. Results and discussion

The magnetic data for complexes showing a thermally induced spin crossover (Fig. 2) was analyzed by using Ising-like model with vibrations (equivalent to the thermodynamic regular solution model) [37] yielding the enthalpy ΔH and entropy ΔS of the spin transition along with the critical temperature T_c and the solid-state cooperativeness Γ. These data are presented in Table 1 and compared with the literature data for similar systems.
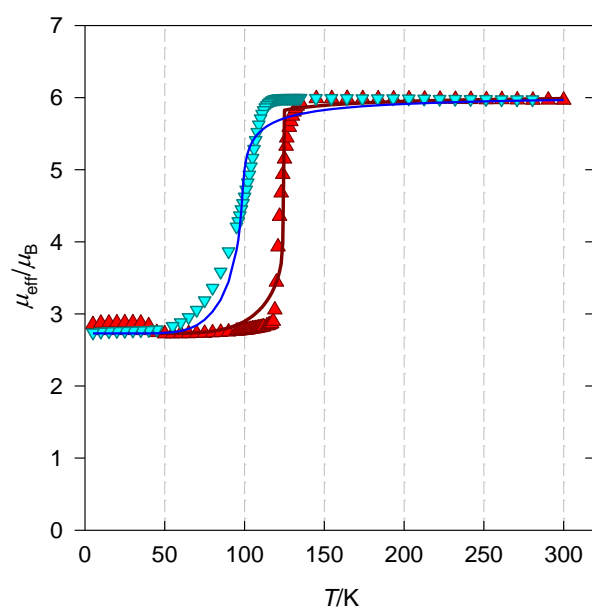

Fig. 2. Temperature dependence of the effective magnetic moment for [Fe(3,5-Cl-salpet)(NCSe)], **1**, in the heating/cooling regime ($M = 661.1$ g mol^{-1}). Lines - fitted with parameters: $g_{LS} = 3.15(9)$, $g_{HS} = 2.06(2)$, energy gap $E/k_B = 249(17)$ K, cooperativeness $\Gamma/k_B = 153(5)$ K, effective mode $\nu_L = 215(8)$ cm^{-1}, $\nu_L/\nu_H = 1.20$ in the heating direction ($R = 0.14$), and $\Gamma/k_B = 91(3)$ K, $\nu_L = 217(2)$ cm^{-1} in the cooling direction ($R = 0.067$).

Table 1. Thermodynamic parameters for mutually related Fe(III) spin crossover complexes. [a]

Compound	T_c/K	ΔH /kJ mol^{-1}	ΔS /J K^{-1} mol^{-1}	(Γ/k_B)/K	Ref.
[Fe(L^{ClCl})(NCSe)]	123 ↑	2.03	17.6	153	This work
	99 ↓	2.03	20.6	91	This work
[Fe(L^{Cl})(NCSe)]	293	6.54	22.3	197	Krüger 2013 [18]
[Fe(L^{Br})(NCSe)]	326	6.03	18.5	215	Krüger 2015 [36]
[Fe(L^{Cl})(NCS)]	280	5.77	20.6	180	Krüger 2013 [18]
[Fe(L^{Br})(N$_3$)]·MeOH	142	1.64	11.5	76	Krüger 2015 [36]
[Fe(*salpet*)(*atz*)]	416	15.3	36.8	284	Herchel 2013 [22]
[Fe(5Cl-*saldptn*)py]BPh$_4$	78	0.44	5.61	63	Boča 2000 [15]
[Fe(3MeO-*saldptn*)py]BPh$_4$	273	4.54	16.6	90	Boča 2000 [15]
[Fe(*saldptn*)py]BPh$_4$	310	5.42	17.5	150	Boča 2000 [15]
[Fe(3EtO-*salpet*)(NCS)]	84 ↑, 82 ↓ *	0.98	11.8	90	Masárová 2015 [38]
[Fe(*napet*)(NCS)]	174	3.08	17.1	135	Masárová 2015 [38]
[Fe(*napet*)(NCS)]·MEK	84				Nemec 2015 [21]
[Fe(*napet*)(NCS)]·DMF	235 ↑, 232 ↓				Nemec 2015 [21]
[Fe(*napet*)(NCS)]·DMSO	138 ↑, 127 ↓				Nemec 2015 [21]

[Fe(*napet*)(NCSe)]·DMF	244			Nemec 2015 [21]
[Fe(*napet*)(NCS)]·MeCN	151	1.92	12.5	87	Nemec 2011 [20]
[Fe(*napet*)(NCO)]	155	2.54	16.3	102	Nemec 2011 [20]
[Fe(*napet*)(NCSe)]·MeCN	170	2.29	13.3	99	Nemec 2011 [20]
[Fe(*napet*)(N_3)]·MeOH	122 $^\uparrow$, 117 $^\downarrow$	1.53	11.2	99	Nemec 2011 [20]

[a] Abbr. for ligands: L^X = 3-X-*salpet* and L^{XX} = 3,5-X-s*alpet*, *saldptn* = *N,N'*-bis(2-hydroxybenzyliden)-1,7-diamino-4-azaheptane, *napet* = *N,N'*-bis(2-hydroxynaphthylidene)-1,6-diamino-4-azahexane, H*atz* = 5-aminotetrazole. [*] - spin crossover between spins 3/2 → 5/2.

The complex **1** shows typical features of the spin crossover between the low-spin (S = 1/2, LS) and the high-spin (S = 5/2, HS) states. At the lowest recorded temperature the effective magnetic moment adopts a value of μ_{eff} = 2.8 μ_B which indicates that g_{LS} ~ 3 is much higher relative to the spin-only value (μ_{eff} = 1.7 μ_B for g_e = 2.0). This value is retained until 100 K when an increase followed by a jump into the high-spin state is observed. The spin crossover proceeds in a narrow interval: $T^\uparrow$(onset) = 118 K and $T^\uparrow$(complete) = 136 K. In the HS-state the value of μ_{eff} = 6.0 μ_B matches the spin-only value. On cooling down a thermal hysteresis is observed. However, the cooling path is more gradual with $T^\downarrow$(onset) = 115 K and $T^\downarrow$(complete) = 54 K.

The asymmetry of the hysteresis loop causes an obstacle for the data fitting. The regular solution model with cooperativeness and/or Ising-like model with vibrations can be applied only for the case of rectangular walls of the hysteresis loop. The angled walls can be reproduced by an extended model with Gaussian distribution of the cooperativeness [37, 39]. In the present case the heating path and the cooling path were fitted independently [40], giving rise to two distinct cooperativeness, $\Gamma^\uparrow$ = 153 K and $\Gamma^\downarrow$ = 91 K. The heating mode is highly cooperative, since $\Gamma^\uparrow > T_c^\uparrow/k_B$ = 123 K; the cooling mode, on the contrary, is gradual because $\Gamma^\downarrow < T_c^\downarrow/k_B$ = 99 holds true.

A comparison of the spin crossover behavior for three related NCSe⁻ containing complexes is given in Fig. 3. It can be seen that the passage from the bisubstituted ligand L^{ClCl} to monosubstituted one L^{Cl} rises the transition temperature substantially but the hysteretic behavior disappears because the cooperativeness is incapable of compensating a substantial increase of ΔH.
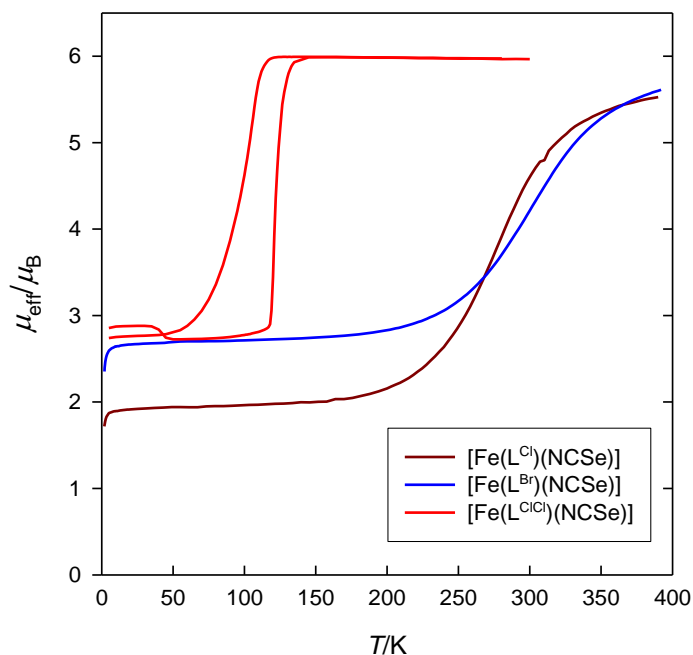

Fig. 3 (color online). Comparison of spin crossover in $[Fe(L^X\text{-}salpet)]$ type complexes with a varied pentadentate Schiff-base ligand $L^X\text{-}salpet$ (X = 3-Cl, 3-Br, and 3,5-Cl) and a coligand NCSe⁻.

Five high-spin complexes $[Fe(3,5\text{-}Cl\text{-}salpet)(N_3)]$, $[Fe(3,5\text{-}Cl\text{-}salpet)(NCS)]$, $[Fe(3,5\text{-}Br\text{-}salpet)(NCS)]$, $[Fe(3,5\text{-}Br\text{-}salpet)(NCSe)]$, and $[Fe(3,5\text{-}Br\text{-}salpet)(N_3)]$ display the effective magnetic moment that is constant down to $T = 20$ K and then it drops down as an effect of the zero-field splitting for Fe(III) centre (see Electronic Supplementary Information).

4. Conclusion

Of seven complexes of the [Fe(3,5-X-*salpet*)(Y)] type, with a pentadentate Schiff base ligand 3,5-Cl-*salpet*, X = Cl$^-$ or Br$^-$, and Y = NCS$^-$, NCSe$^-$ or N$_3^-$, six are high-spin over the whole temperature interval. The complex [Fe(3,5-Cl-*salpet*)(NCSe)] shows a thermally induced spin crossover between $T_c^{\uparrow}$ = 123 K (warming) and $T_c^{\downarrow}$ = 99 K (cooling) with a hysteresis width of ΔT = 24 K. The parameter of the solid-state cooperativeness on heating $\Gamma^{\uparrow} > T_c^{\uparrow}/k_B$ = 123 K causes an abrupt switching whereas in the cooling mode $\Gamma^{\downarrow} < T_c^{\downarrow}/k_B$ = 99 results in rather gradual transition. An analogous monosubstituted complex [Fe(3-Cl-*salpet*)(NCSe)] exhibits a room-temperature switching with T_c = 293 K but the cooperativeness of Γ = 197 K is incapable to induce the thermal hysteresis.

References

[1]   H. A. Goodwin, *Coord. Chem. Rev.* 1976, 18, 293.

[2]   P. Gütlich, *Struct. Bonding* 1981, 44, 83.

[3]   E. König, *Struct. Bonding* 1991, 76, 51.

[4]   P. Gütlich, A. Hauser, H. Spiering, *Angew. Chem.* 1994, 106, 2109.

[5]   P. Gütlich, Y. Garcia, H. A. Goodwin, *Chem. Soc. Rev.* 2000, 29, 419.

[6]   P. Gütlich, Y. Garcia, P. J. van Koningsbruggen, F. Renz: *Introduction to Physical Techniques in Molecular Magnetism, Part 1- Structural and Magnetic Methods* (Eds.: F. Palacio, J. Schweizer, E. Ressouche), University Press, Zaragoza, 2000.

[7]   A. Hauser, J. Jeftic, H. Romstedt, R. Hinek, H. Spering, *Coord. Chem. Rev.* 1999, 190–192, 471.

[8]   P. Gütlich, H. A. Goodwin (Eds.), *Spin crossover in transition metal compounds I, II, III, in Topics in Current Chemistry*, Springer, Berlin, 2004, vol. 233-235.

[9]   P. Gütlich, P. van Koningsbruggen, F. Renz, *Struct. Bonding* 2004, 107, 27.

[10] L. Cambi, L. Szegö, *Ber. Dtsch. Chem. Ges. (A and B Series)* 1931, 64, 2591.

[11] L. Cambi, L. Szegö, *Ber. Dtsch. Chem. Ges. (A and B Series)* 1933, 66, 656.

[12] L. Cambi, L. Malatesta, *Ber. Dtsch. Chem. Ges. (A and B Series)* 1937, 70, 2067.

[13] (a) P. Gütlich, A.B. Gaspar, Y. Garcia *Beilstein, J. Org. Chem.* 2013, 9, 342; (b) A. Bousseksou, G. Molnár, L. Salmon, W. Nicolazzi, *Chem. Soc. Rev*. 2011, 40, 3313; (c) G. Molnár, L. Salmon, W. Nicolazzi, F. Terki, A. Bousseksou, J. *Mater. Chem. C* 2014, 2, 1360.

[14] P. Gütlich, *Eur. J. Inorg. Chem*. 2013, 581.

[15] R. Boča, Y. Fukuda, M. Gembický, R. Herchel, R. Jaroščiak, W. Linert, F. Renz, J. Yuzurihara, *Chem. Phys. Lett*. 2000, 325, 411-419.

[16] F. Renz, P. Kerep, D. Hill, M. Klein, *Hyperfine Interact.* 2006, 168, 981-987.

[17] R. Boča, I. Nemec, I. Šalitroš, J. Pavlik, R. Herchel, F. Renz, *Pure Appl. Chem*. 2009, 81, 1357.

[18] C. Krüger, P. Augustín, I. Nemec, Z. Trávníček, H. Oshio, R. Boča, F. Renz, *Eur. J. Inorg. Chem.,* 2013, 902.

[19] I. Šalitroš, R. Boča, Ľ. Dlháň, M. Gembický, J. Kožíšek, J. Linares, J. Moncoľ, I. Nemec, L. Perašínová, F. Renz, I. Svoboda, H. Fuess, *Eur. J. Inorg. Chem.* 2009, 3141.

[20] I. Nemec, R. Herchel, R. Boča, Z. Trávníček, I. Svoboda, H. Fuess. W. Linert, *Dalton Trans*. 2011, 40, 10090.

[21] I. Nemec, R. Herchel, Z. Trávníček, *Dalton Trans*. 2015, 44, 4474.

[22] R. Herchel, Z. Trávníček, *Dalton Trans*. 2013, 42, 16279.

[23] I. Nemec, R. Boča, R. Herchel, Z. Trávníček, M. Gembický, W. Linert, *Monatsh. Chem*. 2009, 140, 815.

[24] R. Herchel, R. Boča, M. Gembický, J. Kožíšek, F. Renz, *Inorg. Chem*. 2004, 43, 4103.

[25] F. Renz, P. Kerep, *Polyhedron* 2005, 24, 2849.

[26] F. Renz, P. Kerep, *Hyperfine Interact*. 2004, 156/157, 371.

[27] F. Renz,M. Klein, S. Jung, P. Homenya, R. Saadat, D. Nariaki, *Unimagazin*, Leibniz Universität Hannover, 2011, 1–2, 24.

[28] F. Renz, D. Hill, M. Klein, J. Hefner, *Polyhedron* 2007, 26, 2325.

[29] R. Boča, I. Šalitroš, J. Kožíšek, J. Linares, J. Moncoľ, F. Renz, *Dalton Trans*. 2010, 39, 2198.

[30] F. Renz, S. Jung, M. Klein, M. Menzel, A. F. Thünemann, *Polyhedron* 2009, 28, 1818.

[31] F. Renz, C. Zaba, L. Rossberg, S. Jung, M. Klein, G. Klingelhöfer, A. Wünsche, S. Reinhardt, M. Menzel, *Polyhedron* 2009, 28, 2036.

[32] F. Renz, P. Kerep, D. Hill, R. Müller-Seipel, M. Klein, *Hyperfine Interact*. 2006, 168, 1051.

[33] M. Gembický, R. Boča, F. Renz, *Inorg. Chem. Commun*. 2000, 3, 662.

[34] F. Renz, V. Martinez, M. Klein, *Hyperfine Interact*. 2008, 184, 251.

[35] F. Renz, V. Martinez, M. Klein, M. Schott, T. Hoffmann, M. Blumers, I. Fleischer, G. Klingelhöfer, R. Boča, M. Menzel, *Hyperfine Interact*. 2008, 184, 259.

[36] C. Krüger, P. Augustín, Ľ. Dlháň, J. Pavlik, J. Moncoľ, I. Nemec, R. Boča, F. Renz, *Polyhedron,* 2015, 87, 194.

[37] R. Boča, W. Linert *Monatsh. Chem*. 2003, 134, 199.

[38] P. Masárová, P. Zoufalý, J. Moncoľ, I. Nemec, J. Pavlik, M. Gembický, Z. Trávníček, R. Boča, I. Šalitroš, *New. J. Chem*. 2015, 39, 508.

[39] R. Boča, M. Boča, Ľ. Dlháň, K. Falk, H. Fuess, W. Haase, R. Jaroščiak, B. Papánková, F. Renz, M. Vrbová, R. Werner, *Inorg. Chem*. 40 (2001) 3025.

[40] R. Boča, *Program MIF with FIT module*. University of SS Cyril and Methodius, Trnava, © 2015.

6.4   A Rectangular Ni-Fe Cluster with Unusual Cyanide Bridges

Christoph Krüger, Hiroki Sato, Takuto Matsumoto, Takuya Shiga, Graham N. Newton, Franz Renz and Hiroki Oshio

The final publication is available at

http://pubs.rsc.org/en/Content/ArticleLanding/2012/DT/c2dt31152f#!divAbstract.

Preface

The present communication "A rectangular Ni-Fe cluster with unusual cyanide bridges" was published in *Dalton Transaction* in 2012. The work was performed in cooperation with the group of Prof. Dr. Hiroki Oshio in Tsukuba, Japan and deals with a novel asymmetric polycyanide iron complex, $K_2[Fe^{III}(L1)-(CN)_4](MeOH)$ (HL1 = 2,2´-(1H-pyrazole-3,5-diyl)bis-pyridine), and two kinds of enantiomeric nickel-iron squares $\{[Ni(L2^{R/S})]_2[Fe(L1)(CN)_4]_2\}\cdot 6H_2O\cdot 2MeOH$. The heterometallic nickel-iron rectangular molecule with Ni-NC-Fe bridges compromises two nickel ions, two chiral ligands and two tetracyanoferrate moieties. The nickel ion has an octahedral N_6 coordination geometry with donor atoms from the bidentate chiral ligand $L2^{R/S}$ ($L2^{R/S}$ = N-(2-pyridylmethylene)-(R/S)-1-phenylethylamine). Interestingly, the cyanide bridge between Ni und Fe ions shows an Ni-N-C angle of 105.0(3)° in the R-form and 104.8(3)° in the S-form. Magnetic measurements were collected in the range of 1.8-300 K. The values are larger than the expected for the sum of the uncorrelated spins of two Ni(II) and two Fe(III) ions. The data suggests that ferromagnetic interactions between nickel and iron ions are operative through the cyanide and pyrazolate bridges.

The work was performed by the author of this thesis and was supervised and supported by Dr. Takuya Shiga, Dr. Graham N. Newton, Dr. Takuto Matsumoto, as well as Hiroki Sato. The analysis of the single-crystal X-ray diffraction measurements and magnetic data were carried out with the help of Dr. Takuto Matsumoto and Dr. Takuya Shiga. Dr. Takuya Shiga and the author of this thesis wrote the initial manuscript which was refined with Prof. Dr. Franz Renz and Prof. Dr. Hiroki Oshio.

Dalton
Transactions

Dynamic Article Links ▶

www.rsc.org/dalton

COMMUNICATION

A rectangular Ni–Fe cluster with unusual cyanide bridges†

Christoph Krüger,[a,b] Hiroki Sato,[a] Takuto Matsumoto,[a] Takuya Shiga,[a] Graham N. Newton,[a] Franz Renz[b] and Hiroki Oshio*[a]

An asymmetric polycyanide iron complex, $K_2[Fe^{III}(L1)(CN)_4](MeOH)$ (HL1 = 2,2′-(1H-pyrazole-3,5-diyl)bis-pyridine), was synthesized and its complexation compatibility with nickel ions was examined. Two kinds of enantiomeric nickel–iron squares were obtained in the presence of a chiral bidentate capping ligand. The compounds display unusual cyanide bridge geometry and have ferromagnetic interactions between nickel and iron ions.

The cyanide group is a valuable unit for the construction of molecular assemblies with magnetic and electronic interactions between metal ions because it can form linear bridges between neighbouring metal centres. Cyanometallates are well known in the literature, and can form coordination bonds to transition metal ions through their terminal N donor atoms.[1] Many examples of functional cyanide-bridged molecular assemblies have been reported.[2] Indeed, molecular magnets such as single-molecule magnets (SMMs) and single chain magnets (SCMs), the properties of which are reliant upon the interactions mediated by cyanide bridges, can be controllably constructed following modular approaches to molecular design with cyanometallate units.[3,4] For example, combinations of building units with two or three free cyanide groups can often lead to the synthesis of square type $[M_2M'_2]$ molecules.[5] Such discrete molecules have been shown to display dynamic spin transition phenomena such as multi-spin crossover behaviour and electron-transfer-coupled spin transitions (ETCST).[6] The development of new polycyano building blocks may be important for the generation of novel functional molecular systems. Therefore, we have focussed on the syntheses of polycyano iron complexes with a polynucleating ligand. In this work, the bis-bidentate ligand, 3,5-bis(2-pyridyl)-pyrazolate (HL1), was chosen as the capping ligand and a novel tetracyanoferrate complex was developed. Using the tetracyano iron complex as a building block, two cyanide-bridged tetranuclear nickel–iron complexes were synthesized and their magnetic properties were investigated.

The tetracyanoferrate complex, $K_2[Fe^{III}(L1)(CN)_4](MeOH)$ (**1**·MeOH), was synthesized by the reaction of Fe-$(NH_4)_2(SO_4)_2$·$6H_2O$ in boiling water with HL1 and KCN.‡ Single crystal X-ray analysis of **1**·MeOH reveals that the pyrazolate group of the ligand is deprotonated and coordinates to one iron and one potassium ion which occupy the two bidentate sites of L1 (Fig. 1). The second potassium ion connects neighbouring complexes through the CN groups. **1** forms a one-dimensional network structure linked by potassium ions.§ The combination of the tetracyanoferrate complex **1** with $NiCl_2$·$6H_2O$ and the

*[a]Graduate School of Pure and Applied Sciences, University of Tsukuba, Tennodai 1-1-1, Tsukuba 305-8571, Japan.
E-mail: oshio@chem.tsukuba.ac.jp; Fax: +81 29 853 4238;
Tel: +81 29 853 4238
[b]Leibniz Universität Hannover, Institut für Anorganische Chemie, Callinstr. 9, D-30167 Hannover, Germany*
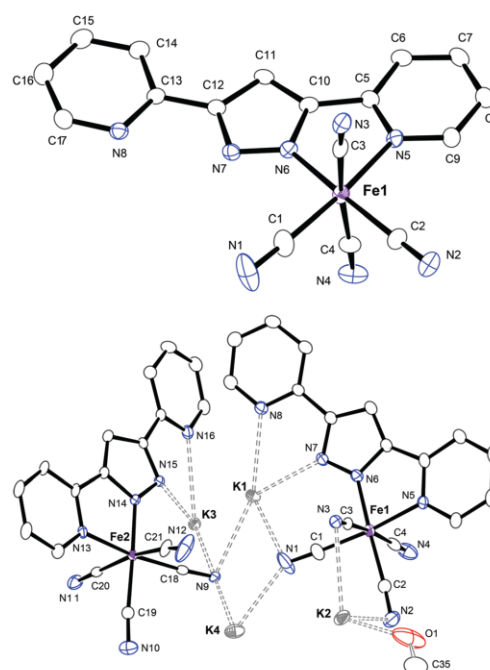
Fig. 1 Molecular structure of **1**. (top) Tetracyanoferrate moiety, (bottom) asymmetric unit. Fe centres in purple; K grey; N blue; O red; C white. Lattice solvent molecules were excluded for clarity.

chiral bidentate ligand L2^R (L2^R = N-(2-pyridylmethylene)-(R)-1-phenylethylamine) yielded a tetranuclear heterometallic complex, {[Ni(L2^R)]$_2$[Fe(L1)(CN)$_4$]$_2$}·6H$_2$O·2MeOH (2·6H$_2$O·2MeOH). The corresponding enantiomer 3 was prepared by the same method using L2^S (L2^S = N-(2-pyridylmethylene)-(S)-1-phenylethylamine).

X-ray structural analysis revealed that 2 and 3 were enantiomers. Complex 3 comprises two nickel ions, two chiral ligands and two tetracyanoferrate moieties, forming rectangular molecules with Ni–NC–Fe bridges, with the complex molecule located on a two-fold axis of symmetry. The nickel ion has an octahedral N$_6$ coordination geometry with donor atoms from the bidentate chiral ligand, the bidentate site of 1 and two cyanide groups, also from 1. Thus the building unit, 1, behaves simultaneously as a tridentate capping group and as a bridging ligand. Two nitrogen atoms (N9 and N10) of the supporting chiral ligand coordinate to the Ni1 atom, along with three nitrogen atoms (N1, N7, and N8) from 1, in which the N7 and N8 donor atoms belong to the bidentate site of L1. Interestingly, the cyanide nitrogen atom N1 bridges between Ni and Fe ions in an unusual manner: with an (Ni1–N1–C1) angle of 105.0(3)° in 2 and 104.8(3)° in 3. To the best of our knowledge, the sharpest Ni–N≡C angle reported in a cyanide-bridged square complex is 147.8(2)°,[7] while the sharpest reported in any species was in a dinuclear nickel complex displaying coordination angles of 111.2–112.9°.[8] The presented compounds thus contain the most acute Ni–N≡C angles observed to date (Fig. 2).

Magnetic susceptibility data for 2·11H$_2$O and 3·11H$_2$O were collected in the temperature range of 1.8–300 K under an applied magnetic field of 500 Oe (Fig. 3 and S2†). The $\chi_m T$ value for 3 was 3.43 emu mol^{-1} K at 300 K, larger than the value (2.75 emu mol^{-1} K) expected for the sum of the uncorrelated spins of two Ni(II) ions and two Fe(III) ions. These discrepancies are explained by the large g values of the nickel and iron ions.[9] As the temperature was lowered, the $\chi_m T$ value of 3 increased, reaching a maximum of 5.04 emu mol^{-1} K at 9.0 K, followed by a steep decrease to 4.24 emu mol^{-1} K at 1.8 K. The temperature dependence of the magnetic susceptibility data suggests that ferromagnetic interactions between nickel and iron ions are operative through the cyanide and pyrazolate bridges. The magnetic behaviour was analyzed for both samples with a Heisenberg spin model of $H = -2J_1 S_{Fe1}(S_{Ni1} + S_{Ni1*}) - 2J_2 S_{Fe1*}(S_{Ni1} + S_{Ni1*})$ for the data above 10 K, using julX.[10] In this simulation, intermolecular interactions based on a molecular field approximation zJ' ($\chi = \chi_0/[1 - \chi_0(2zJ'/Ng^2\mu_B^2)]$) were considered. The obtained best fit parameters for 2 and 3 were g_{Fe} = 2.31, 2.31, g_{Ni} = 2.18, 2.10, J_1 = +7.2, +7.0 cm^{-1}, J_2 = +4.2, +4.0 cm^{-1}, and zJ' = −1.5 K, −1.7 K, respectively. The zJ' parameters imply intermolecular magnetic interactions, but also include contributions from the magnetic anisotropy present in the system. The ferromagnetic arrangement of the spins leads to a spin ground state of S_T = 3. Neither 2 nor 3 showed any out of phase response in their ac magnetic susceptibility, suggesting they were not SMMs.

We synthesised a novel tetracyanoferrate building unit, using which two heterometallic nickel–iron rectangular complexes were obtained. The orientation of the cyanide group on the iron site led to very unusual Ni–N≡C bonding angles in 2 and 3. The investigation into the coordination behaviour of 1 showed

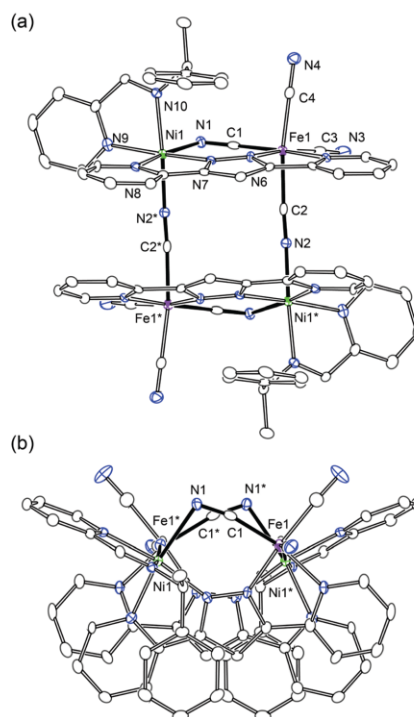Fig. 2   ORTEP diagrams of complex 3. (a) Top view, (b) side view. Selected bond angles: Ni1–N1–C1 104.8(3), Ni1*–N2–C2 170.2(4) (symmetry code: *, −x + 1, −y + 1, z).
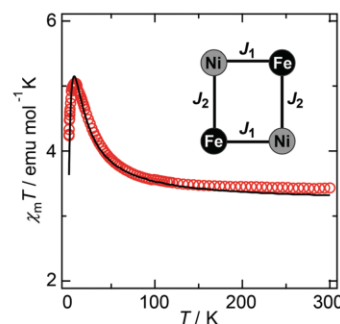

Fig. 3 $\chi_m T$ versus T plots for 3. The solid line indicates the theoretical value (see text).

that it tends to coordinate metal ions in a tridentate manner by adding a cyanide donor to the typically bidentate pyrazole–pyridine binding site, and can bridge to additional metal ions via its free cyanide groups. It is expected that 1 may be used to generate magnetic one-dimensional networks due to its charge of −2 and its four perpendicular cyanide ligands. This work will be

extended to investigate the combination of **1** with other transition metals and supporting ligands.

Notes and references

‡ $K_2[Fe^{III}(L1)(CN)_4](MeOH)$ (**1**·MeOH): To a suspension of HL1 (3.8 g, 17 mmol) in boiling water (100 cm^3), $Fe(NH_4)_2(SO_4)_2$·6H$_2$O (3.9 g, 10 mmol) was added. After stirring for a few minutes, a large excess of KCN (9.77 mg, 150 mmol) was added as a solid to the resultant dark red mixture. After boiling and stirring for a few minutes, the reaction mixture was filtered. The orange filtrate was cooled down to r.t. and left to stand for one day, after which time unreacted ligands had precipitated. The mixture was filtered again and left to stand undisturbed. After a few days, yellow microcrystals of the crude product were obtained. The yellow microcrystals were re-crystallized from methanol/*n*-butanol to afford purple needle crystals of $[\{K_2Fe^{III}(L1)(CN)_4\}_2(MeOH)]$·MeOH (**1**·MeOH). Anal. calcd for **1**·MeOH C$_{18}$H$_{13}$N$_8$FeK$_2$O$_1$: C, 44.00; H, 2.67; N, 22.80. Found: C, 43.71; H, 2.58; N, 22.70%.

$\{[Ni(L2^R)]_2[Fe(L1)(CN)_4]_2\}$·6H$_2$O (**2**·6H$_2$O): To an aqueous solution (5 cm^3) of **1** (31.88 mg, 0.06 mmol) was added a mixture of NiCl$_2$·6H$_2$O (14.26 mg, 0.06 mmol), 2-pyridine carbaldehyde (5.7 μL, 0.06 mmol) and *R*-phenylethylamine (7.6 μL, 0.06 mmol) in methanol (5 cm^3). After stirring for a few seconds, the resulting solution was filtered and left for a few days after which purple crystals were obtained. The crystals were filtered and recrystallized from methanol yielding purple platelet crystals of $\{[Ni(L2^R)]_2[Fe(L1)(CN)_4]_2\}$·6H$_2$O·2MeOH (**2**·6H$_2$O·2MeOH). They were collected by suction filtration and dried in air. Anal. calcd for **2**·11H$_2$O C$_{62}$H$_{88}$N$_{20}$Ni$_2$Fe$_2$O$_{11}$: C, 49.70; H, 4.57; N, 18.70. Found: C, 49.79; H, 4.43; N, 18.57%.

$\{[Ni(L2^S)]_2[Fe(L1)(CN)_4]_2\}$·11H$_2$O (**3**·11H$_2$O): Complex **3**·11H$_2$O was prepared by the same method as **2**, using *S*-phenylethylamine. Anal. calcd for **3**·11H$_2$O C$_{62}$H$_{88}$N$_{20}$Ni$_2$Fe$_2$O$_{11}$: C, 49.70; H, 4.57; N, 18.70. Found: C, 50.00; H, 4.50; N, 18.53%.

§ Crystal data for **1**: C$_{36}$H$_{26}$N$_{16}$Fe$_2$K$_4$O$_2$, M_r = 982.83, monoclinic, $P2_1/c$, a = 8.408(4), b = 20.572(10), c = 24.726(13) Å, β = 99.789(7), V = 4215(4) Å^3, Z = 4, d = 1.549 g cm^{-1}, μ = 1.138 mm^{-1}, $F(000)$ = 1992, GOF = 0.954. A total of 25 983 reflections were collected, 9551 of which were unique ($R_{(int)}$ = 0.1217). R_1 (wR_2) = 0.0740 (0.1833) for 563 parameters and 9551 reflections ($I > 2\sigma(I)$). Crystal data for **2**·6H$_2$O·2MeOH: C$_{64}$H$_{46}$N$_{20}$Ni$_2$Fe$_2$O$_8$, M_r = 1452.33, orthorhombic, $P2_12_12$, a = 13.334(2), b = 20.437(3), c = 11.9421(18) Å, V = 3254.5(9) Å^3, Z = 2, d = 1.482 g cm^{-1}, μ = 1.078 mm^{-1}, $F(000)$ = 1484, GOF = 1.043, Flack parameter of x = −0.004(14). A total of 18 523 reflections were collected, 7251 of which were unique ($R_{(int)}$ = 0.0412). R_1 (wR_2) = 0.0395 (0.0979) for 444 parameters and 7251 reflections ($I > 2\sigma(I)$). Crystal data for **3**·6H$_2$O·2MeOH: C$_{64}$H$_{44}$N$_{20}$Ni$_2$Fe$_2$O$_8$, M_r = 1450.31, orthorhombic, $P2_12_12$, a = 13.319(2), b = 20.390(3), c = 11.9344(18) Å, V = 3241.0(8) Å^3, Z = 2, d = 1.486 g cm^{-1}, μ = 1.082 mm^{-1}, $F(000)$ = 1480, GOF = 1.002, Flack parameter of x = −0.017(15). A total of 20 217 reflections were collected, 7363 of which were unique ($R_{(int)}$ = 0.0511). R_1 (wR_2) = 0.0498 (0.1003) for 444 parameters and 7363 reflections ($I > 2\sigma(I)$). The intensity data were collected on a Bruker SMART APEX diffractometer with graphite-monochromated Mo Kα radiation (λ = 0.71073 Å). Direct methods were used to solve the structure and to locate the heavy atoms using the SHELXL-97 program package. The remaining atoms were found from successive full-matrix least-squares refinements on F^2 and Fourier syntheses. Routine Lorentz polarization corrections and an absorption correction were applied. CCDC 883725–883727 for **1–3**, respectively.

1 W. P. Griffith, *Coord. Chem. Rev.*, 1975, **17**, 177–247; K. R. Dunbar and R. A. Heintz, *Prog. Inorg. Chem.*, 1997, **45**, 283–391 and references cited therein; M. Verdaguer, A. Bleuzen, V. Marvaud, J. Vaissermann, M. Seuleima, C. Desplanches, A. Scuiller, C. Train, R. Garde, G. Gelly, C. Lomenech, I. Rosenman, P. Veillet, C. Cartier and F. Villain, *Coord. Chem. Rev.*, 1999, **190–192**, 1023–1047, and references cited therein; M. Verdaguer, *Science*, 1996, **272**, 698–699.

2 W. Kosaka, K. Nomura, K. Hashimoto and S. Ohkoshi, *J. Am. Chem. Soc.*, 2005, **127**, 8590–8591; W. E. Buschmann, J. Ensling, P. Gütlich and J. S. Miller, *Chem.–Eur. J.*, 1999, **5**, 3019–3028; S. Ohkoshi, H. Tokoro, T. Matsuda, H. Takahashi, H. Irie and K. Hashimoto, *Angew. Chem., Int. Ed.*, 2007, **46**, 3238–3241; S. Ohkoshi, A. Fujishima and K. Hashimoto, *J. Am. Chem. Soc.*, 1998, **120**, 5349–5350; S. S. Kaye and J. R. Long, *J. Am. Chem. Soc.*, 2005, **127**, 6506–6507.

3 P. Gütlich, Y. Garcia and T. Woike, *Coord. Chem. Rev.*, 2001, **219**, 839–879; T. Mallah, S. Thiébaut, M. Verdaguer and P. Veillet, *Science*, 1993, **262**, 1554–1557; S. Ferlay, T. Mallah, R. Ouahès, P. Veillet and M. Verdaguer, *Nature*, 1995, **378**, 701–703; W. R. Entley and G. S. Girolami, *Science*, 1995, **268**, 397–400; S. Ohkoshi, A. Fujishima and K. Hashimoto, *J. Am. Chem. Soc.*, 1998, **120**, 5349–5350; Ø. Hatlevik, W. E. Buschmann, J. Zhang, J. L. Manson and J. S. Miller, *Adv. Mater.*, 1999, **11**, 914–918; S. M. Holmes and G. S. Girolami, *J. Am. Chem. Soc.*, 1999, **121**, 5593–5594; S. Ohkoshi, M. Mizuno, G. J. Hung and K. Hashimoto, *J. Phys. Chem. B*, 2000, **104**, 9365–9367; R. Garde, F. Villain and M. Verdaguer, *J. Am. Chem. Soc.*, 2002, **124**, 10531–10538; E. Coronado, M. C. Giménez-López, G. Levchenko, F. M. Romero, V. García-Baonza, A. Milner and M. Paz-Pasternak, *J. Am. Chem. Soc.*, 2005, **127**, 4580–4581; C. Avendano, M. G. Hilfiger, A. Prosvirin, C. Sanders, D. Stepien and K. R. Dunbar, *J. Am. Chem. Soc.*, 2010, **132**, 13123–13125; R. Boča, I. Šalitroš, J. Kožíšek, J. Linares, J. Moncol and F. Renz, *Dalton Trans.*, 2010, **39**, 2198–2200.

4 D. Li, S. Parkin, G. Wang, G. T. Yee, A. V. Prosvirin and S. M. Holmes, *Inorg. Chem.*, 2005, **44**, 4903–4905; W. Liu, C.-F. Wang, Y.-Z. Li, J.-L. Zuo and X.-Z. You, *Inorg. Chem.*, 2006, **45**, 10058–10065; D. Li, R. Clérac, G. Wang, G. T. Yee and S. M. Holmes, *Eur. J. Inorg. Chem.*, 2007, 1341–1346; C.-F. Wang, W. Liu, Y. Song, X.-H. Zhou, J.-L. Zuo and X.-Z. You, *Eur. J. Inorg. Chem.*, 2008, 717–727; D. Wu, Y. Zhang, W. Huanga and O. Sato, *Dalton Trans.*, 2010, **39**, 5500–5503; Y.-H. Peng, Y.-F. Meng, L. Hu, Q.-X. Li, Y.-Z. Li, J.-L. Zuo and X.-Z. You, *Inorg. Chem.*, 2010, **49**, 1905–1912; N. Hoshino, Y. Sekine, M. Nihei and H. Oshio, *Chem. Commun.*, 2010, **46**, 6117–6119; K. Park and S. M. Holmes, *Phys. Rev. B*, 2006, **74**, 224440-1-10.

5 G. N. Newton, M. Nihei and H. Oshio, *Eur. J. Inorg. Chem.*, 2011, **20**, 3019–3224, and references cited therein.

6 M. Nihei, M. Ui, M. Yokota, L. Han, A. Maeda, H. Kishida, H. Okamoto and H. Oshio, *Angew. Chem., Int. Ed.*, 2005, **44**, 6484–6487; M. Nihei, M. Ui and H. Oshio, *Polyhedron*, 2009, **28**, 1718–1721; I. Boldog, F. J. Muñoz-Lara, A. B. Gaspar, M. C. Muñoz, M. Seredyuk and J. A. Real, *Inorg. Chem.*, 2009, **48**, 3710–3719; A. Rodríguez-Diéguez, R. Kivekäs, R. Sillanpä, J. Cano, F. Lloret, V. McKee, H. Stoeckli-Evans and E. Colacio, *Inorg. Chem.*, 2006, **45**, 10537–10551; C. P. Berlinguette, A. Dragulescu-Andrasi, A. Sieber, J. R. Galán-Mascarós, H. U. Güdel, C. Achim and K. R. Dunbar, *J. Am. Chem. Soc.*, 2004, **126**, 6222–6223; C. P. Berlinguette, A. Dragulescu-Andrasi, A. Sieber, H. U. Güdel, C. Achim and K. R. Dunbar, *J. Am. Chem. Soc.*, 2005, **127**, 6766–6779; M. Shatruk, A. Dragulescu-Andrasi, K. E. Chambers, S. A. Stoian, E. L. Bominaar, C. Achim and K. R. Dunbar, *J. Am. Chem. Soc.*, 2007, **129**, 6104–6116; M. G. Hilfiger, M. Chen, T. V. Brinzari, T. M. Nocera, M. Shatruk, D. T. Petasis, J. L. Musfeldt, C. Achim and K. R. Dunbar, *Angew. Chem., Int. Ed.*, 2010, **49**, 1410–1413; D. Li, R. Clérac, O. Roubeau, E. Harté, C. Mathonière, R. Le Bris and S. M. Holmes, *J. Am. Chem. Soc.*, 2008, **130**, 252–258; Y. Zhang, D. Li, R. Clérac, M. Kalisz, C. Mathonière and S. M. Holmes, *Angew. Chem., Int. Ed.*, 2010, **49**, 3752–3756; M. Nihei, Y. Sekine, N. Suganami and H. Oshio, *Chem. Lett.*, 2010, **39**, 978–979; M. Nihei, Y. Sekine, N. Suganami, K. Nakazawa, A. Nakao, H. Nakao, Y. Murakami and H. Oshio, *J. Am. Chem. Soc.*, 2011, **133**, 3592–3600; J. Mercurol, Y. Li, E. Pardo, O. Risset, M. Seuleiman, H. Rousselière, R. Lescouëzec and M. Julve, *Chem. Commun.*, 2010, **46**, 8995–8997.

7 L. Jiang, T.-B. Lu and X.-L. Feng, *Inorg. Chem.*, 2005, **44**, 7056–7062.

8 F. Meyer, R. F. Winter and E. Kaifer, *Inorg. Chem.*, 2001, **40**, 4597–4603.

9 E. A. Boudreaux and L. N. Mulay, *Theory and Application of Molecular Paramagnetism*, John Wiley & Sons, Inc., New York, 1976, 491; R. Boča, *Struct. Bonding*, 2006, **117**, 1–264; R. L. Carlin, *Magneto-chemistry*, Springer-Verlag, Berlin Heidelberg, 1986.

10 The program julX written by E. Bill was used for the simulation and analysis of magnetic susceptibility data. http://ewww.mpi-muelheim.mpg.de/bac/logins/bill/julX_en.php

7 Conclusion and Outlook

The presented dissertation deals with investigations on structural and magnetic properties of novel Fe^{III} coordination compounds. The first part is devoted to the synthesis and characterisation of mononuclear Fe^{III} complexes $[Fe^{III}(X\text{-salpet})L^1]$ containing a pentadentate Schiff base ligand (X-salpet), as well as an easy replaceable pseudohalide coligand (L^1). Within the scope of this thesis, the investigations were focused on numerous modified pentadentate Schiff base ligands: 3Cl-salpet, 3Br-salpet, 5F-salpet, 5Cl-salpet, 5Br-salpet, 3,5Cl-salpet, 3,5Br-salpet and 3Br5Cl-salpet. These pentadentate ligands have been further developed with various monodentate coligands (L^1 = chloride, cyanate, azide, thiocyanate, selenocyanate, cyanide) to a series of novel Fe^{III} mononuclear complexes. Coligands from the spectrochemical series provide an advantage for a qualitative estimation of electronic strengths and they can also be easily replaced at the sixth coordination site by stronger monomers in methanol solution. Based on previous investigations by Renz, Boca and co-workers,[1] the work was inspired by the possibilities of fine tuning the magnetic properties by ligand modifications and the development of further knowledge in structure-magnetism relationships within the salpet family.

For fine tuning the magnetic properties, a large number of magnetic measurements were carried out and both high or low spin, as well as spin crossover compounds have been observed within the salpet family. On one hand chloride and cyanate coligands result in high spin complexes and on the other hand cyanide monomers induce low spin behaviour due to the stronger impact. The compounds $[Fe^{III}(5Cl\text{-salpet})NCS]$, $[Fe^{III}(5Cl\text{-salpet})NCSe]$, $[Fe^{III}(5Br\text{-salpet})N_3] \cdot CH_3OH$ and $[Fe^{III}(5Br\text{-salpet})NCSe]$ show a gradual spin crossover and are summarised in Table 1 (section 3.2). A further spin crossover complex $[Fe^{III}(5Cl\text{-salpet})N_3]$ with $T_c \approx 150$ K has not been published yet. Within the salpet family, a spin transition seems the most likely for compounds involving azide, thiocyanate or selenocyanate coligands which are suitable for inducing medium ligand field strengths. It is noticeable that $[Fe^{III}(5Cl\text{-salpet})NCS]$ and $[Fe^{III}(5Cl\text{-salpet})NCSe]$ exhibit spin

[1] a) Renz, F.; Hill, D.; Klein, M.; Hefner, J. *Polyhedron* **2007**, *26* (9–11), 2325–2329. b) Renz, F.; Jung, S.; Klein, M.; Menzel, M.; Thünemann, A. F. *Polyhedron* **2009**, *28* (9-10), 1818–1821. c) Nemec, I.; Boča, R.; Gembický, M.; Dlháň, L.; Herchel, R.; Renz, F. *Inorganica Chim. Acta* **2009**, *362* (13), 4754–4759. d) Renz, F.; Zaba, C.; Roßberg, L.; Jung, S.; Klein, M.; Klingelhöfer, G.; Wünsche, a.; Reinhardt, S.; Menzel, M. *Polyhedron* **2009**, *28* (9-10), 2036–2038. e) Boca, R.; Salitros, I.; Kozísek, J.; Linares, J.; Moncol, J.; Renz, F. *Dalton Trans.* **2010**, *39* (9), 2198–2200. f) Šalitroš, I.; Boča, R.; Herchel, R.; Moncol, J.; Nemec, I.; Ruben, M.; Renz, F. *Inorg. Chem.* **2012**, *51* (23), 12755–12767.

transition at 280 and 293 K with ΔT_c = 13 K and [Fe^{III}(5Br-salpet)NCSe] shows a small hysteresis at 326, 317 K. No thermal spin transition is observed for [Fe^{III}(5Br-salpet)NCS]. At first sight this result is a rather unexpected, as the Fe^{III} environment is close to 5Cl-salpet analogous. But structure studies showed that the crystal system of spin crossover compounds is monoclinic with the space group $P2_1/c$ whereas [Fe^{III}(5Br-salpet)NCS] crystallises in a different monoclinic space group Pn. Similar comparisons on dinuclear Fe^{II} compounds have been reported by Real et $al.$[2] {[Fe^{II}(bpym)(NCS)$_2$]$_2$(bpym)}[a] crystallises in the triclinic space group $P\bar{1}$ and shows intramolecular antiferromagnetic coupling between the Fe^{II} ions through the bpym bridge without a spin transition. In contrast, {[Fe^{II}(bpym)(NCSe)$_2$]$_2$(bpym)} exhibits an abrupt spin crossover in the 125 – 115 K temperature region with a small hysteresis loop of 2.5 K. Unfortunately, this crystal structure has not been solved yet. However, if crystal structures and space groups within the salpet family are in agreement, thiocyanate and selenocyanate coligands can be beneficial in tuning the spin crossover.

Investigations on structure properties have been carried out due to the dependence on intermolecular interactions and magnetic behaviour. It is noticeable that the crystal systems of all spin crossover salpet compounds exhibit a high degree of similarity (monoclinic space group $P2_1/c$). In contrast, the only low and high spin complexes crystallise isostructural in the lower symmetric triclinic space group $P\bar{1}$. An exception is [Fe^{III}(5Br-salpet)NCS] which is high spin and crystallises in the monoclinic space group Pn. Moreover, the design of the pentadentate ligand is a crucial factor for covalent and non-covalent intermolecular interactions through the lattice. The spin crossover compounds develop supramolecular dimers linked by rather weak non-covalent N—H--X interactions between the amine group of the pentadentate ligand and a neighbouring substituent of X-salpet. This alignment is supported by $\pi - \pi$ stacking interactions of the neighbouring complex molecules. Based on investigations of spin crossover compounds including various pentadentate ligands it seems that the size and number of substituents at the aromatic ring influences the possibilities of intermolecular interactions. A comparison of [Fe^{III}(5X-salpet)NCSe] with X = F (high spin), Cl (293 K) and Br (326, 317 K) shows that the electronic influence increases with the size of halogens at the aromatic

[2] a) Real, J. A.; Gaspar, A. B.; Munoz, M. C.; Gütlich, P.; Ksenovontov, V.; Spiering, H. In *Spin Crossover in Transition Metal Compounds I*; **2004**; Vol. 1, pp 167–193. b) Real, A.; Zarembowitch, J.; Kahn, O.; Solans, X. *Inorg. Chem.* **1987**, *26*, 2939.
[a] bpym: 2,20-bipyrimidine

ring. The correlation between a single and a double substitution is also notably in e.g. [Fe^{III}(5Cl-salpet)NCSe] (293 K) and [Fe^{III}(3,5Cl-salpet)NCSe] (123, 99 K) which might be explained by the inductive effect.

Despite the further development in structure-magnetism relationships of spin crossover salpet complexes, the problems are still the crystallisation and its correlating entropy. Different crystallisation methods can result in different crystal structures with possible guest inclusions such as solvent molecules. Additional, the entropy which cannot be predicted correlates with the transition temperature. Further structure properties of spin crossover compounds involving pentadentate ligands 3,5Br-salpet and 3Br5Cl-salpet are still under investigations by the Renz group.

First studies on star-shaped heptanuclear complexes [Fe^{II}\{(CN)Fe^{III}(X-salpet)\}$_6$]Cl$_2$ have been carried out including six pentadentate ligands 5Cl-salpet or 5Br-salpet. Indications of a spin crossover in [Fe^{II}\{(CN)Fe^{III}(5Cl-salpet)\}$_6$]Cl$_2$ have been found by Mössbauer spectroscopy from HHHHHL to HHHHHH. In contrast, [Fe^{II}\{(CN)Fe^{III}(5Br-salpet)\}$_6$]Cl$_2$ is only high spin. Moreover, first results on the formation mechanism of the heptanuclear cluster [Fe^{II}\{(CN)Fe^{III}(5Cl-salpet)\}$_6$]Cl$_2$ have been gained by mass spectrometry. Di-, tri-, tetra-, penta- and hexanuclear intermediates have been observed already. Further studies on sequential and concerted mechanisms (section 4.2) on such multinuclear compounds will be performed by the Renz group.

The second part of this thesis deals with the synthesis and characterisation of two rectangular Ni-Fe square complexes. These investigations were inspired by the possibility to develop a switchable chiral molecule with optical properties. Within the scope of this thesis, a novel tetracyanoferrate complex K$_2$[Fe^{III}(L1)(CN)$_4$](MeOH)[a] was developed as a building block. The compound shows pH-dependent solvatochromism effects due to the fact that the ligand HL1 is deprotonable. Crystal structures of the protonated form K[Fe^{III}(HL1)(CN)$_4$](H$_2$O)$_x$ and non-protonated form K$_2$[Fe^{III}(L1)(CN)$_4$](MeOH) were obtained.

The two enantiomeric squares \{[Ni(L2$^{R/S}$)]$_2$[Fe^{III}(L1)(CN)$_4$]$_2$\}·6H$_2$O·2MeOH were formed by K$_2$[Fe^{III}(L1)(CN)$_4$](MeOH), as well as [Ni(L2$^{R/S}$)] involving a chiral bidentate capping ligand L2$^{R/S}$.[b] For both squares ferromagnetic interactions between the nickel and iron ions have been observed. The cyanide-bridge geometry of

---

[a] HL1: 2,2′-(1H-pyrazole-3,5-diyl)bis-pyridine
[b] L2$^{R/S}$: N-(2-pyridylmethylene)-(R/S)-1-phenylethylamine

Ni-N≡C with 104.8° (S-form) and 105.0° (R-form) is unusual and to our knowledge the most acute Ni-N≡C angle observed to date. Further investigations on this type of chiral square complexes with other transition metals such as $[Fe^{III}_2Fe^{II}_2]$ or $[Fe^{III}_2Co^{II}_2]$ will be carried out by the Oshio group.

The development of new polycyano building blocks may be important for the generation of novel functional molecular systems. Their research reflects a modern trend in molecular materials science. Such systems might find applications in hydrogen storage, as molecular sieves and in nanoscale devices.[3]

---

[3] Newton, G. N.; Nihei, M.; Oshio, H. *Eur. J. Inorg. Chem.* **2011**, *2011* (20), 3031–3042.

8   Supplementary Information

8.1   Spin Crossover in Iron(III) Complexes with Pentadentate Schiff Base Ligands and Pseudohalido Coligands

IR spectra

1a

2a'

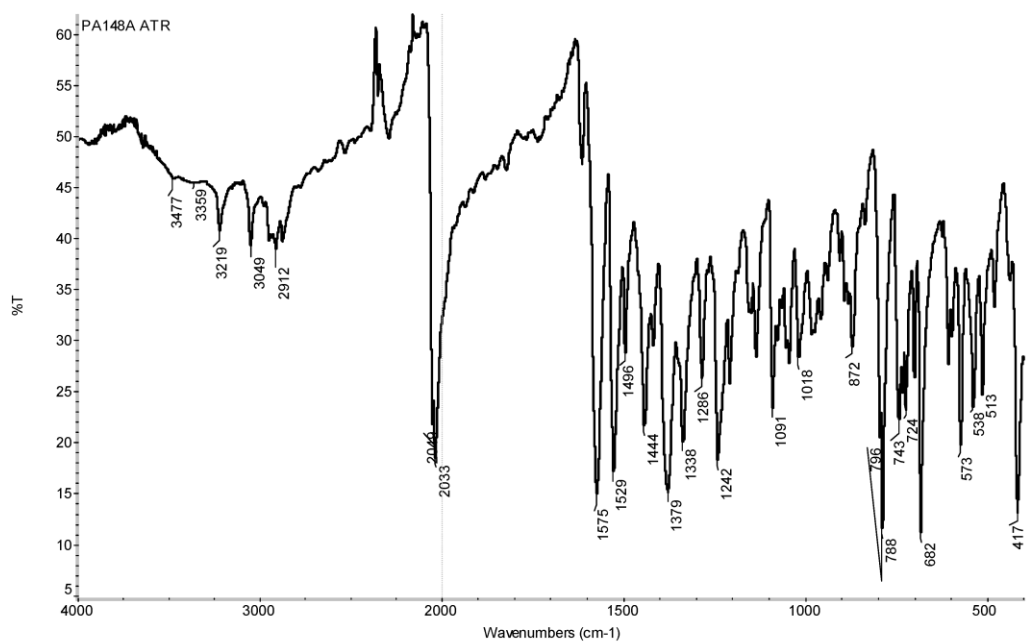**2b**
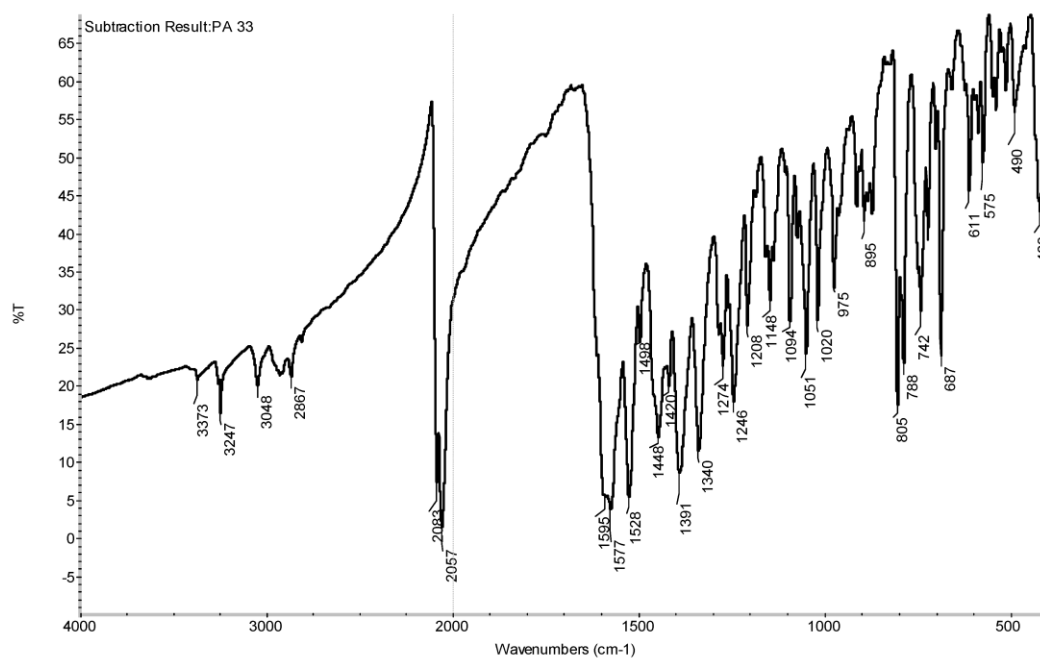

2b'

2c

2d

2e

Subtraction Result:PA 33

8.2 Iron(III) Complexes with Pentadentate Schiff-Base Ligands: Influence of Crystal Packing Change and Pseudohalido Coligand Variations on Spin Crossover

Electronic Supporting Information (ESI)

Iron(III) Complexes with Pentadentate Schiff-base Ligands: Influence of Crystal Packing Change and Pseudohalido Coligand Variations on Spin Crossover

Christoph Krüger, Peter Augustín, Ľubor Dlháň, Ján Pavlik, Ján Moncoľ, Ivan Nemec, Roman Boča and Franz Renz

Magnetic properties: calculation details

The local spin Hamiltonian for **1** and **3** reads

$$\hat{H} = -J\mathrm{h}^{-2}\hat{S}_i \cdot \hat{S}_j + D\mathrm{h}^{-2}(\hat{S}_{zi}^2 + \hat{S}_{zj}^2) + \mu_B \mathrm{h}^{-1} gB \cdot (\hat{S}_{zi} + \hat{S}_{zj}) \qquad (1)$$

where J is the isotropic exchange coupling constant, D is the axial zero-field splitting parameter, g is the isotropic gyromagnetic factor and B is the magnetic field, i and j counts the neighboring interacting centers which are equivalent, therefore the factor 2 in the second and third term. The magnetization is calculated by an iterative way with effective magnetic field (*a molecular field correction*) parameterized by the spin dependent Weiss constant Θ.[1] Taking the derivative of magnetization with respect to the magnetic field the magnetic susceptibility is obtained, which is further corrected for the temperature-independent susceptibility α and presented as effective magnetic moment or eventually the susceptibility product $\chi_{mol}T$. The magnetic susceptibility and magnetization were fitted simultaneously by minimizing a joint functional $F = R(\chi) \cdot R(M)$ where R denotes the discrepancy factors.

The experimental data of **2** and **4** was interpreted by combination of the above mentioned Hamiltonian (1) and the Ising-like model with vibrations.[1,2] The conversion curve from the low-spin to the high-spin state is defined by the high-spin mole fraction $x_H = f(T)$. This interrelates to the so-called fictitious spin $\langle\sigma\rangle_T$ via the formula $x_H = (1 + \langle\sigma\rangle_T)/2$ for which an implicit equation is obeyed

$$\langle\sigma\rangle_T = (F-1)/(F+1) \qquad (2)$$

Here the factor

$$F = \exp[-(E - k_B T \ln r_{ev} - 2\Gamma\langle\sigma\rangle_T)/k_B T] \qquad (3)$$

contains an energy gap E that is proportional to the enthalpy of the spin transition and Γ stands for the solid-state cooperativeness (the intercenter interaction factor). The state degeneracy ratio is

$$r_{ev} = \frac{2S_H+1}{2S_L+1}\left[\frac{1-\exp(-h\bar{\nu}_L/k_B T)}{1-\exp(-h\bar{\nu}_H/k_B T)}\right]^m \qquad (4)$$

where $m = 15$ is the number of active vibration modes in a hexacoordinate complex, $h\bar{\nu}_L$ and $h\bar{\nu}_H$ are the averaged vibration energies (Einstein modes) fixed each other on the basis of experience as $\bar{\nu}_L = 1.15\bar{\nu}_H$. The thermodynamic characteristics of the spin transition are then calculated as

$$\Delta H = R \cdot E$$
$$\Delta S = R \cdot \ln r_{ev}\big|_{x_H=1/2} \qquad (5)$$

and the characteristic temperature at which $x_H = 0.5$ is defined as

$$T_c = \frac{E}{\ln r_{ev}}\bigg|_{Tc} \qquad (6)$$

This quantity has to be determined by an iterative procedure since r_{ev} is a function of temperature. Since the parameters control different parts of experimental dependencies the fitting converged fast. For the model B, the overall high spin fraction is found after renormalization with respect to the fraction of the frozen high spin x_{frz} as

$$x'_H = x_H(1 - x_{frz}) + x_{frz} \qquad (7)$$

while in the model A, $x'_H = x_H$ holds true. By this definition the molecules from the frozen high spin are cooperatively inactive and one has to bear in mind that according to the definitions (5) and (6), $x'_H = 0.5$ at T_c only if no frozen high spin is present (model A), otherwise $x'_H > 0.5$ at T_c. Finally, for the model B the overall susceptibility is composed as

$$\chi_{mol} = x'_H \chi_{5/2} + (1 - x'_H)\chi_{1/2} \qquad (8)$$

It is further worth to notice that while in the model A the decrease of the magnetic moment at low temperature can be only due to the molecular field interaction between the low spin molecules (ZFS does not apply), in the model B also the frozen high-spin state can "feel" the molecular field from the low spin state which occurs in much excess (ZFS can be excluded on

the basis of the unfavorable shape of the magnetization functions[1]). For simplicity the same value of the Weiss constant is taken for the genuine and frozen high spin.

Besides the effective magnetic moment the SCO transition is presented also like the susceptibility product $\chi_{mol}T$ which has the advantage that it is directly proportional to the high spin ratio. This quantity is routinely presented in the cgs-emu units and the relation to the effective magnetic moment in units of Bohr magneton is as follows

$$\mu_{eff}/\mu_B = 2.825 \cdot \sqrt{\chi_{mol}T/\left(cm^3 mol^{-1}K\right)} \tag{9}$$

[1]   R. Boča, *Handbook of Magnetochemical Formulae*, Elsevier, Amsterdam, **2012**.

[2]   a) A. Bousseksou, H. Constant-Machado, F. Varret, *J Phys I France*, **1995**, *5*, 747, b) F. Varret, S. A. Salunke, K. Boukheddaden, A. Bousseksou, É. Codjovi, C. Enachescu, J. Linares, *C.R. Chimie*, **2003**, *6*, 385, c) J. Pavlik, R. Boča, *Eur. J. Inorg. Chem.*, **2013**, 697.
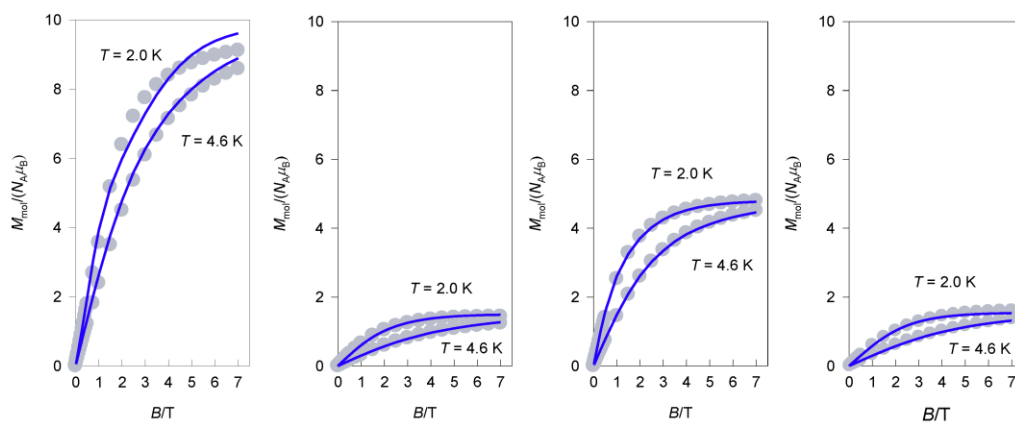
Figure S1. Magnetization as a function of magnetic field for system **1-4** from left to right, circles: experiment, solid line: fitted.
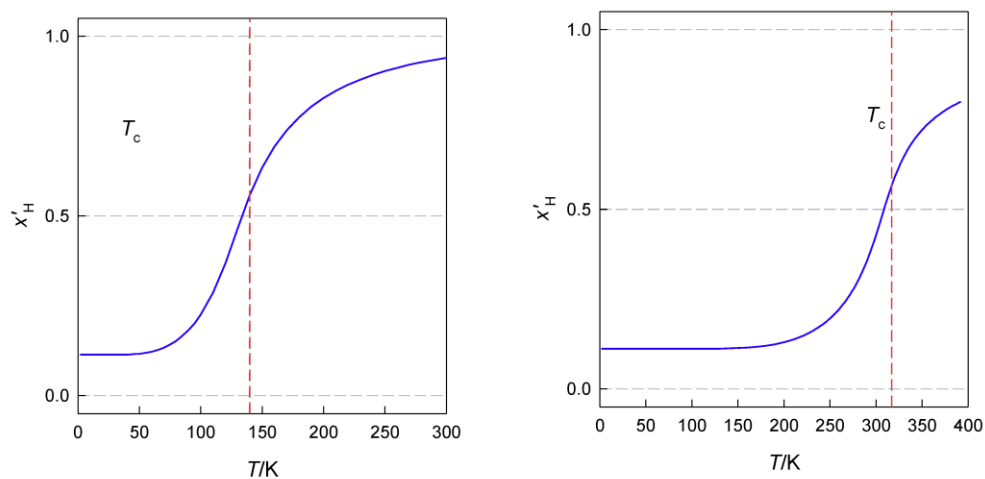
Figure S2. Transition curves for **2** (left) and **4** (right) calculated on the basis of the model B, the renormalized high spin fraction is higher than 0.5 at the critical temperature when the Equations 6 and 7 are employed.

8.3   Hysteretic Spin Crossover in a Mononuclear Iron(III) Complex with a Pentadentate Schiff Base Ligand and NCSe⁻ Coligand

Electronic Supplementary Information

Details of the magnetic data fitting

Temperature dependence of the magnetic susceptibility has been a subject of the fitting to an Ising/like model of spin crossover with vibrations [37]

In fitting the magnetic data three assumptions have been made. (i) The low-spin state of Fe(III) is well described by the Curie-Weiss law enlarged by the temperature-independent (van Vleck) term. The free parameters are the g_L-factor, the Weiss constant Θ_L, and α_L. (ii) The same holds true for the high-spin state, however one can safely fix $g_H = 2.0$ and omit Θ_H and α_H. (iii) There is nothing like a paramagnetic impurity for the Fe(III) complex (as opposite to a frequent situation for Fe(II) ones).

The fourth assumption postulates a model of the spin crossover. This model contains four parameters: (i) the energy difference between LS and HS state Δ_{eff} that is proportional to the enthalpy of the spin transition $\Delta H = R\Delta_{eff}$; (ii) the solid-state cooperativeness J (not to be confused with the exchange coupling constant); (iii) two averaged vibrational frequencies (in fact the Einstein modes) that enter the vibrational partition function. In such a model the equation

$$\langle \sigma \rangle_T = \frac{F-1}{F+1} \tag{1}$$

with

$$f = \exp[-(\Delta_{eff} - kT \ln r_{eff}^T - 2J \langle \sigma \rangle_T)/kT] \tag{2}$$

is to be iterated in order to achieve a selfconsistency. The high-spin mole fraction is related to an fictitious spin *via* $x_H = (1 + \langle \sigma \rangle_T)/2$; the entropic factor is

$$r_{eff}^T = \frac{g_H^{el}}{g_H^{el}} \left[\frac{1 - \exp(h\bar{\nu}_L / kT)}{1 - \exp(h\bar{\nu}_H / kT)} \right]^m \tag{3}$$

for $m = 15$ active modes in a hexacoordinate complex, $h\bar{\nu}_{\text{H}}$ and $h\bar{\nu}_{\text{L}}$ − averaged vibration energies. The transition entropy is then $\Delta S = R\, r_{\text{eff}}^{T}\big|_{x_{\text{H}}=1/2}$. To this end the equilibrium constant is calculated as $K = x_{\text{H}}(1 - x_{\text{H}})$ and this is used in generating the van't Hoff plot $\ln K$ *vs* T^{-1}. The data fitting has been done using the program MIF with the module FIT [40].

The model can be modified by considering a frozen portion of the HS-fraction (equivalent to the fixed paramagnetic impurity x_{PI}). In such a case the g_{LS} is much closer to the spin-only value, typically $g_{\text{LS}} = 2.2 - 2.3$. The resulting thermodynamic parameters of the spin crossover such as ΔH, ΔS, T_{c} and Γ are almost the same.
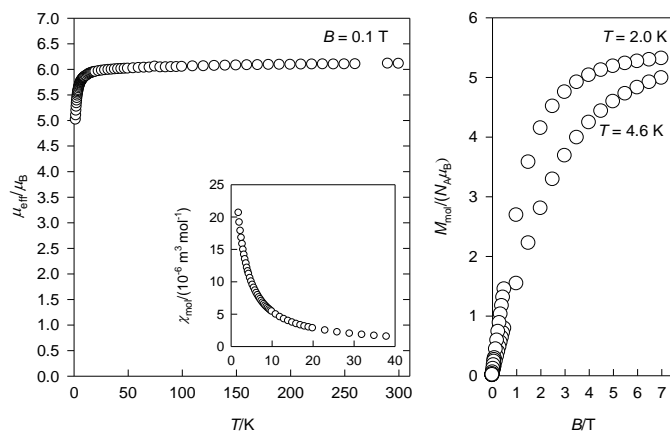
Magnetic data for high-spin complexes
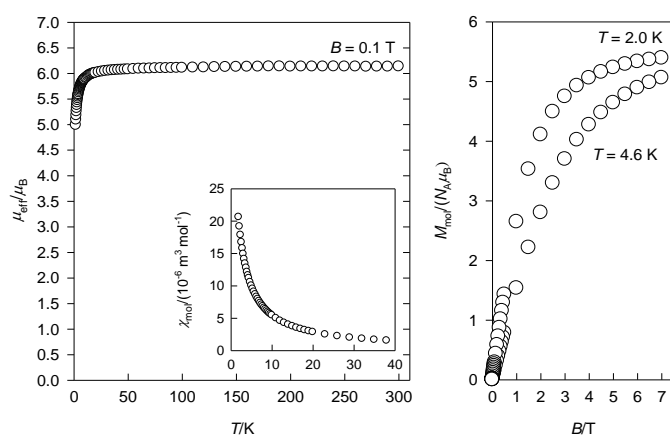
[Fe(3,5-Cl-*salpet*)(N$_3$)], $M = 559.03$ g mol^{-1}
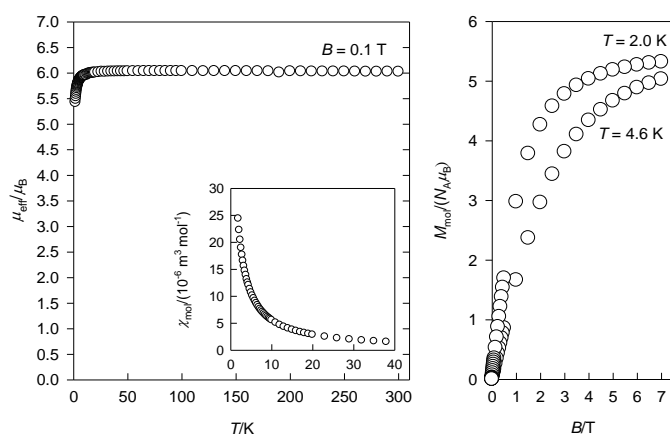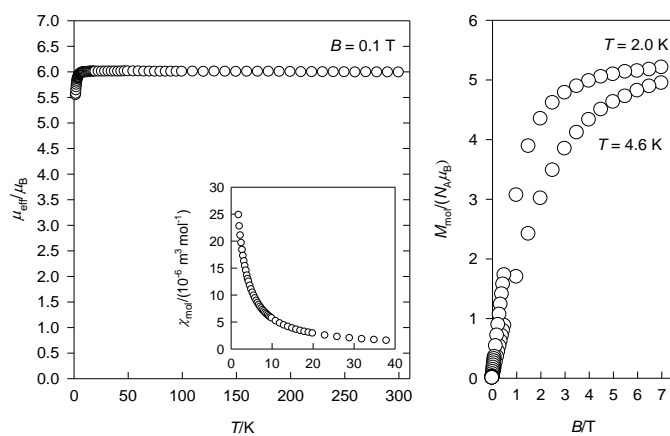

[Fe(3,5-Cl-*salpet*)(NCS)], $M = 575.11$ g mol^{-1}
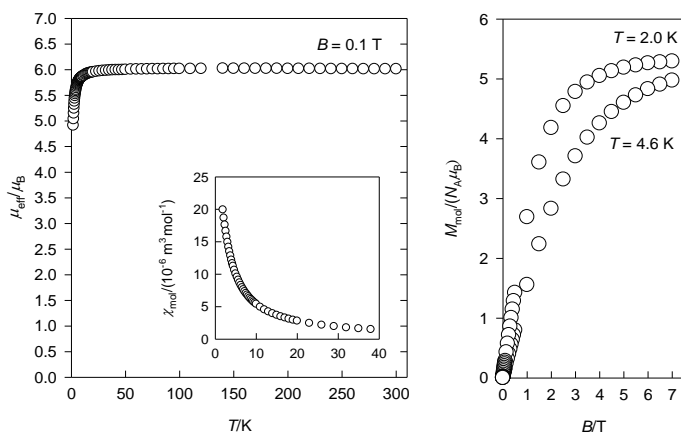
[Fe(3,5-Br-*salpet*)(NCS)], $M = 752.91$ g mol^{-1}

[Fe(3,5-Br-*salpet*)(NCSe)], $M = 799.80$ g mol^{-1}

[Fe(3,5-Br-*salpet*)(N$_3$)], $M = 736.85$ g mol^{-1}

## 8.4   A Rectangular Ni-Fe Cluster with Unusual Cyanide Bridges

Supporting Information

A rectangular Ni-Fe cluster with unusual cyanide bridges

Christoph Krüger, Hiroki Sato, Takuto Matsumoto, Takuya Shiga,

Graham N. Newton, Franz Renz and Hiroki Oshio

Prof. H. Oshio
Graduate School of Pure and Applied Sciences,
University of Tsukuba
Tennodai 1-1-1, Tsukuba, Ibaraki 305-8571 (Japan)
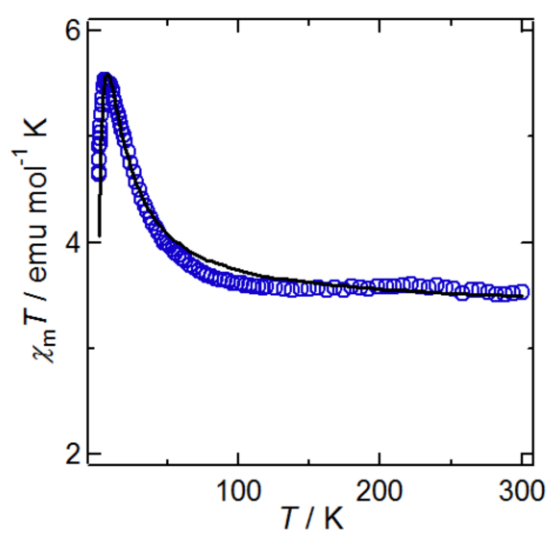FAX: (+81)29-852-4238
E-mail: oshio@chem.tsukuba.ac.jp
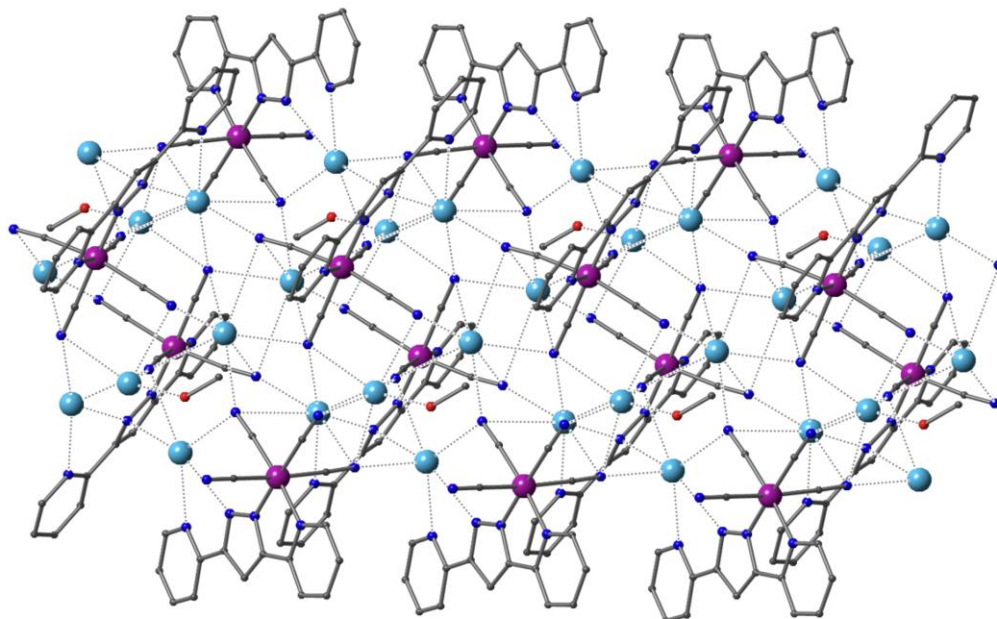
Figure S1. One-dimensional network along the *a* axis of $K_2[Fe^{III}(L1)(CN)_4](MeOH)$ (**1**·MeOH).

(a)

(b)
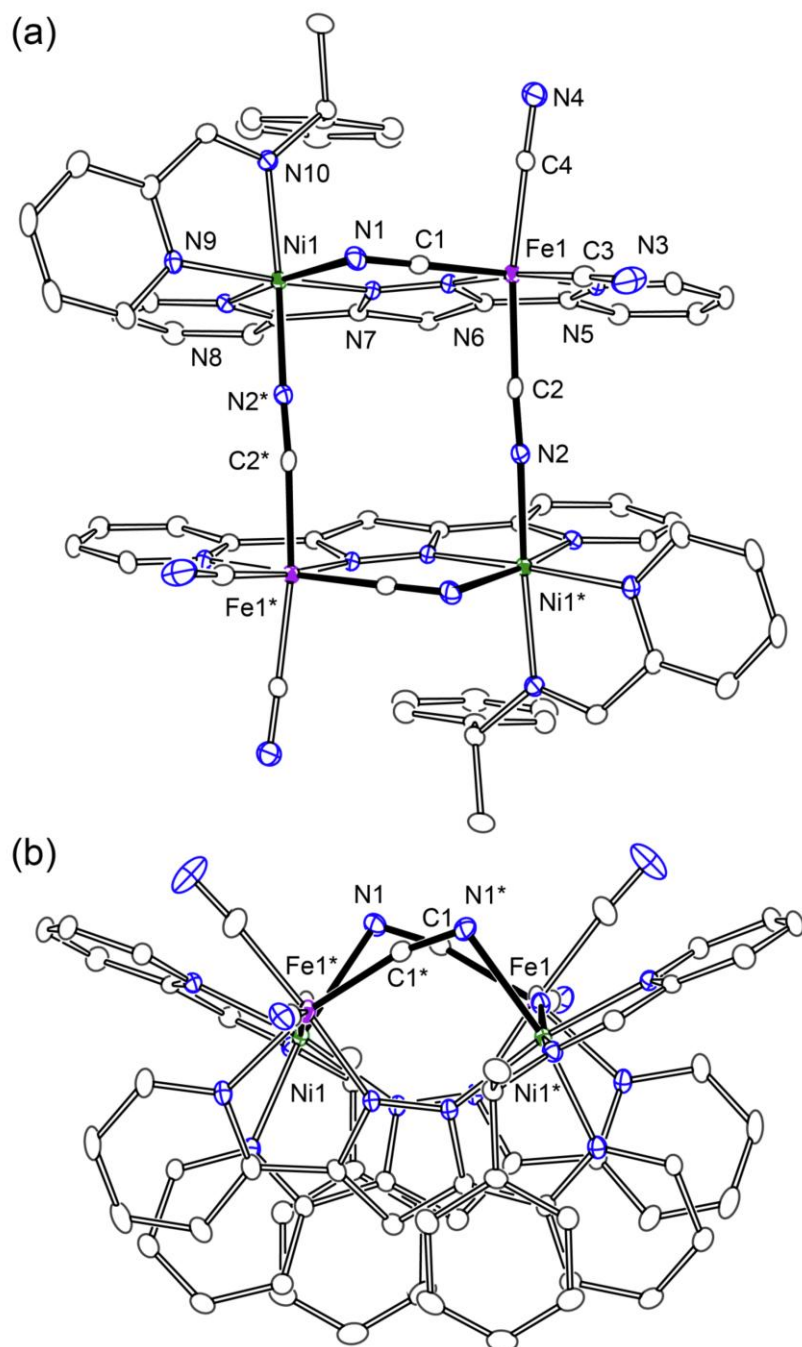
Figure S2. ORTEP drawing of $\{[Ni(L2^R)]_2[Fe(L)(CN)_4]_2\}\cdot6H_2O\cdot2MeOH$ ($2\cdot6H_2O\cdot2MeOH$).
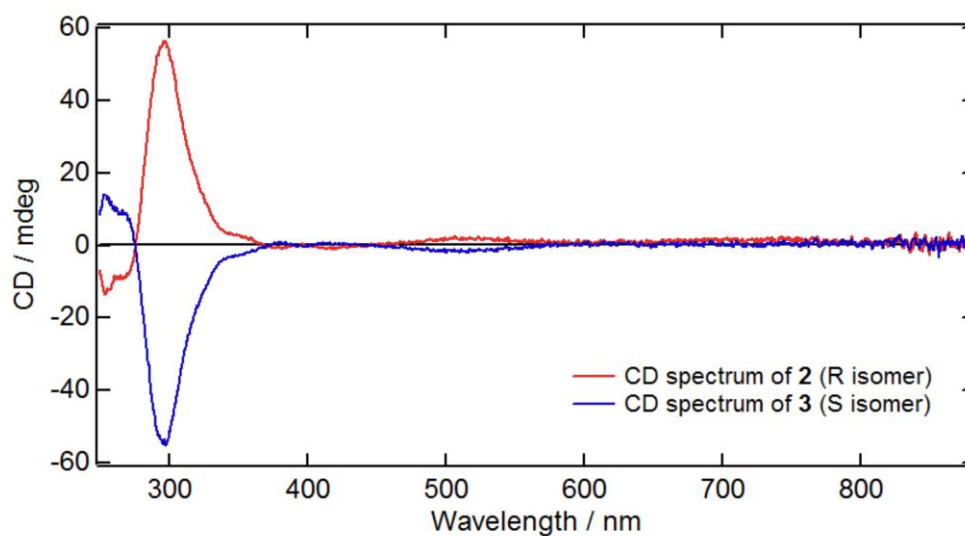
Figure S3. $\chi_m T$ vs. T plot for **2**.
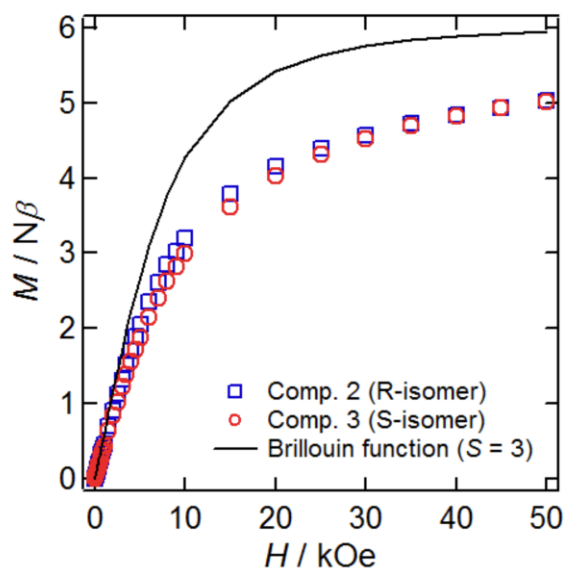
Figure S4.   M vs. H plot of **2** (□) And **3** (○).   The solid line is the indicated Brillouin function of $S = 3$.

Figure S5.   CD spectra of **2** and **3** in methanol.

9   List of Publications

Peer-Review Articles Presented in this Work

Title: "Hysteretic spin-crossover in a mononuclear iron(III) complex with a pentadentate Schiff base ligand and NCSe⁻ coligand"

C. Krüger, L. Heyer, D. Unruh, A. Preiss, Ľ. Dlháň, R. Boča, F. Renz

Inorganica Chimica Acta, **2016**, submitted.

Title: "Iron(III) complexes with pentadentate Schiff-base ligands: Influence of crystal packing change and pseudohalido coligand variations on spin crossover"

C. Krüger, P. Augustin, L. Dlhan, J. Pavlik, J. Moncol, I. Nemec, R. Boca, F. Renz

Polyhedron, **2015**, *87*, 194-201.

Title: "Spin crossover in iron(III) complexes with pentadentate Schiff base ligands and pseudohalido coligands"

C. Krüger, P. Augustín, I. Nemec, Z. Trávnícek, H. Oshio, R. Boca, F. Renz

European Journal of Inorganic Chemistry, **2013**, 902-915.

Title: "A rectangular Ni-Fe cluster with unusual cyanide bridges"

C. Krüger, H. Sato, T. Matsumoto, T. Shiga, G.N. Newton, F. Renz, H. Oshio

Dalton Transaction, **2012**, *41*, 11270-11272.

Further Articles

Title: "Electrospun complexes - Functionalised nanofibres"

T. Meyer, F. Renz, M. Menze, M. Wolff, R. Sindelar, G. Klingelhöfer, D. Unruh, C. Krüger

Hyperfine Interactions, **2015**, accepted.

Title: "Effect of pseudohalides in pentadentate iron(III) complexes studied by DFT and Mössbauer spectroscopy"

M. Wolff, C. Krüger, P. Homenya, L. Heyer, R. Saadat, B. Dreyer, D. Unruh, T. Meyer, G. Klingelhoefer, L. Rissing, R. Sindelar, Y. Ichiyanagi, F. Renz

Hyperfine Interactions, **2013**, *226*, 237-241.

Non Peer-Review Articles

Title: "Klein, flexibel und individuell adressierbar"
F. Renz, L. Rissing, R. Sindelar, C. Krüger, M. Wurz, B. Dreyer
Unimagazin, **2014**, *1/2*.

Title: "Nanopartikel in der Krebsbekämpfung"
F. Renz, A. Kirschning, C. Krüger, K. Seidel
Unimagazin, **2014**, *1/2*.

Oral Presentations

Title: "Vom schaltfähigen Molekül zum intelligenten Material"
C. Krüger, F. Renz
Festkörpernachmittag, ZFM - Zentrum für Festkörperchemie und Neue Materialien, July 23th, **2015**.

Title: "Formation of a mixed-valence heptanuclear iron complex"
C. Krüger, F. Renz
Scientific talk at Slovak University of Technology in Bratislava, Slovakia supported by PPP Slowakei - DAAD, **2015**.

Title: "Iron(III) complexes with pentadentate Schiff base ligands and pseudohalide coligands"
C. Krüger, F. Renz
Scientific talk at Slovak University of Technology in Bratislava, Slovakia supported by PPP Slowakei - DAAD, **2013**.

Title: "A tetracyanide complex in solution and a rectangular Ni–Fe cluster with unusual cyanide bridges"
C. Krüger, F. Renz
Scientific talk at Slovak University of Technology in Bratislava, Slovakia supported by PPP Slowakei - DAAD, **2012**.

Poster Presentations

Title: "A tetracyanate iron(III) unit forms a tetranuclear complex with a chiral ligand"

C. Krüger, H. Sato, T. Matsumoto, T. Shiga, G. N. Newton, F. Renz, H. Oshio

NanoDay, Laboratory of Nano and Quantum Engineering (LNQE), October 10th, **2013**, Hannover, Germany.

Title: "Influence on the coordination sphere of Fe(III) spin crossover compounds"

C. Krüger, S. Klimke, H. Cavers, G. Vaccaro, M. Menzel, R. Stößer, F. Renz

The International Conference on the Applications of the Mössbauer Effect (ICAME), September 1st -6th, **2013**, Opatija, Croatia.

Title: "Nickel-iron rectangle molecule with unusual cyanide bridges"

C. Krüger, H. Sato, T. Matsumoto, T. Shiga, G. N. Newton, F. Renz, H. Oshio

ZFM-Summer School, July 21st-25th, **2013**, Goslar, Germany.

Title: "Variation of pseudohalide coligands in iron(III) spin crossover complexes with pentadentate Schiff base ligands"

C. Krüger, F. Renz

11th Ferrocene Colloquium, February 6th-8th, **2013**, Hannover, Germany.

Title: "Spin crossover in iron(III) complexes with pentadentate Schiff-base ligand and pseudohalido coligands"

C. Krüger, P. Augustín, I. Nemec, Z. Trávníček, H. Oshio, R. Boča, F. Renz

Japanese-German Symposium, October 25th -27th, **2012**, Münster, Germany.

Title: "Magnetic behaviour of iron(III) mononuclear complexes investigated by SQUID and Mössbauer spectroscopy"

C. Krüger, F. Renz, D. Nariaki, H. Oshio

Phase transition and Dynamical properties of Spin Transition Materials (PDSTM), May 22th - 25th, **2012**, Versailles, France.

10 Curriculum Vitae

Christoph Krüger

Biographical Information

Date of birth   February 9, 1987

Place of birth   Berlin

Nationality   German

Education and Professional Experience

03/2012 - 01/2016	Dissertation (PhD) at the Institute for Inorganic Chemistry, Gottfried Wilhelm Leibniz Universität Hannover in the group of Prof. Dr. Franz Renz Title: "Molecular Magnetic Switches – Synthesis and Characterisation of Novel Iron Spin Crossover Compounds"
10/2009 - 02/2012	Master of Science Material- and Nanochemistry, Institute for Inorganic Chemistry, Gottfried Wilhelm Leibniz Universität Hannover Title (master thesis): "Tuning of Molecular Switches"
10/2006 - 09/2009	Bachelor of Science Gottfried Wilhelm Leibniz Universität Hannover
06/2006	Abitur at Gymnasium Walsrode

International Experience

02/2015 – 03/2015	Visiting Researcher at Stanford University (USA) in the group of Prof. Dr. R. N. Zare
10/2010 – 03/2011	Research Student at Tsukuba University (Japan) in the group of Prof. Dr. Hiroki Oshio